Final Report
(Item 2152, ORA 125-6579)

SETTLEMENT BEHAVIOR OF COMPACTED OKLAHOMA SOILS

Prepared by:
Yong Yeow Lim
Gerald A. Miller
Kanthasamy K. Muraleetharan

Planning & Research Division
Oklahoma Department of Transportation
200 N.E. 21st, OKC, OK 73105

Office of Research Administration
The University of Oklahoma
Norman, Oklahoma 73072

February 2003

SETTLEMENT BEHAVIOR OF COMPACTED OKLAHOMA SOILS

Final Report
(Item 2152, ORA 125-6579)

Submitted to:

Planning & Research Division
Oklahoma Department of Transportation
200 N.E. 21st Street
Oklahoma City, Oklahoma 73105

Prepared by:
Yong Yeow Lim
Gerald A. Miller
Kanthasamy K. Muraleetharan

School of Civil Engineering and Environmental Science
The University of Oklahoma
Norman, Oklahoma 73019

From:
The Office of Research Administration
The University of Oklahoma
Norman, Oklahoma 73019

February 2003

TECHNICAL REPORT DOCUMENTATION PAGE

1. REPORT NO.	2. GOVERNMENT ACCESSION NO.	3. RECIPIENT'S CATALOG NO.
FHWA/OK 02(03)	FHWA/OK 02(03)	

4. TITLE AND SUBTITLE	5. REPORT DATE
Settlement Behavior of Compacted Oklahoma Soils	February 2003
	6. PERFORMING ORGANIZATION CODE
7. AUTHOR(S)	8. PERFORMING ORGANIZATION REPORT
Yong Yeow Lim, Gerald A. Miller, Kanthasamy K. Muraleetharan	ORA 125-6579
9. PERFORMING ORGANIZATION NAME AND ADDRESS	10. WORK UNIT NO.
The University of Oklahoma Norman, Oklahoma 73019	
	11. CONTRACT OR GRANT NO. Item No. 2152
12. SPONSORING AGENCY NAME AND ADDRESS	13. TYPE OF REPORT AND PERIOD COVERED
Oklahoma Department of Transportation Planning & Research Division 200 N.E. 21st Street Oklahoma City, OK 73105	Final Report (April 1999-November 2001)
	14. SPONSORING AGENCY CODE

15. SUPPLEMENTARY NOTES

16. ABSTRACT

Numerous highway embankments experience post-construction settlement problems, such as bridge approach settlement that results in the "bump at the end of the bridge." One of the causes may be wetting-induced collapse settlement or simply, collapse settlement. Collapse settlement is a time-dependent process resulting from post-construction increases in moisture content. The post-construction settlement of numerous Oklahoma highway embankments raised questions as to whether the current Oklahoma Department of Transportation embankment specifications and construction practices are adequate in addressing collapse settlement, and prompted the current study to examine the influence of soil type on collapse potential of Oklahoma soils.

One-dimensional oedometer tests were conducted to study the potential for collapse settlement of 22 Oklahoma soils and shales under conditions typically encountered in compacted fills. Results show that factors related to fine composition, such as clay-size fraction, plasticity index, liquid limit, activity, and AASHTO group index can be used for preliminary estimation of collapse index. Statistical analysis of the oedometer test data indicates that variables having the most impact on collapse index are moisture content, dry unit weight, plasticity index, and clay-size fraction.

Settlement charts were developed to facilitate the estimation of collapse settlement of fills for different conditions, including fill height, moisture content, and soil type. Three scale centrifuge models compacted at different conditions and a case history of an embankment that has experienced significant collapse settlement are presented. Predictions based on one-dimensional oedometer-based method and settlement charts are compared to measured collapse settlements at the embankment centerlines. Given the uncertainty with field estimates of settlement, the comparison showed a reasonable agreement between predictions and field estimates of collapse settlement at the embankment centerlines; the limited evidence suggests that predictions based on one-dimensional assumptions tend to underestimate actual settlements possibly due to the two-dimensional nature of embankments.

The review of literature regarding settlement of compacted fills, the laboratory test results obtained, and the field study of an actual embankment suggest the need for embankment design and specifications that will account for collapse susceptibility of different soil types. Specifications should demand for exceptional quality control and more stringent compaction requirements during embankment construction, particularly for large embankments, collapse-susceptible soils, and embankments susceptible to flooding.

17. KEY WORDS	18. DISTRIBUTION STATEMENT
Collapse Settlement, Compacted Soil, Embankment, Centrifuge Test	No restrictions. This publication is available from the office of Planning and Research Division, Oklahoma, DOT.

19. SECURITY CLASSIF. (OF THIS REPORT)	20. SECURITY CLASSIF. (OF THIS PAGE)	21. NO. OF PAGES	22. PRICE
Unclassified	Unclassified	154	

Disclaimer

The contents of this report reflect the views of the authors who are responsible for the facts and the accuracy of the information presented herein. The contents do not necessarily reflect the official views of the Oklahoma Department of Transportation or the Federal Highway Administration. This report does not constitute a standard, specification, or regulation. While trade names may be used in this report, it is not intended as an endorsement of any machine, contractor, process, or product.

Acknowledgements

The authors would like to thank the people in the Department of Biology at the University of Oklahoma and at the Army Corps of Engineers Waterways Experiment Station in Vicksburg, Mississippi for their assistance in conducting Scanning Electron Microscopy and centrifuge testing, respectively. Also, thanks to folks in the Soils and Foundations Branch and Planning and Research Division of the Oklahoma Department of Transportation for facilitating the successful completion of this project. Special thanks is extended to Dr. James B. Nevels and his field crew, and Mr. Curtis Hayes, for their help in the field phase of this study and cooperation in the use of laboratory equipment.

This research was funded by the Oklahoma Department of Transportation, while the centrifuge testing reported in this report was funded by the National Science Foundation (Grant No. CMS 9501718). This support is gratefully acknowledged.

Table of Contents

List of Tables

List of Figures

List of Symbols

C_{α} = compression ratio

C_{σ} = recompression ratio

γ_d = dry unit weight

I_d = slake durability index

I_e = collapse index

I_J = jar soaking index

LL = liquid limit

PI = plasticity index

PL = plastic limit

R = relative compaction

r^2 = coefficient of determination

s_u = undrained shear strength

w = moisture content

w_n = natural moisture content

Summary

Numerous highway embankments experience post-construction settlement problems, such as bridge approach settlement that results in the "bump at the end of the bridge." One of the causes may be wetting-induced collapse settlement or simply, collapse settlement. Collapse settlement is a time-dependent process resulting from post-construction increases in moisture content. The post-construction settlement of numerous Oklahoma highway embankments raised questions as to whether the current Oklahoma Department of Transportation embankment specifications and construction practices are adequate in addressing collapse settlement, and prompted the current study to examine the influence of soil type on collapse potential of Oklahoma soils.

One-dimensional oedometer tests were conducted to study the potential for collapse settlement of 22 Oklahoma soils and shales under conditions typically encountered in compacted fills. Results show that factors related to fines composition, such as clay-size fraction, plasticity index, liquid limit, activity, and AASHTO group index can be used for preliminary estimation of collapse index. Statistical analysis of the oedometer test data indicates that variables having the most impact on collapse index are moisture content, dry unit weight, plasticity index, and clay-size fraction.

Settlement charts were developed to facilitate the estimation of collapse settlement of fills for different conditions, including fill height, moisture content, and soil type. Three centrifuge scale models compacted at different conditions and a case history of an embankment that has experienced significant collapse settlement are presented. Predictions based on one-dimensional oedometer-based method and settlement charts are compared to measured collapse settlements at the embankment centerlines. Given the uncertainty with field estimates of settlement, the comparison showed a reasonable agreement between predictions and field estimates of collapse settlement at the embankment centerlines; the limited evidence suggests that predictions based on

one-dimensional assumptions tend to underestimate actual settlements possibly due to the two-dimensional nature of embankments.

The review of literature regarding settlement of compacted fills, the laboratory test results obtained, and the field study of an actual embankment suggest the need for embankment design and specifications that will account for collapse susceptibility of different soil types. Specifications should demand for exceptional quality control and more stringent compaction requirements during embankment construction, particularly for large embankments, collapse-susceptible soils, and embankments susceptible to flooding.

Chapter 1: Introduction

1.1 General

Based on a review of literature and a survey of 48 state departments of transportation, Briaud et al. (1997) identify several factors that cause settlement of highway embankments and lead to the "bump at the end of the bridge." Among the primary causes were settlement of the natural soil beneath the embankment and compression of the embankment fill material. With regard to the latter, poor compaction of the fill, poor fill materials, and high embankments (more than 10 m) were cited by transportation agencies as being the primary conditions leading to approach settlement. Only one agency indicated collapsible soils as a condition leading to embankment settlement; however, it is possible that in some cases where poor compaction of the fill, poor fill materials, and high embankments existed, wetting-induced collapse in the fill contributed to the settlement problem. In a different survey, Stark et al. (1995) listed collapse mechanism as one of the factors leading to settlement of highway embankments in Illinois.

In a survey of 758 bridge approaches in Oklahoma, Laguros et al. (1990) found that the two most statistically significant factors correlated to settlement are the age of the approach and the height of the embankment. A comprehensive laboratory investigation was also conducted on two embankments from the survey list that exhibited excessive settlements. These researchers found that poor quality materials, post-construction wetting, high embankment, and settlement of embankment soils have contributed to the overall settlements of these embankments. Among other possibilities, some of these factors are consistent with a collapse mechanism. Collapse settlement increases with increasing rate of wetting and greater embankment height. These results raised questions as to whether the current Oklahoma Department of Transportation (ODOT) embankment specifications and construction practices are adequate in addressing collapse settlement, and prompted the current study to examine the influence of soil type on collapse potential of Oklahoma soils.

Research to date is limited regarding the influence of soil type on collapse potential of compacted soil, particularly in regard to natural sources of fill compacted within typical embankment specifications. In addition, the influence of moisture content within specifications has received little attention. Some correlation has been established between collapse potential and index properties of soils; however, the research involved primarily silty and sandy soils, as well as artificially mixed soils containing clay.

As part of this research, laboratory oedometer testing was conducted on a variety of compacted natural soils to establish empirical correlation between collapse index and various soil properties. In addition, a simple method of predicting the centerline settlement of two-dimensional (long) embankments was developed and predictions were compared to measured settlements of three centrifuge model embankments and one actual embankment. In addition to collapse settlement, settlement attributed to self-weight compression was studied.

1.2 Objectives

This research focused on evaluating the settlement potential of various Oklahoma soils as well as suggesting design and construction methods to overcome settlement problems of embankments. The primary objectives of this research were:

1. To characterize the one-dimensional compression behavior of selected Oklahoma soils and shales under conditions typical of compacted embankments. In particular, the rate and magnitude of compression were examined.
2. To identify, via laboratory testing, typical soils and shales native to Oklahoma that are susceptible to collapse settlement under conditions frequently encountered in compacted fills.
3. To characterize, via index and physical properties, typical Oklahoma soils and shales and to relate these characteristics to the soil's degree of susceptibility to collapse settlement.
4. To develop a protocol to identify collapse-susceptible soils.
5. To develop and verify, through a field study and a centrifuge testing program, a simple method of predicting the centerline settlement of two-dimensional (long) embankments.

6. To prepare recommendations for addressing collapse-susceptible soils in embankment design and construction.

1.3 Report Layout

This report is organized into seven chapters. Chapter 2 reviews published studies on soil and highway embankment settlements. Chapter 3 provides detailed descriptions of the test soils as well as the sample preparation, test procedures, and results for oedometer testing. Correlation between collapse index and each of the soil properties as well as the predictive model for collapse index are also presented in this chapter. Chapter 4 presents the preparation, instrumentation, testing, and results of three centrifuge model embankments. Comparisons of the predicted and measured centerline settlements of the model embankments are also presented in this chapter. Chapter 5 presents results from a field study of an actual embankment as well as comparisons of the predicted and measured centerline settlements of the embankment. Chapter 6 is devoted to some recommendations for embankment design and construction synthesizing results of current research and that in the literature. Finally, the conclusions for this study are presented in Chapter 7. This chapter also includes recommendations for future study on the understanding of collapse behavior in compacted soils.

Chapter 2: Literature Review

2.1 General

The primary mechanisms for the compression of embankment fill are self-weight settlement, collapse settlement, and settlement due to shale deterioration. Self-weight settlement is the vertical deformation of soil due to overburden pressure. Collapse settlement is defined as the densification of an initially stable soil as a result of inundation with water (Barden et al. 1973, Mitchell 1993). The addition of water that triggers collapse in compacted fills can be due to post-construction alterations in moisture content caused either by rainfall, ingression of capillary water from foundation soils, or post-construction flooding. Shale deterioration due to weathering can lead to a weakening of the soil structure that results in settlement sometime after the soil compaction is completed. This phenomenon is common to non-durable shales that do not break down during field compaction, but soften and disintegrate as a result of post-construction wetting (Strohm et al. 1978). A detailed discussion of these settlement mechanisms is presented in this chapter.

2.2 Compression of Unsaturated Soils

The compression of unsaturated soils can be divided into three stages, that is, initial compression, consolidation, and creep (Yoshimi 1958). Each phase probably occurs simultaneously; however, they are considered to act separately. These stages are defined as follows: (1) initial compression is the immediate response caused by the compression of pore air and the soil skeleton; (2) consolidation is the stage of compression that involves the outflow of pore fluids under a significant pore pressure gradient; and (3) creep is the long-term process involving rearrangement of aggregates under a constant applied stress with little pore pressure gradient. Several researchers (Yoshimi 1958, Witsman and Lovell 1979, DiBernando and Lovell 1980) report similar compression-time relationships for compacted soils. Typically, a large amount of compression takes place within the first minute of loading, and further compression with time is

limited. Such behavior was noted for laboratory-compacted silty clays, highly plastic clays, and shales.

The rate of self-weight compression of an unsaturated soil depends on the degree of saturation in the soil. At a moisture content dry of the optimum moisture content (OMC), pore water pressure dissipates rapidly due to continuous air voids (Barden 1974). Hence, self-weight settlement generally is complete shortly after construction and thus, does not pose many problems for constructed facilities (DiBernardo and Lovell 1980). At moisture contents much wetter than the OMC, high pore water pressure develops due to occluded air voids, and as a result, the rate of compression is slower. For the latter case, the rate of compression can be predicted using the theory of consolidation or any of the more complex theories attempting to consider the effects of occluded air (Barden 1974).

Lambe (1958a and 1958b) discusses the effect of soil structure on the behavior of compacted clays. He indicates that a clayey soil compacted dry of optimum generally results in a flocculated structure, whereas that compacted wet of optimum generally results in a dispersed structure. Seed and Chan (1959) substantiate Lambe's findings and demonstrate that for the same compacted dry unit weight, a flocculated structure generally exhibits higher soil suction and higher compressibility (at higher stress levels) compared with a dispersed structure.

DiBernardo and Lovell (1980) found that the initial moisture content and compaction pressure are the principal variables that affect the compressibility of the highly plastic clay they studied. There is a marked difference in the compressibility behavior of soils at applied vertical stresses lower and higher than the compaction prestress. Compaction prestress is the preconsolidation pressure induced during compaction. Soils experience very little compression at applied vertical stresses lower than the compaction prestress; however, when the applied vertical stress exceeds the level of compaction prestress, more compression occurs. In addition, the authors show that there is a marked difference in the compressibility behavior for samples compacted at moisture contents wet and dry of the OMC depending on the range of vertical

stresses applied. At an applied vertical stress lower than the compaction prestress, the wet-of-optimum samples are more compressible (due to the dispersed soil structure as suggested by Seed and Chan) than the dry-of-optimum samples, whereas at a higher vertical stress, the opposite holds true.

2.3 Collapse Mechanism

Both compacted and naturally deposited soils experience collapse (Lawton et al. 1986). A literature review performed by Lawton et al. (1991b) has shown that nearly all types of compacted soils (even clean sands, pure clays, and soils containing substantial gravel fractions) are collapsible under suitable conditions. The conditions that lead to collapse in both compacted and naturally deposited soils are well documented in the literature. Collapse is generally associated with the following conditions (Barden et al. 1973, Mitchell 1993): (1) the soil fabric is open; (2) the soil is unsaturated; (3) some metastable bonding such as capillary tension and/or natural cementation is present such that the soil is stable under the existing stress and moisture conditions; and (4) the stress level is high enough to cause shear failure at the particle contacts following the loss of metastable bonding.

When a collapsible soil contacts water, the metastable bonding is destroyed through the elimination of capillary tension and dissolution of natural cementation resulting in shear failure at the particle contacts. Due to the behavioral differences of compacted and naturally deposited soils, discussion of collapse phenomena will be limited to compacted soils, unless otherwise stated.

The mechanisms of collapse in cohesive and cohesionless compacted soils are different. In cohesionless soils, such as sands and gravels, the metastable bonding is typically provided by capillary tension. The elimination of capillary tension is also partly responsible for collapse phenomena in cohesive soils. For example, Fredlund and Gan (1995) report that collapse phenomena for the silt and silty sand they studied is primarily related to the reduction of matric suction during inundation. According to Fredlund and Gan, there is a direct relationship between

the reduction in volume and the decrease in matric suction observed during collapse in oedometer tests.

Collapse in cohesive soils may also occur because of a softening of the macropeds (clusters of clay particles) upon wetting. This model was proposed by Jennings and Burland (1962), later verified using scanning electron microscopy by Barden et al. (1973) and Booth (1977), and refined by Hodek and Lovell (1979) as cited by Lawton (1992). In this model, a cluster of many clay particles called macropeds acts as the binder between coarser particles; when wetted, the macropeds soften and lubricate the intergranular contacts, thereby causing collapse. The macropeds in dry of optimum conditions are brittle and shrunken with larger inter-aggregate pores; upon wetting, the macropeds soften with the adsorption of water to the clay particles and as a result, collapse occurs. On the other hand, the macropeds in soil wet of optimum are plastic and swollen and the addition of water primarily fills the small inter-aggregate pores, with little softening of macropeds; thus, collapse is unlikely.

The collapse potential of a soil is typically measured in the laboratory using standard incremental loading oedometer equipment and employing simple modifications to the standard loading procedure. Two widely accepted methods exist, the single- and double-oedometer methods. Test procedures for each method are discussed in Chapter 3.

2.4 Factors Affecting Collapse

Moisture Condition, Dry Unit Weight, & Stress State

Collapse potential for a given compacted soil depends on the prewetting moisture condition, dry unit weight of the soil, and the total overburden stress (Lawton 1986). Generally, collapse potential increases with increasing total overburden stress, decreasing dry unit weight, and decreasing prewetting moisture content. There is one exception, however, to this general trend; collapse potential reaches maximum at some value of vertical stress, known as compaction prestress. Beyond compaction prestress, collapse potential decreases with increasing vertical stress (Lawton et al. 1992), as shown in Figure 2.1. Witsman and Lovell (1979) suggest the use

of Casagrande construction for the determination of compaction prestress from stress-strain curves, acknowledging that extending the use of Casagrande construction to compacted, unsaturated soils may be inappropriate.

For the silt Fredlund and Gan (1995) tested, the amount of collapse decreased linearly with increasing initial moisture content if the initial dry unit weight of specimens was kept constant. Similarly, amount of collapse was observed to decrease linearly with increasing initial dry unit weight for a given moisture content. For a given dry unit weight, collapse potential is lower at higher moisture contents for several reasons. The wetter and more compressible as-compacted soil has already experienced a significant amount of load-induced compression before inundation (Lawton et al. 1986) resulting in an increase in dry unit weight and degree of saturation. Lawton et al. (1986) emphasize that the underlying reason collapse potential decreases with increasing moisture content for a given dry unit weight is the increased degree of saturation at higher moisture content. On the macro-scale, the macropeds developed at higher moisture contents are more plastic and swollen. The addition of water creates little softening of macropeds; therefore, collapse potential is reduced (Lawton et al. 1989). For a given moisture content, collapse potential reduces at higher dry unit weights because of the lower void ratios or less open soil fabric (Basma and Tuncer 1992).

Degree of Wetting

Partial wetting may prevail in field situations; thus, estimated collapse settlements based on full-wetting collapse potential, as in the laboratory oedometer tests, may not be realized in such situations (Houston and Houston 1992). Lawton (1986) reports that single-oedometer samples of clayey sand attained an average degree of saturation of 92 percent after soaking. Witsman and Lovell (1979) employed backpressure saturation techniques in triaxial collapse tests to achieve complete or near-complete saturation; however, they determined that little additional collapse was observed during backpressure saturation. Houston and Houston (1992) discuss a method to predict the collapse settlement due to partial wetting. Houston and Houston noted that collapse

potential obtained from typical laboratory collapse tests is conservative if partial wetting is expected in the field.

Soil Type

As brought up earlier, research to date does not adequately address the influence of soil type on collapse potential of compacted soil, particularly in regard to natural sources of fill compacted within typical embankment specifications. In addition, the influence of moisture content within specifications has received little attention. Limited attempts have been made to correlate collapse potential and index properties of soils. The available studies, however, involved primarily silty and sandy soils, as well as artificially mixed soils containing clay.

Steadman (1987) studied the effect of fines content on the magnitude of collapse in artificially generated sand-silt-clay mixtures. The researcher concluded that as the fines fraction increases, in either clay or silt fraction, the magnitude of collapse increases. Furthermore, soils containing equal amounts of silt and clay collapsed more than soils containing either more clay or more silt, but clayey soils showed more overall. His findings are based on results of 50 double-oedometer tests conducted on specimens prepared at dry unit weights corresponding to 85 and 90 percent relative compaction, as determined from the modified Proctor procedure, and a moisture content 3 percent below the OMC.

In a comparable study, Alwail et al. (1994) report that collapse potential increases with increasing clay-size fraction and clay-to-silt ratio. They performed double-oedometer tests on 25 soil combinations of sand-silt-clay mixtures compacted at dry unit weight corresponding to 90 percent relative compaction, as determined from the modified Proctor procedure, and a moisture content 3 percent below the OMC.

Mishu (1963), as cited by Witsman and Lovell (1979), studied the one-dimensional collapse behavior of two compacted natural clays. Mishu reports that under similar conditions, the more plastic soil exhibited larger collapse.

While useful, these studies do not encompass natural variability in soil as nearly all the studies involved mixtures of sand, silt, and clay from the same stock. Furthermore, the influence of moisture content is generally not addressed. Results presented in this report represent 88 tests on 22 broadly different natural soils from Oklahoma.

Few empirical relationships can be found in the literature for predicting collapse potential for compacted soils. The majority of these were developed for naturally deposited soils and thus, are not relevant for compacted soil. However, one study reported by Basma and Tuncer (1992) involved a multiple regression analysis on results of 138 single-oedometer tests. The tests were conducted on eight natural silty and sandy soils (including two sands, five sandy lean clays, and a fat clay) prepared at relatively low dry unit weights and moisture contents. The majority of the samples were compacted at a relative compaction of 80 percent, as determined from the standard Proctor procedure, and moisture contents of between 10 to 13 percent dry of the OMC. Factors that had the most impact on the magnitude of collapse were initial moisture content, dry unit weight, pressure at wetting, uniformity coefficient, and/or difference between sand and clay-size fractions. While relevant, this study is of limited use in the current research, which is focused on soils compacted within or close to within typical embankment specifications, i.e., relative compaction of 95 percent (standard Proctor effort) and moisture contents between 4 percent below and 2 percent above the OMC.

Compaction Method

Compaction methods may have an impact on collapse potential of laboratory- and field-compacted clays. Lawton et al. (1992) report that the influence of compaction method on collapse behavior has been relatively ignored by researchers, even though it is widely recognized that compaction methods may have a significant affect on the engineering properties of cohesive soils (Seed and Chan 1959).

Lawton et al. (1992) determined that the compaction method has little influence on collapse potential at dry or wet of the OMC for the clayey sand they studied. The authors added that whether this result is also valid for other laboratory- or field-compacted soils is unknown.

Noorany and Stanley (1994) claim that samples subjected to static compaction will exhibit greater expansion and lower collapse compared to kneading compaction. They added that tamping, using a Harvard miniature compactor, produces results between kneading and static compaction; however, they did not provide any experimental data to support their findings.

Stress-Strain Anisotropy

While collapse is often evaluated in the laboratory using one-dimensional single- and double-oedometer tests, stress-strain conditions in many field applications are not one-dimensional. For instance, stress-strain conditions within a long embankment are closely represented by plane strain. Lawton et al. (1991a) conducted collapse testing under anisotropic stress-strain conditions in a triaxial apparatus. They found that the magnitude of volumetric strain associated with wetting is a function of the mean normal total stress and is independent of principal total stress ratio. However, axial collapse increases and radial collapse decreases with increasing principal total stress ratio for a given mean normal total stress. Using these relationships along with the knowledge of the in-situ horizontal stresses (can be estimated using in-situ testing techniques, such as the pressuremeter test) within an embankment, a more reliable prediction of strain conditions can be obtained (Lawton et al. 1991a).

Pore Fluid Chemistry

Two studies regarding the influence of pore fluid on collapse potential in the literature were conducted by Mellors (1995) and Lawton et al. (1993). Mellors investigated the influence of different pore fluids on the collapse potential of natural deposits of loess with approximately 20 percent clay-size fraction. The researcher's results indicate that specimens flooded with either water or sodium hexametaphosphate solution collapsed by the nearly the same amount with insignificant differences. The specimens flooded with saturated solution of calcium chloride

(with a concentration of calcium ions that is significantly higher than that found in tap water) collapsed slightly less and specimens flooded with inorganic fluids collapsed the least. The influence of pore fluids on collapse potential of soils with higher clay-fractions, however, is unknown. Lawton and his associates report that dilute aqueous solutions of calcium chloride and sodium chloride (calcium and sodium ions are commonly found in tap water) have slight effect on the magnitude of collapse of a clayey sand.

2.5 Mitigation of Collapse Settlement

Compaction Parameters

Extensive research has been performed to reduce collapse by controlling compaction parameters. Proctor (1933) discovered the relationship between maximum dry unit weight and OMC for a compacted soil in his quest for a way to limit the settlement of earth dams when soil becomes completely saturated. Sherard et al. (1963) report that many groups of engineers, including the Army Corps of Engineers, prefer to compact fine-grained soils at or above the OMC to avoid cracks that would develop from differential settlement in earth dams. Lawton (1986) found that significant reductions in collapse potential could be achieved by compacting and maintaining the moisture content wet of the line of optimums. Because collapse potential decreases significantly on or above the line of optimums, McMahon and Kropp (2000) proposed a compaction specification that is based on achieving a minimum degree of saturation represented by the line of optimums.

Critical degree of saturation for a given soil is the prewetting degree of saturation above which negligible collapse potential exists for a given range of relative compaction and overburden pressure (Lawton et al. 1992). Based on a literature survey by Lawton et al. (1992), the critical degree of saturation is typically within 15 percent of degree of saturation represented by the lines of optimums.

Preparing the soil at high levels of relative compaction may reduce collapse. The critical relative compaction is defined as the dry unit weight or relative compaction above which little or

no collapse will occur regardless of moisture conditions; however, it depends on stress level (Lawton et al. 1989). The concept of critical relative compaction exists in both nonexpansive and expansive soils. In expansive soils, collapse potential can be reduced by compacting at a higher dry unit weight, but swelling increases with increasing dry unit weight as shown in Figure 2.2. Therefore, excessive swelling potential can be induced in the soil if compacted to a very high unit weight (Lawton et al. 1989).

Lawton (1986) proposed a compaction specification involving selecting a best combination of placement moisture content and dry unit weight for each fill depth that would result in negligible wetting-induced volume change. Lawton's specification involves applying both the concepts of critical degree of saturation and that of critical relative compaction. The U.S. Bureau of Reclamation constructs large earth dams with soils compacted with varying placement moisture contents with depth to reduce collapse potential (Clevenger 1952). Similarly, Noorany and Stanley (1994) recommend varying placement moisture content and dry unit weight with depth to minimize collapse in large structural fills. Nwaboukei and Lovell (1985), however, believe that such a compaction specification is extremely difficult to achieve in the field.

Chemical Stabilization

Miller et al. (1997) report the successful use of cement kiln dust (CKD) to nearly eliminate the collapse potential for three shales. The single-oedometer samples were placed at dry unit weight corresponding to 95 percent relative compaction, as determined from standard Proctor procedure, with moisture contents dry of the OMC and conducted at two different stress levels of 383 and 1532 kPa. According to the authors, the reduction in collapse potential is attributed to the cementitious properties of the CKD. Likewise, Lawton et al. (1993) found that hydrated calcitic lime and Portland cement are capable of reducing collapse potential of the clayey sand they studied. Even though Miller et al. (1997) and Lawton et al. (1993) did not explicitly mention it in their work, it is possible that the decreased plasticity index of these treated shales may also have contributed to the negligible collapse potential.

Although chemical stabilization appears promising in reducing collapse potential in compacted soils, the potential negative effects of chemical stabilization need to be considered. These include the durability issues of stabilized soils under influence of freezing and thawing and/or wetting and drying cycles, and the potentially harmful reactions between various compounds in the soil and chemical stabilizers (such as, lime-sulfate reactions).

2.6 Time Rate of Collapse

Lawton et al. (1992) and Leonards and Girault (1961) report that typical deformation versus time plots for single-oedometer collapse tests on clayey soils are similar in shape to those obtained from consolidation tests on fine-grained soils as depicted in Figure 2.3. Fredlund and Gan (1995) report similar results on the silty sand and silt they tested. Lawton et al. (1992) point out that three distinct regions of collapse are evident in the deformation versus time plot (see Figure 2.3). Region 1 represents the time required for water to move through the porous stones and enter the sample. In region 2, a majority of collapse takes place as a result of reduction in capillary tension, weakening of clay bridges, and/or softening of macropeds. Collapse is essentially complete in region 3, though some minor creep deformation continues.

Lawton et al. (1992) report that collapse occurs rapidly, usually within several hours or less, in the single-oedometer specimens. Booth (1977) found that the majority of collapse occurred in less than 25 minutes for three sands he tested. Fredlund and Gan (1995) report comparable results on the silty sand and silt they tested. For the lean clay studied by Huang (1989), as cited by Lawton et al (1992), the time for complete collapse was considerably longer, i.e., 4 hours.

Lawton et al. (1992) studied the effect of clay content on rate of collapse from single-oedometer tests using varying proportions of Ottawa sand and kaolin. They found that the time rate of collapse increased with increasing clay-size fraction and collapse occurred in less than 2 hours even for high clay-size fractions. According to these authors, collapse occurs rapidly on wetting at low clay contents because few macropeds are formed. Collapse occurs more slowly at

higher clay contents as a result of the relatively low permeability of the macropeds; as a result, considerably longer time is required for complete softening and distortion of macropeds to take place.

The time required for collapse to occur in the field is related to the process of wetting and the rate of water infiltration (Lawton et al. 1992). Kellner and Rose (1971) report that the collapse settlement of highway embankments subjected to post-construction lake impoundment occurred at nearly the same rate as lake impoundment. On the other hand, for fills not subjected to flooding, settlement may occur over longer periods. Many authors (Brandon et al. 1990, Lawton et al. 1992, Vicente et al. 1994, McMahon and Kropp 2000) report that many structural fills in California subjected to water infiltration from rainfall and landscape irrigation experienced noticeable collapse settlement several years after construction.

2.7 Shale Deterioration

Shales undergo three basic modes of deterioration, according to DiMillio and Strohm (1981). These three modes are (1) deterioration due to chemical weathering (related to breakdown of primary mineral components), (2) physicochemical deterioration (related to clay mineral hydration, swelling, and dispersion), and (3) physical deterioration (related to rock strength). According to Strohm and his associates, the classification of shales according to their long-term durability represents the most critical step in the design of shale embankments. They acknowledge the use of slake durability index, I_d, (as determined from slake durability test) and jar soaking index, I_J, (as determined from jar slake test) to classify the deterioration of shales. These researchers recommend that durable shales ($I_d > 90$ and $I_J = 6$) can be placed as rock fill in thick lifts of 0.6 to 0.9 m and soft shales ($I_d < 60$ and $I_J \leq 2$) need to be placed as soil fill in thin lifts of 0.2 to 0.3 m. Intermediate shales ($I_d = 60$ to 90 and $I_J = 3$ to 5), however, require special treatment such as high relative compaction and effort to prevent wetting.

As noted earlier, shale deterioration due to weathering can lead to a weakening of the soil structure, resulting in settlement sometime after the embankment is completed. This phenomenon

is common to non-durable shales (Strohm et al. 1978). Sherard et al. (1963) claim that non-durable shales do not break down during field compaction; however, these shales deteriorate or soften when they come into contact with water. Strohm et al. (1978) attribute the excessive settlement of many highway shale embankments to deterioration or softening of non-durable shales into clays due to the presence of water.

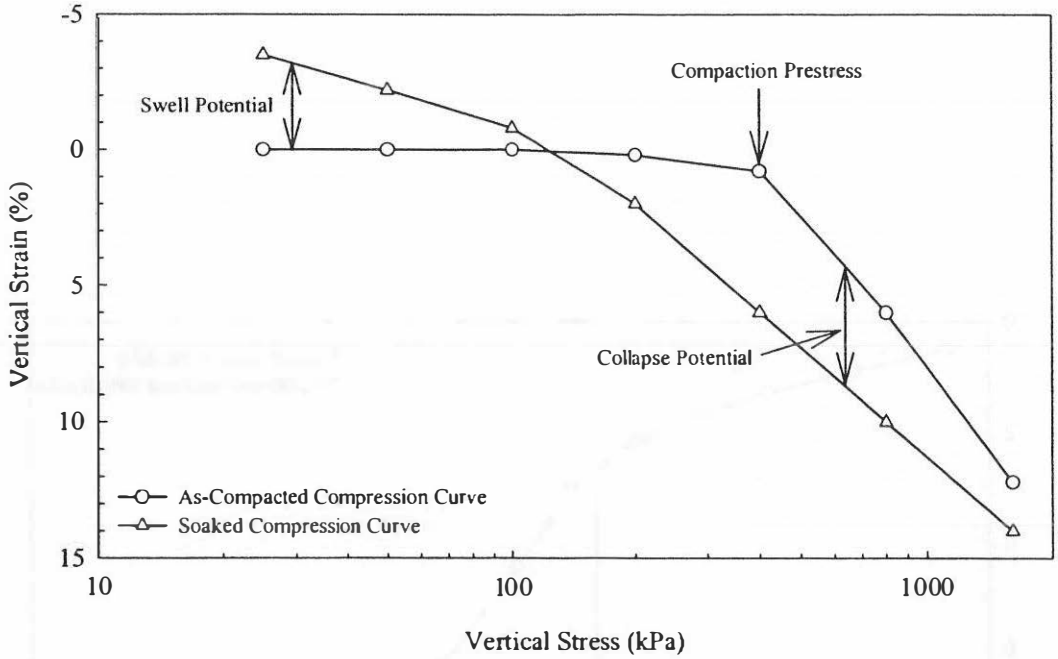

Figure 2.1: Collapse potential as determined from double-oedometer tests (after Lawton et al. 1992)

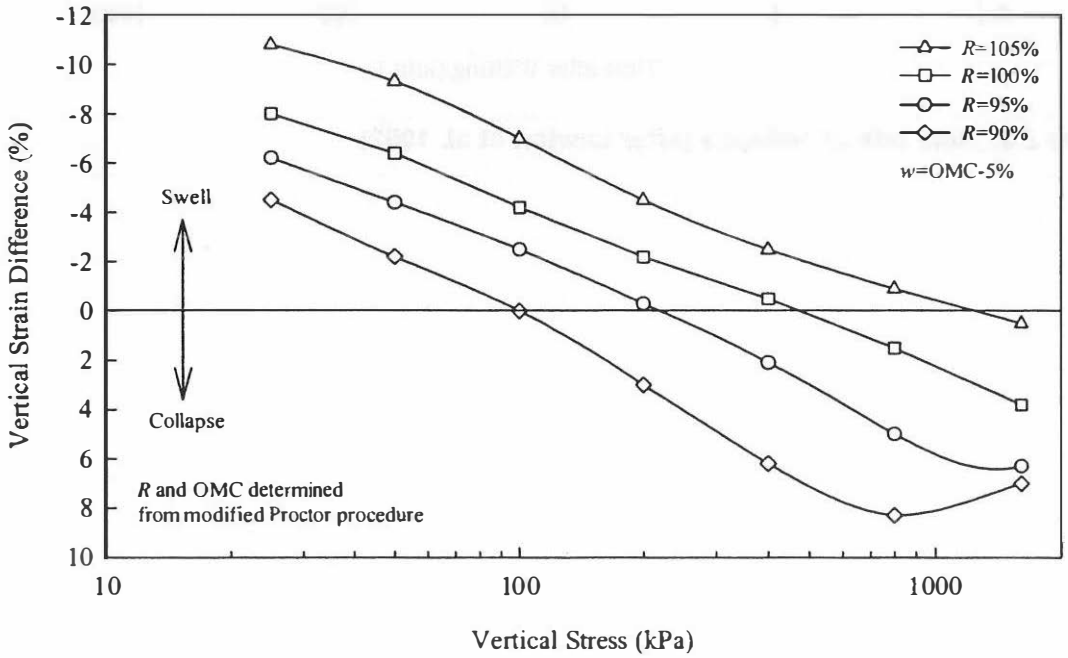

Figure 2.2: Collapse and swelling potential as a function of dry unit weight (after Lawton et al. 1989)

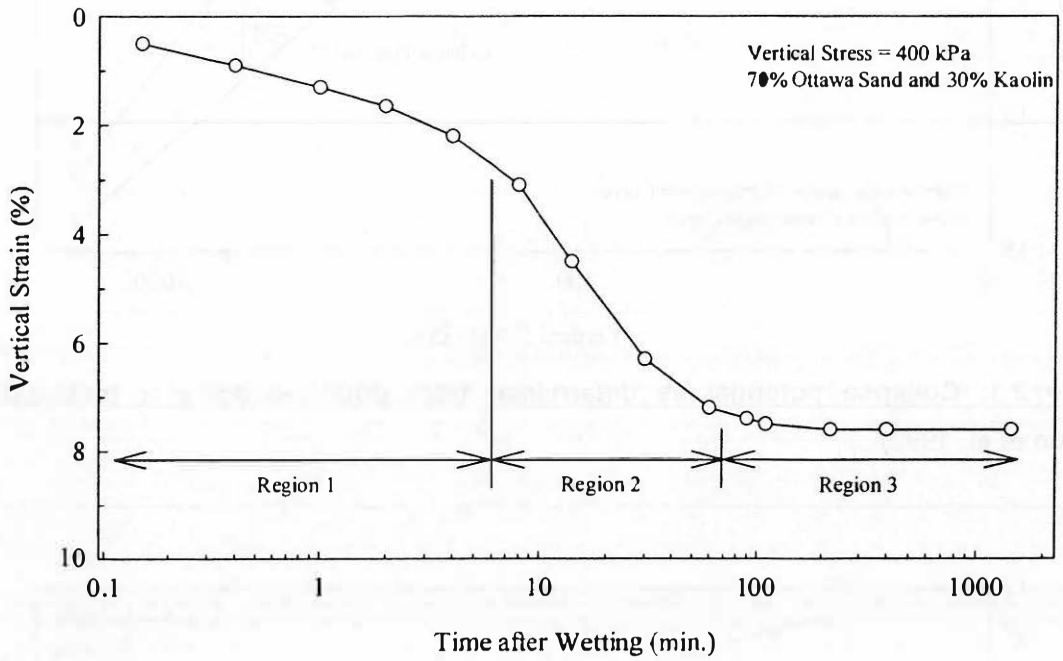

Figure 2.3: Time rate of collapse (after Lawton et al. 1992)

Chapter 3: Oedometer Testing

3.1 Introduction

One-dimensional oedometer tests were conducted on 22 Oklahoma soils and shales to study the potential for self-weight and collapse settlements of Oklahoma soils and shales under conditions typically encountered in compacted fills. Of particular interest was the development of simplified methods for identifying collapse-susceptible soils and predicting collapse settlement of compacted fills. To attain the first goal, single-parameter correlation was established between collapse index and individual soil parameters, and multiple linear regression was performed to correlate multiple soil parameters and collapse index. The empirical correlation can be used to provide a crude estimate of collapse index so as to serve as a basis for screening collapse-susceptible soils. To achieve the second goal, settlement charts were developed to estimate collapse settlement of fills under different conditions, including fill height, moisture content, and soil type. If the correlation and settlement charts suggest that an embankment soil will exhibit significant vertical settlement, then a more detailed settlement analysis of the embankment could be initiated. A detailed description of the test soils, sample preparation, test procedures, test matrix, test results, and experimental variability is presented.

3.2 Test Soils

Soil sampling was conducted such that soils representative of the broad classes of soil types in Oklahoma were obtained. Twenty-two soils and shales, representing many of the AASHTO soil classes, were used in this work. These include seven clays, three low-plastic silts, weathered sandstone, six non-plastic sands, and five weathered shales. A brief description of each test soil and the collection location is given in Table 3.1.

The soils selected for this study were subjected to standard tests, including tests for grain-size distribution (ASTM D 422), Atterberg limits (ASTM D 4318), specific gravity (ASTM D 854), and standard Proctor compaction (ASTM D 698). In addition, shale samples were

subjected to slake durability tests (ASTM D 4644). These tests were performed to classify the soils, characterize the compaction behavior, guide the preparation of oedometer samples, and relate the soil properties to collapse index. Properties of the test soils are listed in Table 3.2.

3.3 Sample Preparation

All the soil required for oedometer samples was prepared by air drying, except for those with low clay content (sands and silts), which were oven dried. Next, samples were pulverized and then passed through a U.S. standard No. 10 sieve. Water was added to the soil and the thoroughly mixed soil was compacted into the oedometer ring in three equal layers to give the required dry unit weight. Tap water was used for all oedometer testing as comparisons between results of tests conducted with de-ionized and tap water showed negligible difference; similar findings were reported by Mellors (1995) and Lawton et al. (1993). Oedometer rings had three different sizes: (1) 63.5 mm diameter × 25.4 mm height, (2) 63.5 mm diameter × 19.1 mm height, and (3) 69.9 mm diameter × 19.1 mm height. Oedometer rings were greased with petroleum gel to reduce side friction. To simulate compaction in the field, laboratory compaction consisted of tamping with a 15.8-mm diameter metal rod to achieve nearly uniform application of compaction energy to the top of each of the three layers. Compaction of each layer was conducted to achieve the desired dry unit weight. After compaction, samples were sealed and left in a humidity chamber overnight.

3.4 Test Procedures

Single-Oedometer Method

The single-oedometer method was the primary tool for evaluating the collapse susceptibility of the test soils. The test procedure followed that suggested by ASTM D 5333, except that tap water was used instead of distilled water. This method consists of loading a sample at its as-compacted moisture content using standard loading increments (load increment ratio of unity) to an applied vertical stress of 200 kPa, allowing the sample to come to equilibrium under the applied stress,

and then inundating the oedometer sample with water. The vertical strain difference or collapse index was determined at the end of a 24-hour period following inundation. To minimize change in specimen moisture content, a loose-fitting plastic membrane was placed over the sample oedometer cell during as-compacted compression.

Double-Oedometer Method

The double-oedometer method, proposed by Jennings and Knight (1957), was conducted to investigate the potential for volume change over a broad range of stress levels. The method requires testing two nominally identical samples. One sample is initially inundated with water under a small seating load and allowed to swell until primary swelling is complete. Next, the sample is loaded in standard increments. The other sample is tested at the as-compacted moisture content using standard incremental loading procedures with the exception that loading increments are only maintained for one hour. The vertical strain difference between the as-compacted and inundated compression curves at a given stress level is assumed to be the collapse or swell potential that would occur in the as-compacted sample if it were loaded to that stress level and then inundated. To minimize changes in moisture content of the as-compacted specimen, a loose-fitting plastic membrane was similarly placed over the sample oedometer cell during as-compacted compression.

The influence of temperature on collapse behavior of soil is unknown; however, it is well recognized that temperature variation can have significant influence on consolidation (Finn 1951, Paaswell 1967). The oedometer tests were conducted under nearly constant room temperature of 22±2 °C.

Both the single- and the double-oedometer methods have their own advantages and hence both were employed in this study. The double-oedometer method can investigate the potential for volume change over a broad range of stress levels. On the other hand, the single-oedometer method more closely mimics the sequence of loading and wetting that occurs under field conditions. Many researchers (Booth 1977, Justo et al. 1984, Lawton et al. 1989, Miller et al.

1997) found that the two methods generally show only small difference in the predicted magnitudes of collapse. Swelling potential, however, was different for each method (Justo et al. 1984, Lawton et al. 1989, Miller 1997). Justo et al. (1984) found that the volume change in the expansion zone depends significantly on the stress at which water was added in the soaked specimen.

3.5 Test Matrix & Sample Designation

The single-oedometer test was conducted on each soil sample prepared at a dry unit weight corresponding to 95 percent relative compaction, as determined from the standard Proctor procedure, and four different moisture contents equal to 4 and 2 percent below the OMC, OMC, and 2 percent above the OMC. Each collapse test was conducted at a vertical stress of 200 kPa. To evaluate test repeatability, single-oedometer tests were performed in triplicate for one soil and in several cases, duplicate tests were performed to investigate unusual results.

The dry unit weight and moisture contents adopted in the preparation of single-oedometer samples correspond to conditions frequently encountered in compacted fills. The ODOT embankment specifications call for compaction to at least 95 percent of the maximum dry unit weight, as determined by standard Proctor procedure, and to moisture content within 2 percent of the OMC. There are provisions to allow for moisture contents up to as much as 4 percent below of the OMC for AASHTO designated A-4 and A-5 soils (silty soils with plasticity index ≤ 10).

The double-oedometer test was conducted to verify the agreement between the two loading-wetting sequences and to provide an estimate of volume change behavior over a broad range of stress levels. These tests were conducted on four soils (Minco Silt, Blaine Shale, Hennessey Shale 1, and Boggy Shale) prepared at 95 percent relative compaction and at a moisture content of 4 percent below the OMC. Double-oedometer tests were performed in triplicate for two soils to evaluate test repeatability and duplicate tests were performed in some cases to investigate unusual results.

Each test was labeled to indicate the type of test (C= single-oedometer collapse, A = as-compacted, S = soaked), molding moisture content, and sample number; therefore, each test identification number has three components. A test identification number that does not bear the sample number represents the average results of replicate samples. For instance, the designation A-4-1 refers to the first sample prepared at a moisture content of 4 percent below the OMC and tested in as-compacted condition.

3.6 Results & Discussion of Single-Oedometer Tests

Results of the single-oedometer test are summarized in Figures A-1 through A-22 of Appendix A. Typical stress-strain plots for the single-oedometer test are given in Figure 3.1 for Vanoss clay. Average values of collapse index at four different moisture contents and degrees of saturation are tabulated in Table 3.3 and summarized in Figures 3.2 and 3.3.

Collapse Index

Referring to figures and table mentioned, several important observations are made as follows:

1. Collapse index varied from 0 to 7.1 percent, which indicates negligible to moderately severe collapse according to the collapse index criteria set forth by ASTM D 5333.
2. Collapse can occur over a wide range of dry unit weights depending on soil type. Dry unit weight alone cannot be used to assess collapse susceptibility because different soils may be stable for different ranges of dry unit weight, stress state, and moisture condition.
3. Satisfying the dry unit weight criterion alone (i.e. relative compaction) is not sufficient to prevent collapse settlement in compacted soils because compaction moisture content has a significant influence on collapse potential.
4. Cohesionless soils compacted within ODOT embankment specifications are not collapse-susceptible. Thus, they are ideal fill materials for embankments. Most cohesionless soils employed in this study are classified under the AASHTO designated A-1, A-2, and A-3 groups, which are generally regarded as being satisfactory for embankment construction according to the AASHTO standard. Gracemore Sand 4 and Slaughterville Sand fall into the

AASHTO designated A-4 group, yet are not collapse-susceptible because of their cohesionless nature.

5. Slightly cohesive silty soils from the AASHTO designated A-4 group, which excludes Gracemore Sand 4 and Slaughterville Sand, compacted within ODOT embankment specifications exhibited a slight degree of collapse (with collapse index of less than 2 percent). However, for large embankments 1 to 2 percent of collapse strain can result in significant settlement. Thus, the categorization of collapsible soils according to collapse index given in ASTM D 5333 should be applied with care.
6. Clayey soils from the AASHTO designated A-6 and A-7 groups showed the greatest collapse index in the range of 0.5 to 7.1 percent. Such soils are generally regarded as being less desirable for embankments; therefore, special attention should be given to the design and construction of embankments using clayey soils.
7. Generally, collapse index decreases nearly linearly with increasing moisture content for the given relative compaction of 95 percent. Depending on soil type, reduction in collapse index with increasing moisture content varied from negligible in cohesionless soils to substantial in clays, as indicated by the slope of the first-order regression lines in Figures 3.2 and 3.3. Some test results exhibited slight deviation from this general trend; exceptions are noted for cohesionless sands with low collapse index.

   As discussed in Section 2.3, the reduction of collapse index with increasing compaction moisture content for cohesive soils is due macroped softening and lower matric suction that developed at higher moisture contents. Also, a reduction in collapse index may result because the wetter and more compressible as-compacted soil has already experienced significant amounts of load-induced compression before inundation and hence an increased dry unit weight before inundation as generally indicated in Table 3.3.
8. For some soils, generally those with higher plasticity index, collapse index is significant at, and wet of the OMC.

9. Slake durability index, as determined from slake durability tests on four test shales, did not correlate with collapse index. Slake durability test was not performed on Hennessey Shale 2 because no intact shale fragments could be obtained. Slake durability index varied from 5.4 to 29.1 percent for the shales investigated, which are classified as soft non-durable according to the slake durability index criteria suggested by Strohm et al. (1978). Because slake durability test measures the durability of intact shale fragments, it is believed that the breaking down of the shales to a soil-like consistency prior to compaction accounts for the lack of correlation between slake durability index and collapse index.

Statistical Correlation

To enable screening for a potential embankment soil with regard to collapse susceptibility, single-parameter correlation was established between collapse index and individual soil parameters. In addition, multiple linear regression was performed to correlate multiple soil parameters and collapse index. These empirical relationships were developed from a database of 88 single-oedometer test combinations representing 22 soils prepared at 95 percent relative compaction and four different moisture contents.

Single-parameter correlation reveals that collapse index increases with increasing plasticity index, liquid limit, activity, and clay-size fraction for a given molding moisture content and compaction effort. A plot of collapse index versus plasticity index is depicted in Figure 3.4. A complete set of such plots is included in Figures A-23 through A-25 of Appendix A for the remaining soil parameters. The demonstrated trend of increasing collapse index with increasing clay-size fraction for compacted soils reported in this study further supports the model based on artificially mixed soil in which increased collapse index is correlated with an increase in clay-size fraction (Steadman 1987, Alwail et al. 1994). The increase of collapse index with increasing clay-size fraction could be related to the increased number of macropeds and higher matric suction developed with greater clay-size fraction. Greater swelling could result from the increased clay-size fraction at low stress levels; however, such swelling is probably out-weighed

by the increased softening and distortion of the macropeds at high stress levels, so the net result is an increase in collapse index (Lawton et al. 1992). In addition, greater clay-size fraction results in higher matric suction for a given moisture content and hence greater collapse (Rao and Revanasiddappa 2000). The increase of collapse index with increasing plasticity index, liquid limit, and activity can be explained in the same manner, as these parameters are indicators of fine composition (type and amount of clay minerals).

The AASHTO group index that is widely used in determining the quality of soil material for use in soil structures correlates fairly well with collapse index. Group index reflects the plasticity index, liquid limit, and clay-size fraction of the soil. Collapse index increases with increasing value of group index for a given molding moisture content and compaction effort, as shown in Figure 3.5. As expected, plasticity index, liquid limit, and clay-size fraction exhibited fairly reasonable correlation with one another as illustrated in Figure 3.6. The single-parameter correlation between collapse index and various soil parameters indicates that factors related to fine composition can be used for preliminary assessment of collapsible compacted soils.

Multiple linear regression analysis was performed on the same database using a commercially available statistics software package, Statistical Analysis System (SAS), to develop a predictive model for collapse index. The predictive model was obtained through the backward elimination technique and has a coefficient of determination, r^2 of 0.76. The collapse index (I_e) is described in terms of compaction moisture content (w), dry unit weight (γ_d), plasticity index (PI), and clay-size fraction (C), and is given as:

$$I_e\,(\%) = 9.805 - 0.261\ w\,(\%) - 0.424\,\gamma_d\,(\mathrm{kN/m^3}) + 0.0580\ PI + 0.0697\ C\,(\%) \qquad (1)$$

The beauty of this model is that only easily obtained soil parameters are required and the model encompasses the range of moisture contents from 4 percent dry to 2 percent wet of the OMC. The advantage of the predictive model, over the single-parameter correlation, is that the influence of moisture content on collapse index can be investigated. On the other hand, the

single-parameter correlation has the advantage of predicting collapse index using a single soil parameter. As with any empirical correlation, those presented here may be specific to the conditions for which they were developed. Specifically, they are generally applicable to compacted natural soils prepared at 95 percent relative compaction, having range of moisture contents from 4 percent dry to 2 percent wet of the OMC, and following similar oedometer testing procedures.

Significant scatter in the data is observed in the correlation. This can be partly explained by the dependence of collapse index on many interacting factors, including environmental factors (moisture content, unit weight, soil structure, and stress level) and composition factors (fine composition and pore fluid chemistry). Also, experimental variability may have contributed to the scatter. Analysis of the replicated tests indicates that variability in collapse index increases with soil plasticity; average and maximum differences in collapse index for duplicated tests are 0.6 and 1.5 percent, respectively. In the single-parameter correlation, the r^2 consistently decreases with increasing compaction moisture content for all cases. This suggests a lower dependence of collapse index on soil type at higher compaction moisture contents.

As-Compacted Compressibility

Referring to the stress-strain plots given in Figure 3.1 and others in Appendix A, three important observations are made, as follows:

1. With few exceptions for cohesive soils, the as-compacted compressibility prior to inundation at a vertical stress of 200 kPa is greater for samples with higher moisture content. A notable increase in compressibility is recognized for samples compacted at a moisture content 2 percent above the OMC. Such a trend can be explained by the difference in soil structure and the values of matric suction as described in Section 2.3.
2. In general, specimens prepared at a moisture content 4 percent dry of the OMC had comparable compressibility at stress levels less than 200 kPa regardless of soil type, as evidenced from the portion of as-compacted compression curve prior to inundation.

Compressibility at higher moisture content, on the other hand, varied over a wider range and is observed to depend on soil type, which is consistent with the findings of the U.S. Bureau of Reclamation as cited by Sherard et al. (1963). Specifically, cohesive soils generally exhibit greater compression compared to cohesionless soils at higher moisture contents.

3. No visible trend is observed regarding the influence of moisture content on the compressibility of the cohesionless specimens. One possible explanation is that matric suction changes are less significant for cohesionless sands. Therefore, the 6 percent change in moisture content encompassed in this study is likely too small to produce any significant change in matric suction that would influence the compressibility of these samples.

Time Rate of Collapse

Plots of vertical strain versus time for each test are given in Figures A-26 through A-33 of Appendix A. Typical plots for cohesionless and cohesive soils are given in Figures 3.7 and 3.8, respectively. Referring to these figures, several important observations are made as follows:

1. Time rate of collapse for cohesionless soils is faster than that of cohesive soils.
2. Collapse occurs quickly in cohesionless soil samples with majority of collapse occurring in less than 30 minutes.
3. Comparing different cohesive soils, there is a significant difference in time required for complete collapse. Some cohesive soils (Hennessey Shales I and 2, Wellington Shale, Boggy Shale, Heiden Clay, and Dennis Clay) require considerably longer times, up to 24 hours, to complete collapse.
4. Shapes of vertical strain versus time for all soils, except the six cohesive soils exhibiting a slower rate of collapse, are generally similar at all the moisture conditions investigated. They are similar in shape to those obtained from consolidation tests on fine-grained soils; in short, they have a Type I shape, as described by Leonards and Girault (1961).
5. The shape of the vertical strain versus time plots changes considerably with molding moisture content for the six cohesive soils exhibiting a slower rate of collapse. As shown in Figure

3.8, significant time lags between initial inundation and subsequent collapse are observed in Heiden Clay compacted on the dry side of the OMC. The wet-side sample, however, did not exhibit such behavior.

The reasons for the delay of collapse in these samples are thought to be a result of the reduced permeability of the dry-side sample. The specimen prepared at a lower moisture condition possessed a lower degree of saturation and hence, a lower coefficient of permeability when compared with a sample prepared at higher moisture content. The reduced permeability outweighs the increase in the suction gradient at the wetting front and hence, resulted in lower flow velocity in the drier sample.

To substantiate this hypothesis, moisture contents were taken at different times during inundation at 200 kPa vertical stress for three replicated Heiden Clay oedometer specimens prepared at 95 percent relative compaction and a moisture content 4 percent dry of the OMC. Visual inspection of the dissected samples and moisture content measurements indicated that the wetting front did not move significantly far into the core for samples that were submerged in water for 30 and 260 minutes of soaking. Moisture content measurements for soaking at 30, 260, and 1800 minutes were 18.9, 21.6, and 25.4 percent, respectively. This simple test tends to substantiate that time rate of collapse for the cohesive soil is related to the unsaturated permeability of the soil specimens.

Time Rate of As-Compacted Compression

The time rate of compression for one soil, i.e., Hennessey Shale 1, at four different moisture contents (including 4 and 2 percent below the OMC, OMC, and 2 percent above the OMC) was analyzed. A complete set of results for all moisture levels is included in Figures A-34 through A-36 of Appendix A. Typical time rate of compression plot for OMC+2 percent moisture level is given in Figure 3.9 for Hennessey Shale 1.

Results show that a large portion of compression takes place upon initial application of load. After the initial rapid compression, little further compression can be observed. As the

degree of saturation for these samples are below 85 percent (see Table 3.3), Yoshimi (1958) attributed such a rapid rate of compression to the outflow of pore air. The subsequent negligible compression, according to Yoshimi, is due to the dissipation of residual pore air pressure and rearrangement of soil aggregates.

Figure 3.10 shows the relative compression versus time at different moisture conditions. Relative compression is defined as the compression at a given time divided by total compression at 60 minutes. It is interesting to note that the relative compression curves at different moisture conditions are virtually the same. DiBemardo and Lovell (1980) suggested that such phenomena occur if the air voids are interconnected. The practical significance of these data is that the settlement due to as-compacted compressibility is likely to be achieved during the construction period if the air voids are interconnected (DiBernardo and Lovell 1980).

Two important observations are made based on plots of relative compression at various stress levels versus time, as given in Figure 3.11 and others in Appendix A:

1. The relative compression at any given time increases with increasing stress level.
2. Significant increases in relative compression with increasing stress level are observed at early times; with increasing time, however, relative compression increases are lower with increase in stress level. This is possible because the dissipation of residual pore air pressure and rearrangement of aggregates occurred quickly at lower stress levels.

3.7 Results & Discussion of Double-Oedometer Tests

Results of double-oedemeter tests for selected soils are given in Figures A-37 through A-40 of Appendix A. A typical result from a double-oedometer collapse test is given in Figure 3.12, and a comparison of collapse index from single- and double-oedometer tests is shown in Figure 3.13. Several important observations are made as follows:

1. Single- and double-oedometer collapse potentials are in reasonably good agreement for the soils tested as shown in Figure 3.13. Therefore, single- and double-oedometer test results can be used interchangeably with confidence in the collapse region.

2. Double-oedometer data indicate that Minco Silt does not exhibit swelling behavior, as expected for silt. On the other hand, double-oedometer data for Hennessey Shale, Boggy Shale, and Blaine Shale show swelling at low pressures in addition to collapse at higher pressures, as expected for moderately plastic clayey soils. The transition from swelling to collapse occurs at a vertical stress where the as-compacted and soaked compression curves diverge. Observing the double-oedometer curves given in Appendix A, this point is between 50 and 100 kPa for the clayey soils tested in the current research.
3. Double-oedometer data for all samples exhibit a maximum collapse potential at the compaction prestress; beyond the maximum, the collapse potential decreases with increasing vertical stress.
4. The compaction prestress is between 400 and 600 kPa for the soils tested at 95 percent relative compaction and a moisture content of 4 percent dry of the OMC. At applied stresses less than the compaction prestress, samples compacted at the dry side of the OMC are relatively incompressible. Once applied stress increased above the level of compaction prestress, samples underwent significant deformation. In a practical sense, soil compacted at the dry side of the OMC is relatively incompressible under typical embankment loading conditions, i.e., below the maximum vertical stress of 400 kPa typical at the base of a 20-m high embankment.
5. Allowing soil to take up water, whether swelling takes place or not, reduces the compaction prestress. Soaked prestress is less than the compaction prestress in all cases.

3.8 Charts for Preliminary Settlement Estimates

Collapse index is a useful indicator of a soil's susceptibility to collapse settlements; however, it can be misleading for judging the magnitude of collapse settlements in fills. For example, in the ASTM D 5333 standard, a collapse index of 2 percent would be classified as slight and may suggest to the engineer that collapse settlements will be insignificant. Yet, a 2 percent vertical strain over a 10-m thick fill would cause a settlement of 0.2 m, which is significant. While

classification criteria in ASTM D 5333 may be reasonable for modestly thick fills, a more useful way to assess the importance of collapse would be to predict collapse settlement taking into account the fill or embankment height.

Two problems exist with regard to predicting collapse settlements in embankments using results of single-oedometer tests. First, stress conditions in embankments are not one-dimensional and second, a single-oedometer test gives the collapse potential at one level of stress. These problems can be addressed in different ways that vary in complexity. At the most complex level, a finite element analysis incorporating soil models that capture collapse behavior may be most appropriate but impractical for everyday practice. This approach would likely require sophisticated laboratory testing, beyond the simple oedometer tests, to determine constitutive model parameters. Another less complex approach would be to predict vertical stresses below the embankment centerline using available elastic solutions (e.g. Poulos and Davis 1974) and combine these with laboratory collapse test data from oedometer tests. This approach would be similar to using oedometer test results and stress distribution theory for predicting footing settlements, and would therefore likely suffer from the same shortcomings. At the simplest level, one could assume that one-dimensional conditions exist below the embankment centerline (i.e., vertical stress equals unit weight times depth below embankment centerline) and simply perform a one-dimensional settlement analysis using oedometer collapse test data. All of these approaches require knowledge of wetting-induced volume change behavior over the range of stresses encountered in the embankment, which necessarily requires multiple single-oedometer tests or double oedometer tests.

To further exploit the collapse test database presented previously, a simple method was used to produce collapse settlement curves for one-dimensional fills of various heights and having different soil characteristics. The curves shown in Figure 3.14 allow for a simple prediction of collapse settlement below a one-dimensional fill based on soil plasticity index, moisture condition relative to the OMC, and fill height. Such curves are intended to give

engineers a simple tool for quickly assessing whether collapse settlements are likely to be problematic, thus possibly warranting further laboratory testing (such as collapse tests), more in depth analysis, design modifications and increased quality control measures.

A number of assumptions are encompassed in the settlement curves presented in Figure 3.14. Assumptions and analysis involved are described below.

1. Collapse strain is assumed to increase linearly with the logarithm of vertical stress from the point at which the as-compacted and soaked compression curves diverge up to the compaction prestress as shown in Figure 3.15. Beyond the compaction prestress the collapse potential is assumed to be constant. These critical points, designated A and C in Figure 3.15, appear to be dependent on soil characteristics; however, given the limited double-oedometer data available for soils in the database, the values at A and C are assumed to be 70 kPa and 400 kPa, respectively. Within the range of values observed for these points from double-oedometer tests, a sensitivity analysis showed that these assumptions are reasonable and conservative in most cases for embankments less than 20 m in height. Further research is being conducted to better define points A and C for different soils.
2. Collapse index estimates obtained from the single-parameter correlation equation for plasticity index (see Figure 3.4) are used to define the collapse strain at 200 kPa, designated point B in Figure 3.15.
3. Complete wetting is assumed and swelling is ignored in the development of the settlement curves.
4. Only, collapse settlement is considered. Settlements due to embankment self-weight at constant moisture content are not included.

In reality, stress and strain conditions below the embankment centerline are not one-dimensional. However, this assumption is more correct at the center of long, wide embankments with shallow side slopes as compared to short ones with a narrow crest width and steep side slopes. Elastic solutions for embankment stresses suggest that one-dimensional stress conditions

are roughly approximated at the centerline of embankments with modest crest widths (Poulos and Davis 1974). If one assumes that one-dimensional conditions are roughly approximated below the centerline of an embankment, then a crude estimate of embankment settlement can be obtained using Figure 3.14.

3.9 Experimental Variability

The experimental variability of the oedometer test is quantified based on comparisons of collapse index, soaked compression curves, and as-compacted compression curves from nominally identical samples. In general, the test results are rather variable for the cohesive soils based on collapse strain difference of replicate tests. Generally, a maximum collapse strain difference of 1.5 percent can be expected for cohesive soils. Replicate samples showing such a magnitude of collapse strain difference are Bosville Clay, Lomill Clay, Bethany Clay, and Dennis Clay. A large vertical strain difference of 3.2 percent was measured at a stress level of 1600 kPa in soaked compression curves of three replicate Minco Silt specimens. Because this series of tests was conducted in the early part of the research, they are considered anomalous. Unlike the cohesive soils, less deviation, in terms of strain difference of replicate tests, is observed in the collapse potential of cohesionless soils.

A possible cause of data scatter includes inherent variability in sample preparation and resulting non-homogeneous samples. Slight deviation from the target moisture content and dry unit weight may have notable influence on the compressibility and collapse potential of soils. As discussed in Section 2.4, the compressibility and collapse potential of compacted soils are dependent on the void ratio and degree of saturation. The non-homogeneity of samples probably resulted from an unevenly distributed loose soil before tamping and non-uniform application of compaction energy to the top of each layer. As small clods were present in the soil mixture, and with each layer being very thin, uniform distribution of the loose soil can be a formidable task. In addition, uniform application of compaction energy is difficult when a small diameter rod is utilized for tamping, because the operator can inadvertently compact one side more than the

other. Visual inspection performed at the end of each test indicated that some cohesive specimens were tilted. This suggests the presence of non-uniformity in some samples.

Vibrations generated during handling can alter the dry unit weight of cohesionless samples, and may account for the scatter in test results. Because samples have to be assembled in the oedometer cell and later into the oedometer, vibrations generated during assembling are inevitable. Other possible causes of variability include instrumentation error and inherent inaccuracies in measurements.

Table 3.1: General characteristics of the test soils

Soil	General characteristics	Location
Gracemore Sand 1 [a]	Light brown, alluvial soil	NW/4 of Section 18, T8N, R2W, Cleveland County (Norman)
Gracemore Sand 2	Light brown, alluvial soil	NW/4 of Section 18, T8N, R2W, Cleveland County (Norman)
Gracemore Sand 3 [a]	Light brown, alluvial soil	NW/4 of Section 18, T8N, R2W, Cleveland County (Norman)
Gracemore Sand 4 [a]	Light brown, alluvial soil	NW/4 of Section 18, T8N, R2W, Cleveland County (Norman)
Vanoss Sand	Reddish-brown, residual soil	SW/4 of Section 5, T8N, R2W, Cleveland County (Norman)
Darnell Sandstone	Very pale-brown, weathered sandstone	Section 27, T3N, R8E, Pontotoc County (Lula)
Slaughterville Sand	Brown, residual soil	SW/4 of Section 35, T9N, R3W, Cleveland County (Norman)
Minco Silt	Brown, residual soil	Grady County (Tuttle)
Blaine Shale	Brown, weathered shale	---
Grainola Silt	Dark brown, residual soil	SW/4 of Section 33, T9N, R2W, Cleveland County (Norman)
Teller Silt	Dark brown, residual soil	SW/4 of Section 6, T8N, R2W, Cleveland County (Norman)
Hennessey Shale 1	Red, weathered shale	I-35 just south of the Canadian River, Oklahoma City
Hennessey Shale 2	Red, weathered shale	NW/4 of Section 14, T9N, R3W, Cleveland County (Norman)
Vanoss Clay	Dark brown, residual soil	SW/4 of Section 5, T8N, R2W, Cleveland County (Norman)
Doolin Clay	Dark grayish-brown, residual soil	SE/4 of Section 23, T9N, R3W, Cleveland County (Norman)
Wellington Shale	Dark gray, weathered shale	---
Boggy Shale	Light olive, weathered shale	---
Bethany Clay	Pale brown, residual soil	SW/4 of Section 6, T8N, R2W, Cleveland County (Norman)
Heiden Clay	Olive-gray, residual soil	Choctaw County (Highway 70)
Lomill Clay	Dark brown, residual soil	SW/4 of Section 21, T9N, R3W, Cleveland County (Norman)
Bosville Clay	Light brown residual soil	---
Dennis Clay	Olive-gray, residual soil	---

[a]Gracemore Sands 1, 3, and 4 are artificially mixed from Gracemore Sand 2.

Table 3.2: Properties of the test soils

Soil	AASHTO class.	USCS class.	Specific gravity	Liquid limit	Plasticity index	Fines (%)	Clay-size Fraction (%)	Activity	Max. dry unit wt. (kN/m^3)	OMC (%)	Slake durability index
Gracemore Sand 1	A-1-b (1)	SW-SM	2.65	NP	NP	10	---	---	17.8	9.6	---
Gracemore Sand 2	A-3 (1)	SP	2.65	NP	NP	2	---	---	16.5	8.8	---
Gracemore Sand 3	A-3 (1)	SW-SM	2.65	NP	NP	9	---	---	17.8	10.3	---
Gracemore Sand 4	A-4 (0)	SM	2.66	NP	NP	37	---	---	16.4	14.5	---
Vanoss Sand	A-2-4 (0)	SM	2.68	NP	NP	31	10	---	19.4	8.6	---
Darnell Sandstone	A-3 (1)	SP	2.68	NP	NP	4	---	---	16.7	14.0	---
Slaughterville Sand	A-4 (0)	SM	2.67	NP	NP	39	15	---	18.8	11.1	---
Minco Silt	A-4 (4)	CL	2.68	28	8	73	15	0.53	17.7	14.6	---
Blaine Shale	A-4 (7)	CL	2.81	28	10	84	32	0.32	17.2	17.6	5.4
Grainola Silt	A-4 (8)	CL	2.72	31	9	88	24	0.39	17.1	15.0	---
Teller Silt	A-4 (5)	CL	2.71	32	10	69	25	0.40	17.6	14.8	---
Hennessey Shale 1	A-6 (13)	CL	2.81	34	13	97	51	0.25	16.8	19.6	29.1
Hennessey Shale 2	A-6 (14)	CL	2.81	33	15	96	38	0.39	17.4	15.5	---
Vanoss Clay	A-6 (17)	CL	2.73	40	25	76	30	0.82	17.2	16.8	---
Doolin Clay	A-7-6 (33)	CH	2.75	52	34	92	37	0.92	15.6	20.8	---
Wellington Shale	A-7-6 (18)	ML	2.84	47	19	86	44	0.44	15.9	22.0	24.9
Boggy Shale	A-7-6 (24)	CL	2.82	45	24	94	48	0.50	16.5	17.0	15.2
Bethany Clay	A-7-6 (31)	CH	2.77	53	34	87	44	0.78	16.5	18.6	---
Heiden Clay	A-7-6 (39)	CH	2.83	63	36	94	57	0.63	15.6	19.4	---
Lomill Clay	A-7-6 (47)	CH	2.82	70	43	95	68	0.63	14.6	25.3	---
Bosville Clay	A-7-6 (15)	CL	2.72	41	26	67	37	0.70	16.8	15.7	---
Dennis Clay	A-7-6 (34)	CH	2.75	51	32	97	49	0.65	16.3	19.4	---

Table 3.3: Average value of collapse index, degree of saturation, and dry unit weight at different molding moisture conditions

Soil	Collapse Index (%)				Initial Degree of Saturation (%)				Initial Dry Unit Wt./ Prior to Inundation Dry Unit Wt. (kN/m^3)			
	-4%	-2%	0%	+2%	-4%	-2%	0%	+2%	-4%	-2%	0%	+2%
Gracemore Sand 1	0.1	0.2	0.2	0.2	29	40	51	59	16.8 / 17.1	16.9 / 17.2	17.1 / 17.5	17.0 / 17.3
Gracemore Sand 2	0.1	0.2	0.1	0.0	18	27	35	42	15.3 / 15.4	15.4 / 15.5	15.6 / 15.7	15.5 / 15.6
Gracemore Sand 3	0.2	0.3	0.2	0.1	33	42	49	63	16.8 / 17.0	16.9 / 17.2	16.8 / 17.0	16.9 / 17.1
Gracemore Sand 4	0.3	0.4	0.2	0.5	44	51	57	65	15.4 / 15.6	15.4 / 15.7	15.2 / 15.4	15.3 / 15.5
Vanoss Sand	0.5	0.4	0.3	0.1	29	40	53	67	18.2 / 18.4	18.0 / 18.1	18.2 / 18.3	18.4 / 18.6
Darnell Sandstone	0.2	0.1	0.1	0.1	40	48	57	65	15.9 / 16.1	15.9 / 16.1	15.8 / 16.0	15.9 / 16.0
Slaughterville Sand	0.5	0.3	0.1	0.2	41	52	63	75	17.5 / 17.7	17.7 / 17.9	17.7 / 17.9	17.9 / 18.1
Minco Silt	1.5	0.5	0.4	0.1	52	60	70	79	16.7 / 17.0	16.9 / 17.1	17.1 / 17.4	16.9 / 17.4
Blaine Shale	2.5	2.5	0.9	0.4	55	64	73	81	16.2 / 16.4	16.3 / 16.5	16.2 / 16.5	16.3 / 16.8
Grainola Silt	1.7	1.0	0.5	0.7	48	55	63	72	16.1 / 16.2	16.2 / 16.4	16.1 / 16.4	16.3 / 16.6
Teller Silt	0.9	0.5	0.2	0.2	48	58	68	79	16.4 / 16.5	16.4 / 16.6	16.6 / 16.8	16.8 / 17.1
Hennessey Shale 1	2.4	1.9	1.3	0.8	61	69	76	84	16.0 / 16.1	16.0 / 16.2	16.0 / 16.2	16.0 / 16.4
Hennessey Shale 2	4.1	3.7	2.8	2.2	48	56	68	75	16.4 / 16.6	16.6 / 16.7	16.6 / 16.7	16.8 / 17.2
Vanoss Clay	2.9	2.8	1.4	0.5	58	67	74	83	16.6 / 16.8	16.5 / 16.7	16.5 / 16.8	16.6 / 17.1
Doolin Clay	5.3	3.5	1.4	1.0	59	66	73	80	15.1 / 15.4	15.3 / 15.8	15.5 / 16.1	15.0 / 15.6
Wellington Shale	4.0	2.5	2.5	1.7	61	67	73	79	15.1 / 15.3	15.1 / 15.3	15.2 / 15.4	15.2 / 15.4
Boggy Shale	6.9	7.1	5.1	4.2	48	56	64	72	15.6 / 15.8	15.6 / 15.8	15.6 / 15.8	15.6 / 16.0
Bethany Clay	4.9	4.6	2.8	1.7	55	63	70	78	15.5 / 15.6	15.7 / 15.9	15.7 / 15.9	15.7 / 16.0
Heiden Clay	5.6	4.9	4.7	3.2	50	54	65	72	14.7 / 15.0	14.8 / 15.0	14.9 / 15.2	14.8 / 15.1
Lomill Clay	4.0	3.9	3.1	2.5	59	65	73	80	14.0 / 14.2	13.8 / 14.1	13.8 / 14.1	13.9 / 14.5
Bosville Clay	4.6	4.1	3.8	3.4	47	57	63	73	15.9 / 16.0	16.0 / 16.1	16.0 / 16.2	16.1 / 16.4
Dennis Clay	6.0	5.7	3.2	2.1	55	62	70	79	15.5 / 15.7	15.3 / 15.5	15.5 / 15.7	15.6 / 16.0

Note: Percentages above each column represent moisture content difference relative to the OMC, i.e., OMC-4%, OMC-2%, OMC, and OMC+2%.

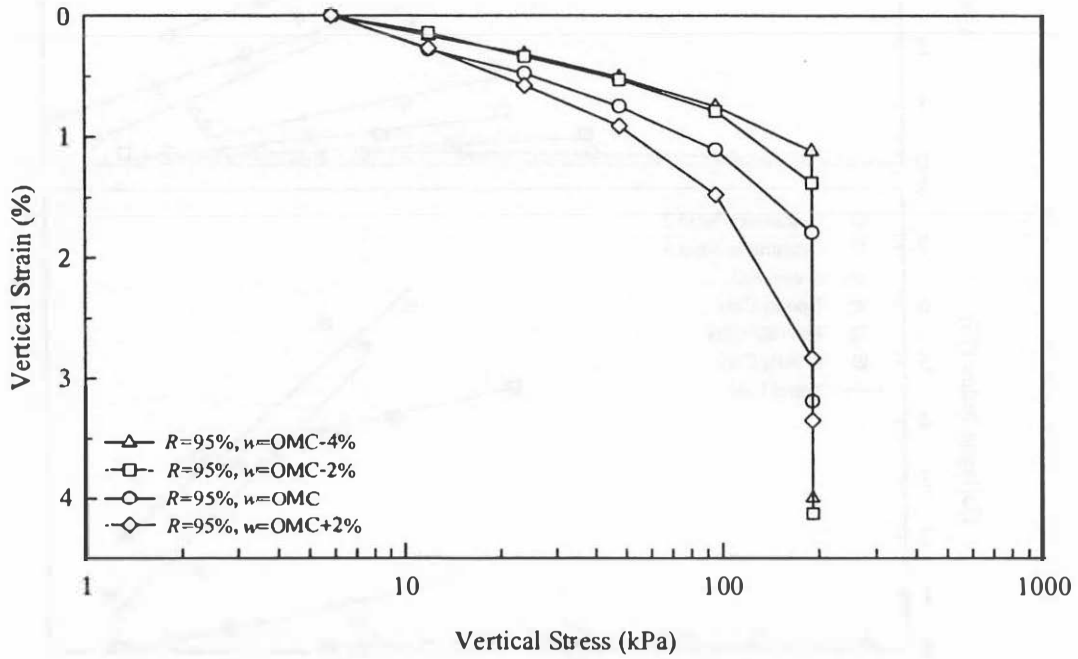

Figure 3.1: Results of single-oedometer tests for Vanoss Clay

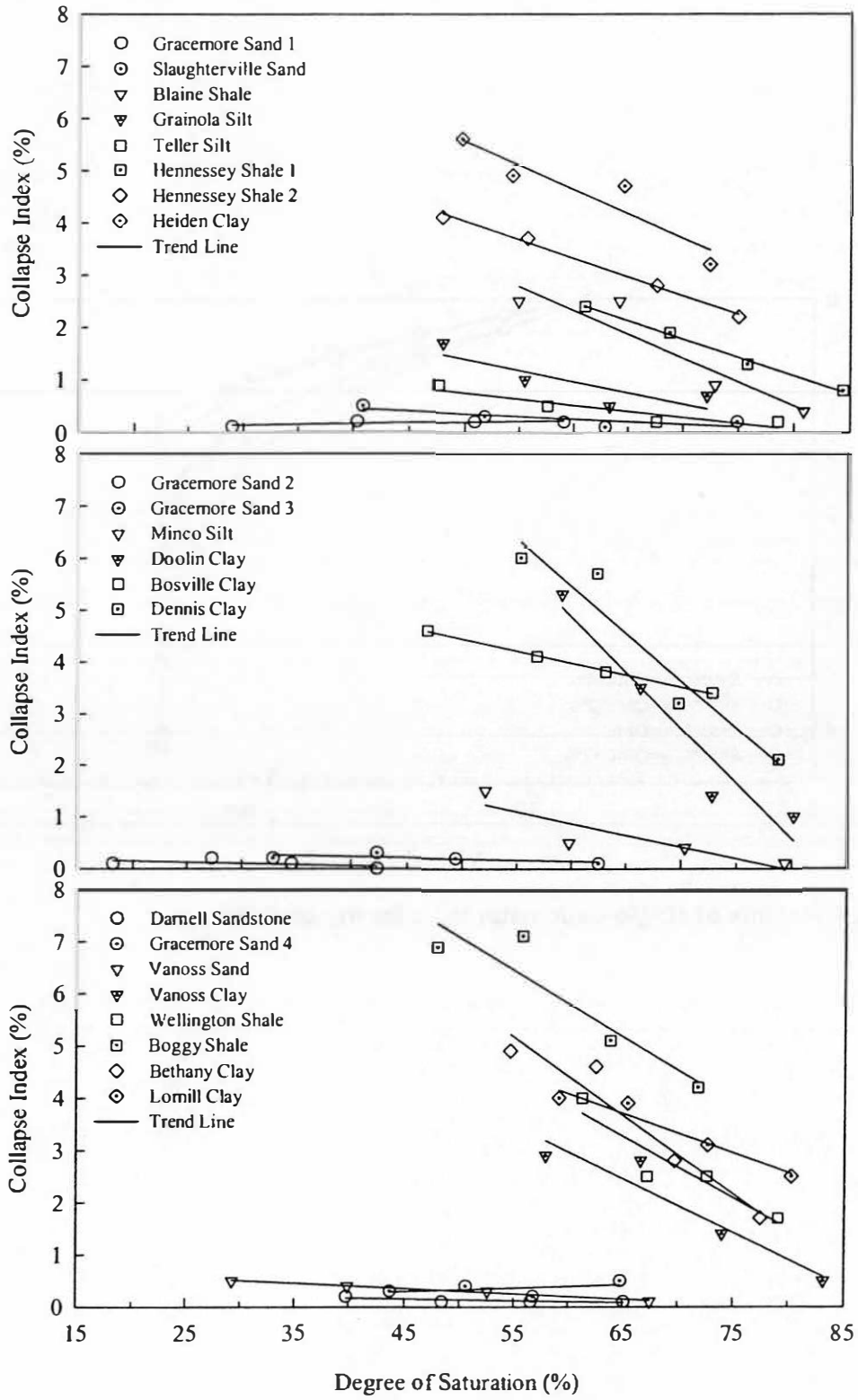

Figure 3.2: Average value of collapse index versus initial degree of saturation

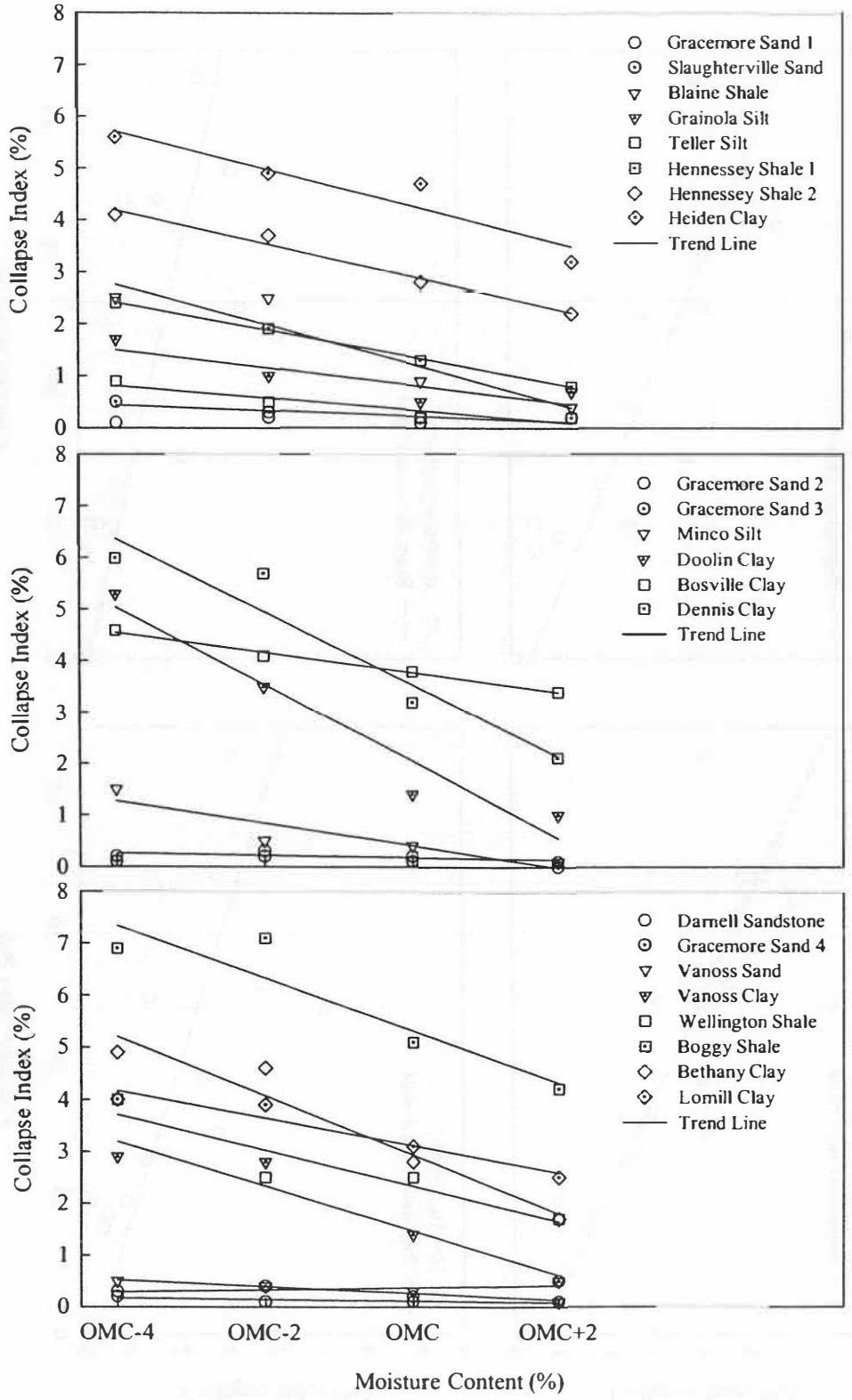

Figure 3.3: Average value of collapse index versus initial moisture content

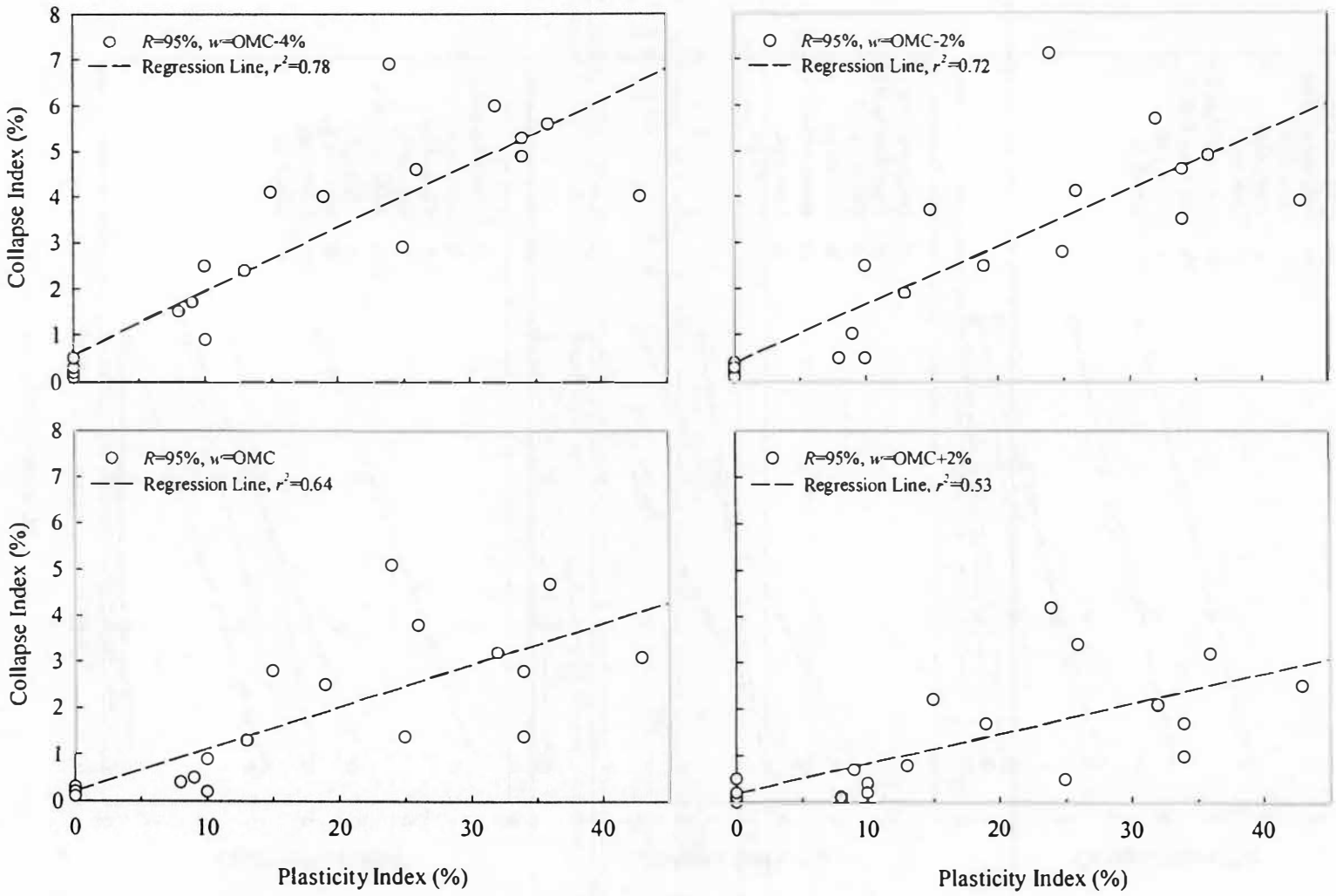

Figure 3.4: Average value of collapse index versus plasticity index

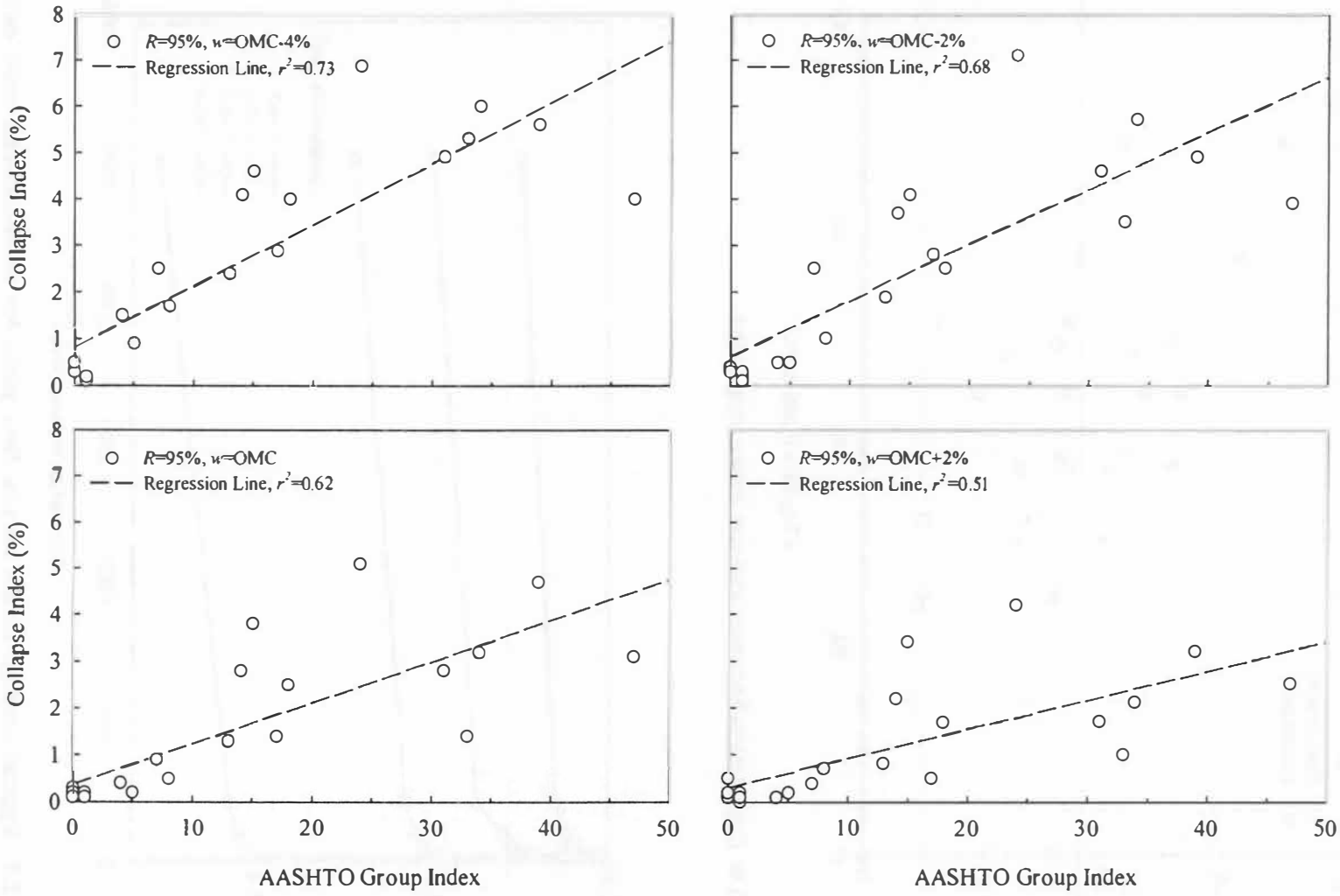

Figure 3.5: Average value of collapse index versus AASHTO group index

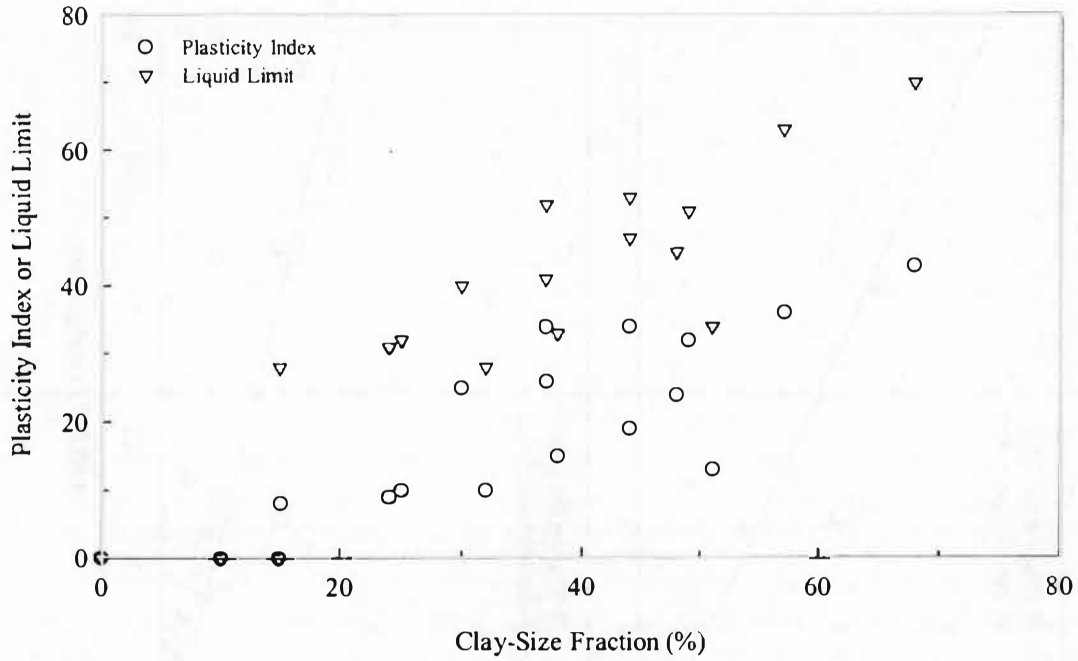

Figure 3.6: Correlation between various index properties

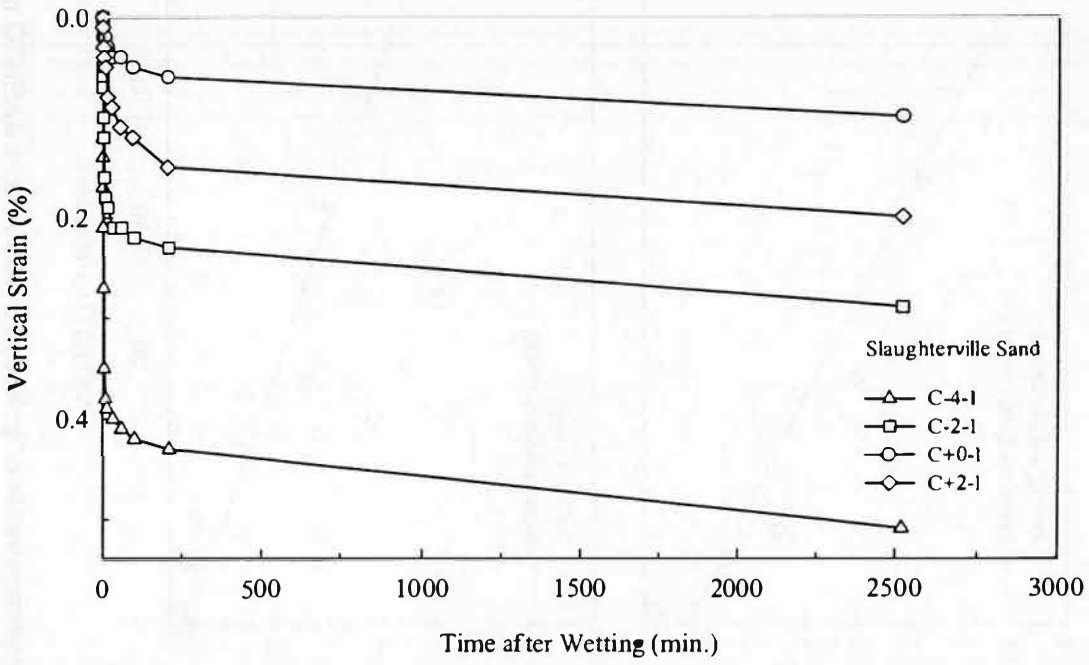

Figure 3.7: Typical vertical strain versus time plots for cohesionless soils during single-oedometer collapse at a vertical stress of 200 kPa

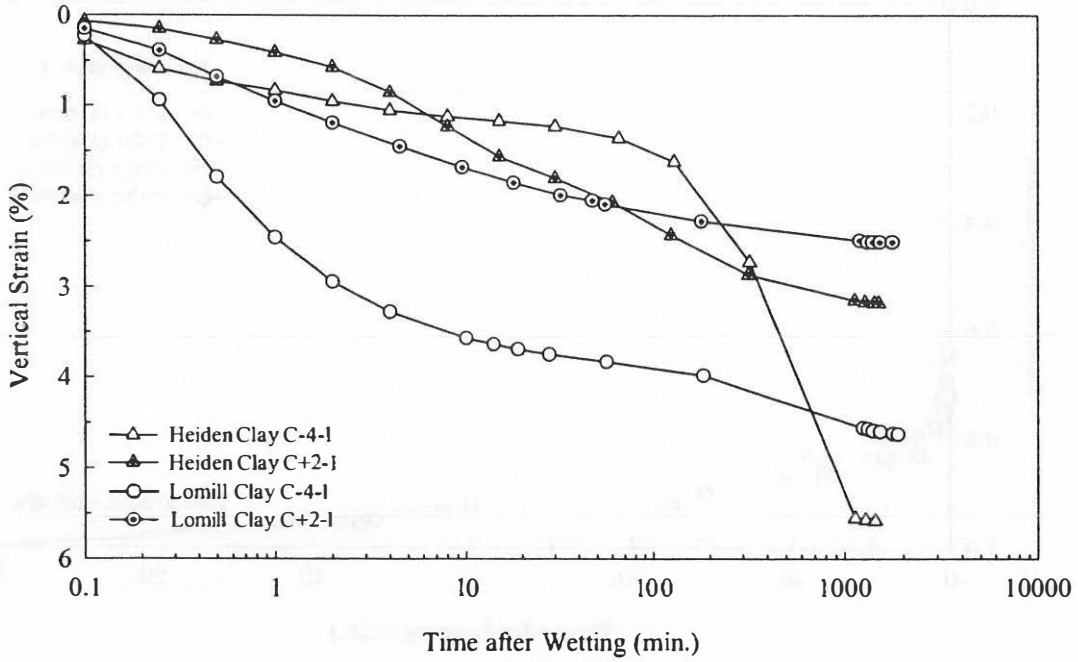

Figure 3.8: Typical vertical strain versus time plots for cohesive soils during single-oedometer collapse at a vertical stress of 200 kPa

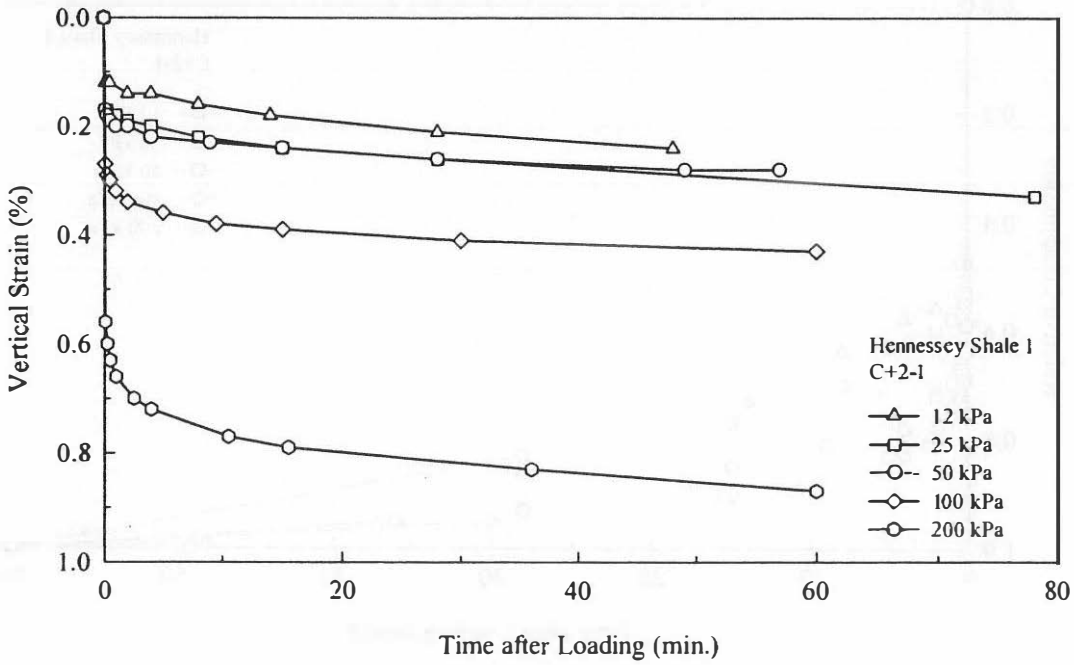

Figure 3.9: Typical time rate of compression curves for as-compacted samples

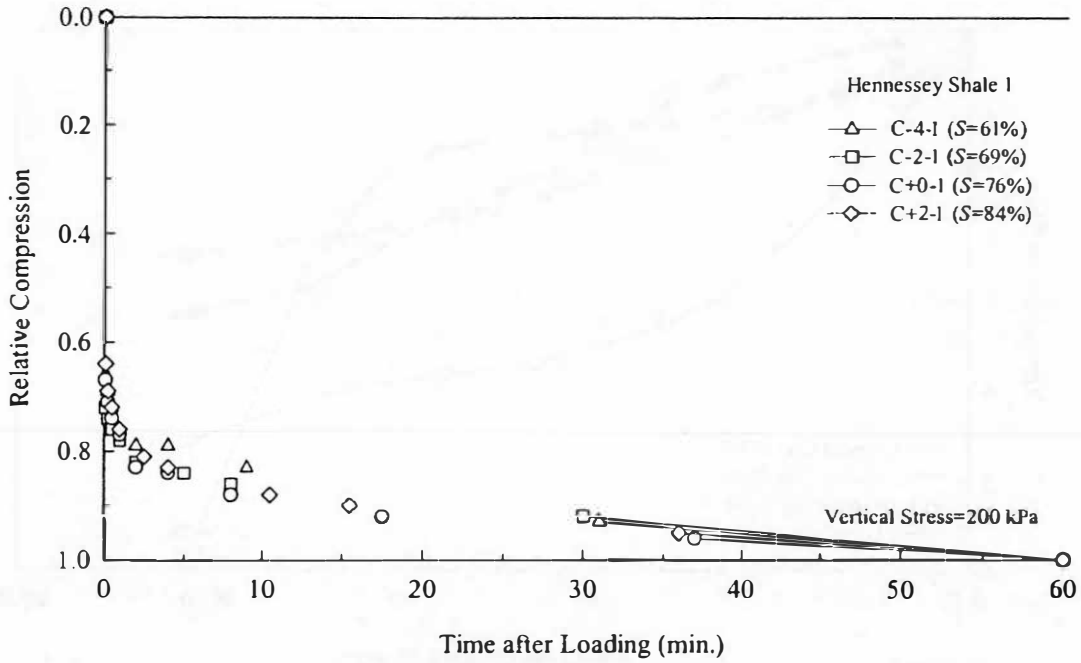

Figure 3.10: Relative compression versus time for as-compacted samples at different moisture contents

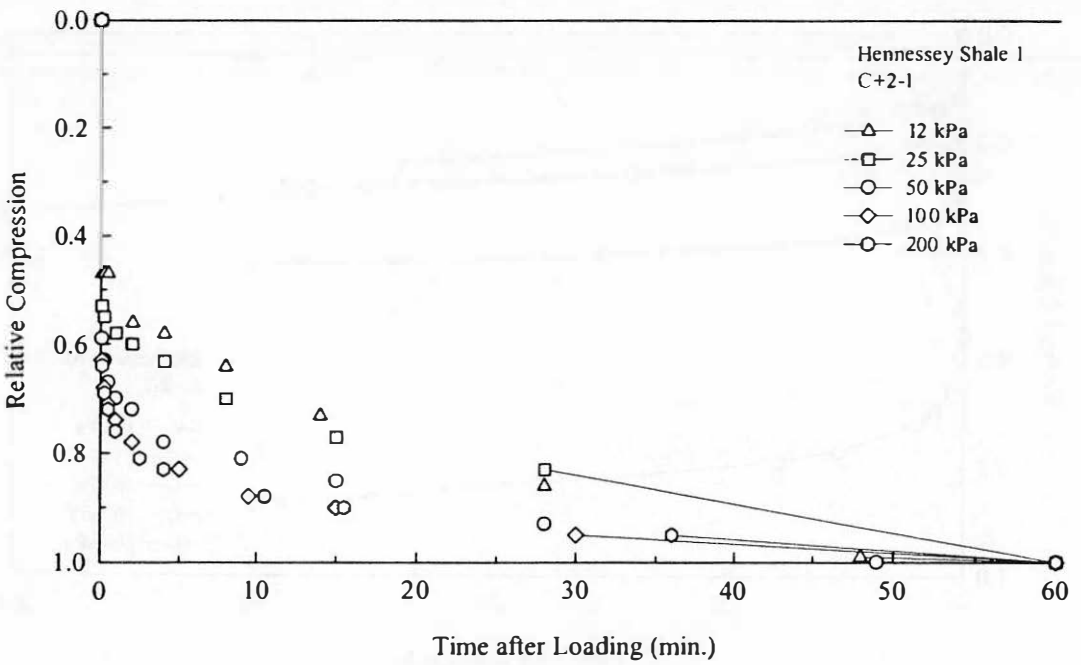

Figure 3.11: Typical relative compression versus time for as-compacted samples at various stress levels

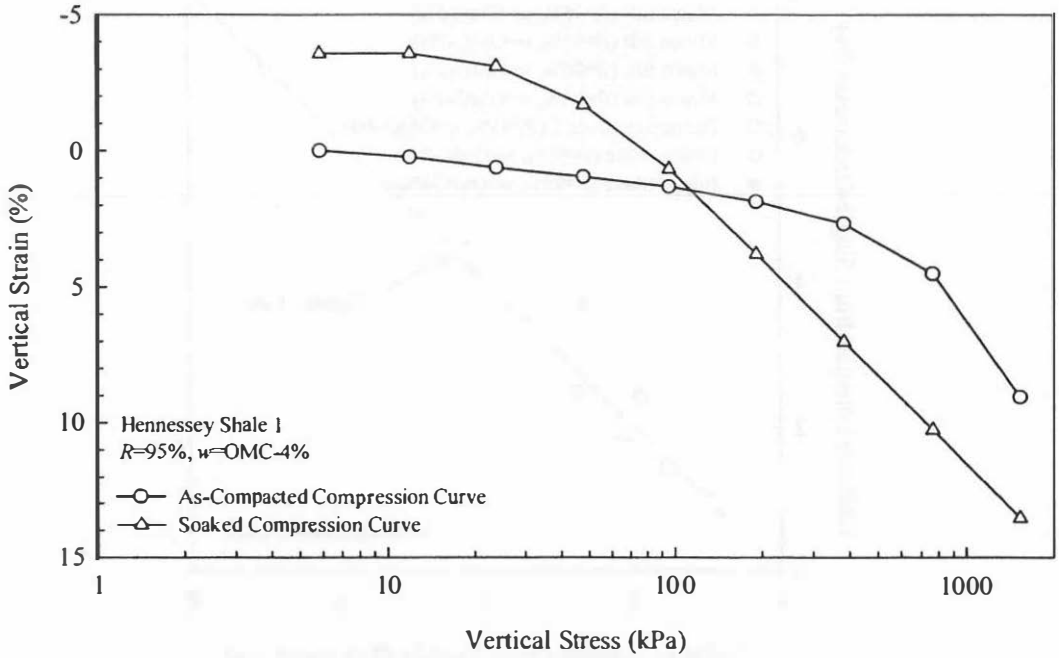

Figure 3.12: Stress-strain plots for double-oedometer test on Hennessey Shale 1

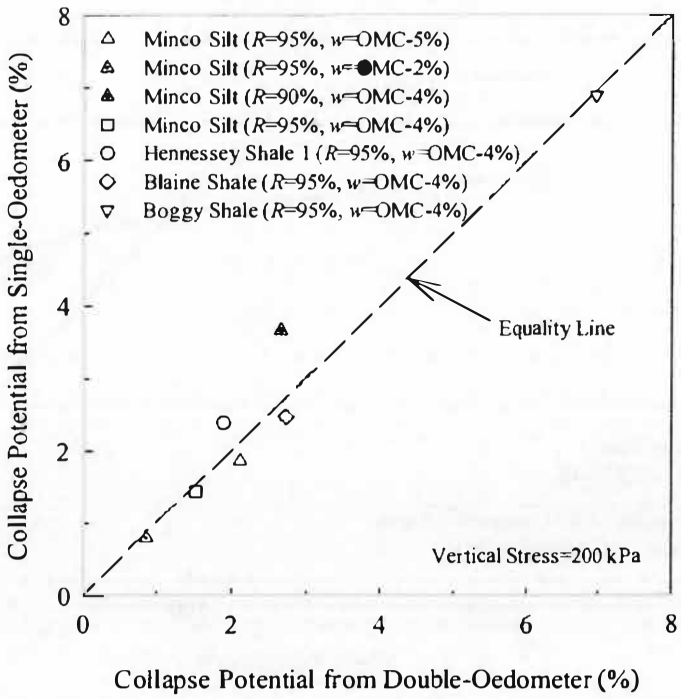

Figure 3.13: Comparison of collapse potential from single- and double-oedometer tests

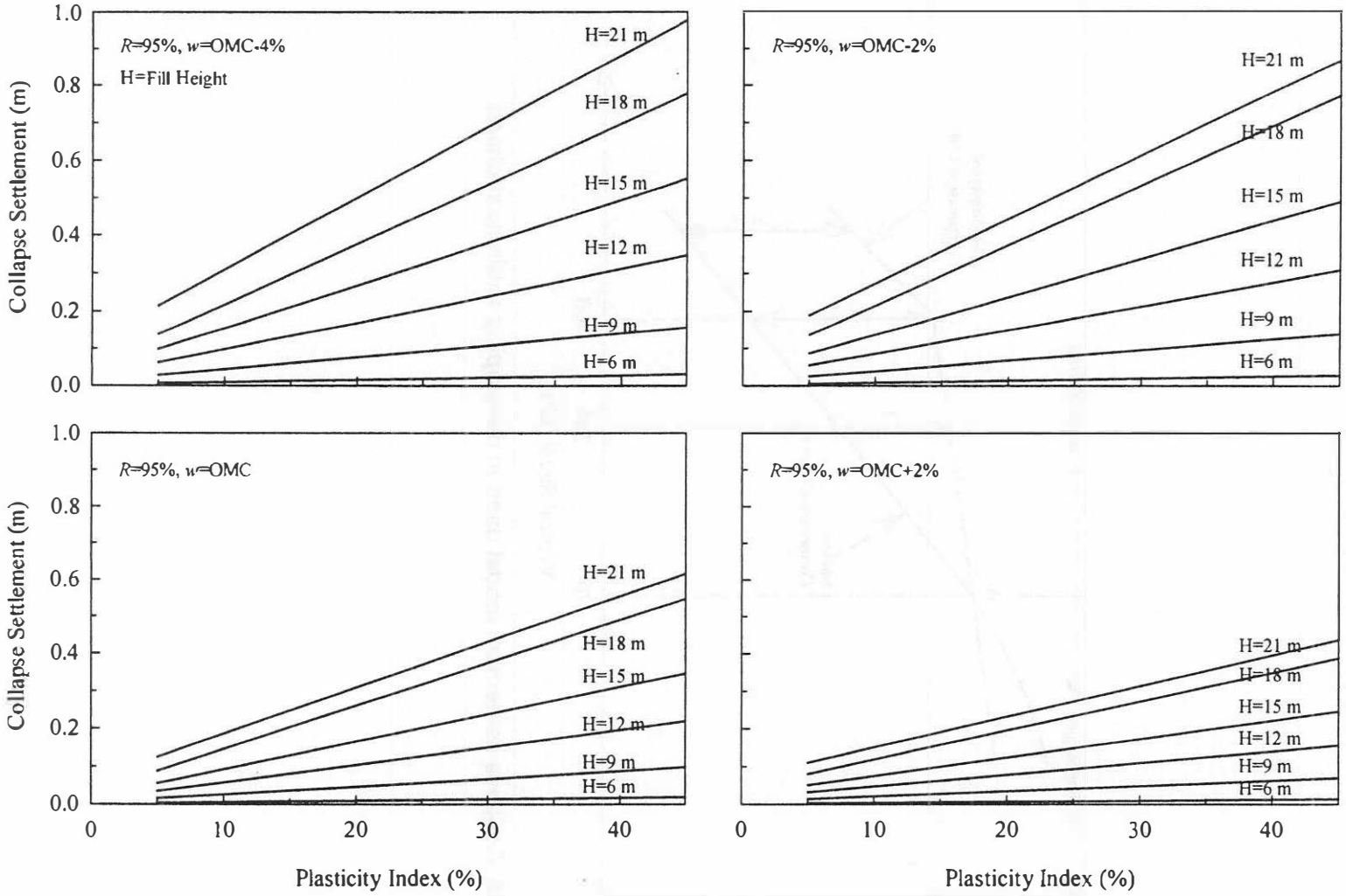

Figure 3.14: Predicted relationship between collapse settlement and plasticity index

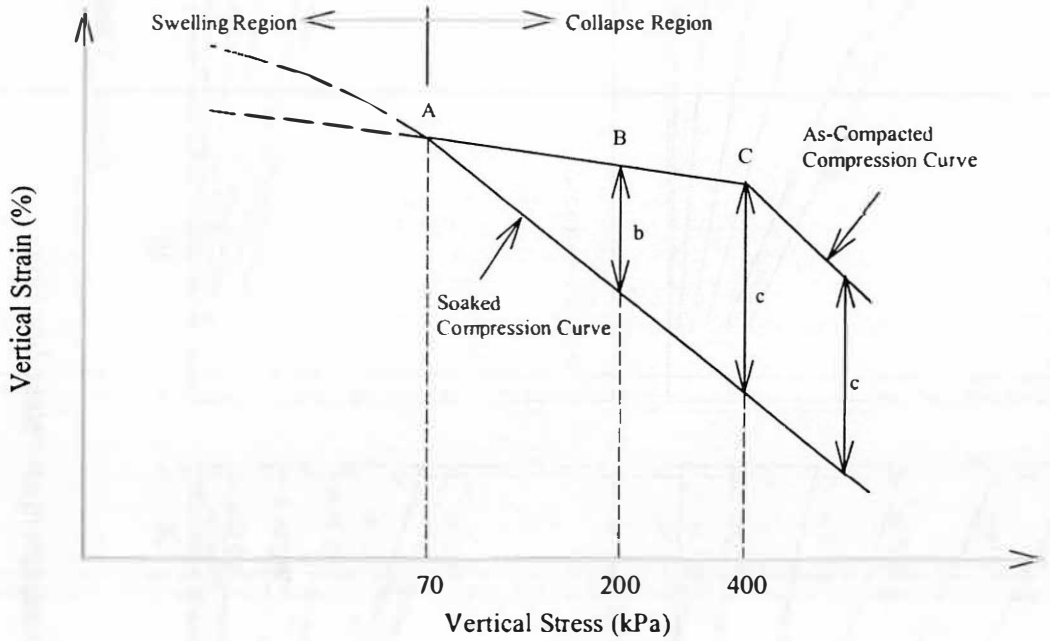

Figure 3.15: Collapse settlement model used in developing settlement charts

Chapter 4: Centrifuge Testing

4.1 Introduction

Collapse is often evaluated in the laboratory using the one-dimensional oedometer test; however, stress-strain conditions within an embankment are three-dimensional. For this reason and because of the substantial resources associated with full scale testing, scale centrifuge models were used to produce experimental settlement data for a simulated long embankment (i.e. plane strain). Centrifuge testing was carried out to produce experimental data for model embankments to discern between self-weight and collapse settlements as well as to compare simple one-dimensional oedometer-based predictions to the settlements at the centerline of embankment models. This chapter provides descriptions of the centrifuge facility, model preparation, and instrumentation. In addition, test results, settlement predictions, and the accuracy of predictions are discussed.

4.2 Centrifuge Facility

Centrifuge model embankments were constructed and tested in the Army Corps of Engineers Centrifuge facility located in Vicksburg, Mississippi. Figure 4.1 (a) illustrates the centrifuge used in this study. It has three main components: centrifuge arm, swinging platform, and balancing counterweight. The finished model is constructed inside the model container, which is mounted on the swinging platform. The swinging platform swivels outward during spinning and is stabilized by the balancing counterweight to ensure smooth rotation. The centrifuge platform has a 6.5-m radius with a range of gravitational acceleration from 10 to 350 times earth's gravity (g). It has a maximum payload of 8,000 kg up to 143 g, reducing to 2000 kg at 350 g.

4.3 Model Preparation & Testing

Three centrifuge model embankments (or models) were analyzed in this study. Minco Silt was selected for use in the centrifuge testing to facilitate the measurement of matric suction using the miniature pore pressure transducers (PDCR 81s). Soil required for each model was prepared by

oven drying (due to low clay content), pulverizing, and then passing through a U.S. standard No. 4 sieve. The soil was allowed to come to room temperature before tap water was added and thoroughly mixed with the soil. The moist soil was stored in sealed buckets and left overnight to promote a more thorough distribution of water throughout the soil. Practical limitations prevented a longer seasoning period, and therefore, great care was taken during mixing to incrementally weigh and distribute the water evenly over the oven-dry soil that was partitioned in mixing trays.

Each model was prepared the next day. The mixed soil was compacted into three equal layers in the centrifuge box to the target dry unit weight using a standard effort rammer (ASTM D 698). The aluminum centrifuge box had an open top with a dimension of 1.07 m long by 0.30 m wide by 0.46 m high. Longitudinal walls were detachable and one was made of transparent Plexiglas. Sintered stainless steel porous stones on the bottom of the centrifuge box and a groove system underneath allowed water to be introduced via an electronically controlled valve.

The shape of each model was obtained by replacing the detachable walls with two templates outlining the shape of the embankment and then trimming the compacted soil using a stainless steel bar with a sharpened, beveled edge. One face of each model was carefully marked with India Ink after removing the templates. Horizontal and vertical ink lines aid in sketching and photographing the undeformed and deformed shapes of the models.

The longitudinal sidewalls were covered with polystyrene sheets and reattached to the centrifuge box. Additional polystyrene strips were placed between the soil and the longitudinal walls as shown in Figure 4.1 (b). This was done to minimize friction between the soil and longitudinal walls so that each model would simulate a long embankment. The ink lines and embankment outlines were visible through and traced upon the Plexiglas walls.

Modified miniature pore pressure transducers (PDCR 81s) that are capable of measuring matric suction were incorporated into the models at various depths and locations. The modification of PDCR 81s for matric suction measurement is given by Muraleetheran and

Granger (1999). The PDCR 81s were saturated in a metal vacuum chamber filled halfway with a saturation fluid of 50 percent de-aired water mixed with 50 percent glycerin by weight. The PDCR 81s were first held above the saturation fluid under 90 kPa vacuum for about two minutes to remove any air that was in the porous disk and the gap behind the disk. The vacuum chamber was then inverted to submerge the PDCR 81s in the saturation fluid for about two hours. Finally, vacuum was released, and the PDCR 81s were ready to measure matric suction. Linear variable differential transformers (LVDTs) were placed at various locations on the models to measure horizontal and vertical deformations as depicted in Figure 4.1 (c). To prevent drying of the soil between preparation and testing of the models in the centrifuge, moist towels were placed over the models.

One purpose of centrifuge testing was to discern self-weight settlement from collapse settlement. This was achieved by spinning up each model to an acceleration of 165 g in the centrifuge and allowing sufficient time for self-weight settlement before water was introduced. The end of self-weight settlement was determined by observing the point at which the vertically oriented LVDTs appeared to cease moving. Water was introduced from the bottom of the centrifuge box in three steps until the whole model was nearly submerged as shown in Figure 4.1 (d). Water at each level was maintained until collapse settlement had ceased before introducing additional water. Water levels were monitored with an on-board camera focused on a ruler. Observations during flight indicated that water levels were increased uniformly on both sides of the model and that the wetting front in the soil moved at nearly the same rate as the increasing water level.

Following each test, the deformed ink lines and shape of each model were traced on the longitudinal Plexiglas walls. Centerline profiles of the models were recorded using a profiler. Models were then dissected, and moisture content samples were taken at various locations in the models.

4.4 Model Dimensions & Instrumentation

Each of the three models was constructed with a height of 0.127 m and a crest width of 0.121 m, with a side slope of three horizontal units to one vertical unit (3:1). To obtain the prototype dimensions, the model dimensions are multiplied by 165 in accordance with centrifuge scaling laws. These models correspond to having a height of 21 m in the prototype scale.

Six pore pressure transducers were incorporated into each model at various depths and locations to measure matric suction. Of the six pore pressure transducers, three responded correctly in Model No. 1, none in Model No. 2, and four in Model No. 3. These pore pressure transducers did not respond correctly due to de-saturation of the porous stones resulting from delays between transducer installation in the model and centrifuge testing. As discussed by Muraleetharan and Granger (1999), there is a narrow window of time in which the pore pressure transducers equipped with high-air entry porous stones properly measure matric suction. The dimensions and locations of sensors (LVDTs and pore pressure transducers) for each model are shown in Figure 4.2.

4.5 Results & Discussion of Oedometer Tests

Three series of double-oedometer tests corresponding to the dry unit weight and compaction moisture content of the three models were performed on Minco Silt. An additional three series of single-oedometer tests inundated at 400 kPa were performed for comparisons with double-oedometer test results. Both single- and double-oedometer tests were performed in triplicate for quality control purposes. Test results are illustrated in Figure 4.3 and tabulated in Tables B-1 through B-3 of Appendix B. Referring to the test results, several important observations are made, as follows:

1. Single- and double-oedometer data are in reasonably good agreement.
2. Incomplete saturation prevailed in the single-oedometer test specimens. These samples attained an average degree of saturation of 86 percent at the end of a 24-hour soaking period; as a result, incomplete collapse could have occurred. Assuming complete collapse is realized

under such conditions may be justified for natural deposits of silts and possibly for compacted silts. Houston and Houston (1992) report that natural deposits of silts have a limited increase of collapse strain when the degree of saturation increases from approximately 85 or 90 percent to 100 percent. A literature review performed by Osipov and Sokolov (1995) show comparable findings.

3. Swelling behavior is nonexistent in double-oedometer results, as expected for silt.
4. Collapse index varied from 0.4 to 1.8 percent, which indicates a slight degree of collapse according to ASTM D 5333.
5. Collapse potential increases as compaction moisture content and dry unit weight decrease, as evidenced by both the single- and double-oedometer data. With regard to the moisture content, for a relative compaction of 95 percent, the collapse potential is about twice as large for a moisture content of 9.6 percent compared to a moisture content of 12.6 percent. The effect of dry unit weight is partially revealed by comparing Figures 4.3 (b) and (c) for relative compaction of 90 and 95 percent, respectively. While the moisture content is 1 percent higher for the 90 percent relative compaction, the collapse potential at 90 percent relative compaction is similar to the sample with 95 percent relative compaction. It can be reasoned that if the moisture content for 90 percent relative compaction were the same as 95 percent relative compaction, then the collapse potential would be even greater for the former. This indicates that lower dry unit weight leads to greater collapse potential for similar moisture content, as expected.
6. The point at which the as-compacted and soaked compression curves diverge gives an indication of the vertical stress above which collapse may occur. Observing the double-oedometer curves in Figure 4.3, this point is near 50 kPa for Minco Silt. Thus, for similar field conditions, collapse may occur in soil where the overburden depth exceeds about 3 m.

4.6 Results & Discussion of Centrifuge Tests

Moisture Content Measurements

Moisture content measurements were taken at various points in time to quantify the moisture changes in the test soil and are summarized in Table 4.1. Figure 4.4 depicts moisture content measurements taken after dissecting the models at the end of testing. Moisture content measurements were made prior to compaction or at the end of compaction and prior to testing for the quantification of moisture loss due to time lag between model preparation and testing of the models. Although moist towels were placed over the models to minimize moisture loss, average prewetting moisture contents were 1.1 to 1.7 percent lower than compaction moisture contents for Model Nos. 1 and 2.

Moisture content measurements taken after dissecting the models at the end of testing reveal that average moisture contents for Model Nos. 1 and 3 were 1 to 2 percent lower than Model No. 2 possibly due to the higher dry unit weights of Model Nos. 1 and 3. This result is consistent with moisture content measurements taken at the end of a 24-hour soaking period in the corresponding single-oedometer tests, as indicated in Table 4.1, although moisture content measurements from the single-oedometer tests were consistently lower in all cases.

Deformations & Pore Pressure Responses

Tracings of the undeformed and deformed ink lines are shown in Figure 4.5. Tracings indicate that centerline deformations were lowest for Model No. 1 and greatest for Model No. 2. This is consistent with the oedometer results (see Figure 4.3) in that more settlement is expected for soils with lower moisture content and dry unit weight. Tracings also demonstrated the two-dimensional nature of embankment settlement in that compression is observed at the centerline and is accompanied by some outward bulging at the lateral margins.

LVDT readings for each model are summarized in Table 4.2. A comparison of centerline settlement data from tracings and LVDT measurements is presented in Table 4.3. Settlement data are presented for self-weight and collapse compressions resulting from each wetting sequence.

Figure 4.6 depicts data from LVDTs and pore pressure transducers located as shown in Figure 4.2 for Model No. 3. Data for Model Nos. 1 and 2 are shown in Figures B-1 and B-2 of Appendix B. Note that the LVDT measurements have not been scaled to the prototype dimensions (multiply by a factor of 165 to calculate prototype deformations). The following observations are made based on the three sets of centrifuge data:

1. Centerline deformation corresponding to self-weight and collapse settlements is clearly visible in the centerline (CL) LVDT response for Model No. 2 and 3. Due to faulty LVDT, centerline deformation for Model No. 1 was not obtained. Similarly, centerline deformation for Model No. 2 was not obtained at the third water level due to faulty LVDT.
2. Self-weight settlement occurred quickly as the acceleration was increased, suggesting that in actual embankments compacted dry of the OMC, self-weight settlement may occur during construction.
3. Right and left horizontal (RH and LH) LVDT responses indicate a small amount of outward horizontal movement in each model. Except for Model No. 1, nearly all of the horizontal movement appears to occur during spin-up to 165g and then remains essentially constant. RH and LH LVDTs for Model No. 1 recorded additional horizontal outward movement during subsequent wetting, in addition to the outward movement during spin-up. Tracings for each model given in Figure 4.5 confirm outward movement at the locations of RH and LH LVDTs.
4. Right and left vertical (RV and LV) LVDTs for Model Nos. 2 and 3 recorded considerable downward movement during spin-up, as well as some upward movement during subsequent wetting. RV and LV LVDTs did not function correctly in Model No. 1. The downward movement that occurred during self-weight deformation is attributed to the displacement of soil in response to gravity. Subsequent upward bulging of the slope is a result of the two-dimensional nature of wetting-induced volume change. Tracings confirm the bulging and upward movement at lateral margins of the models.

5. Readings from the RV and LV LVDTs differ because of local variation in unit weight and moisture content resulting from imperfect compaction. In addition, the LVDT foot placement may be slightly different in each case, and there may be slight geometrical imperfections in the models as well.
6. Of the six pore pressure transducers, three responded correctly in Model No. 1 and four in Model No. 3. None of the pore pressure transducers responded correctly in Model No. 2. Matric suctions recorded by the transducers prior to inundation with water were between 5 and 40 kPa, as shown in Figure 4.6 and Figure B-1 in Appendix B. Tensiometer measurements of Minco Silt compacted at conditions similar to those in the models yield matric suction values of between 40 and 70 kPa. Measured matric suctions in the models are lower than expected; however, this may have been partly due to de-saturation of the porous stones resulting from delays between transducer installation in the model and centrifuge testing. As mentioned earlier, there is a narrow window of time in which the pore pressure transducers equipped with high-air entry porous stones properly measure matric suction.
7. For pore pressure transducers that responded correctly, matric suction increased during spin-up. This phenomenon is likely caused by the increased dry unit weight during spin-up. Although both dry unit weight and degree of saturation increased during spin-up, it is believed that the increase in dry unit weight outweighs the increased degree of saturation, resulting in a higher matric suction. The soil-water characteristic curves for Minco Silt depicted in Figure 4.7 show that higher values of matric suction were measured in Minco Silt compacted at a higher dry unit weight.
8. It is noted that the matric suction values, as determined from the soil-water characteristic curves in Figure 4.7, are lower than those from direct measurements at a similar moisture content. Because samples used for soil-water characteristic curves were prepared at 6 percent moisture content, while models were compacted at much higher moisture contents of between 10.6 and 12.6 percent, the difference in matric suction values may be partly due to the

difference in soil fabric resulting from different compaction moisture contents (Muraleetharan and Granger 1999).

9. Pore pressure transducers responded at nearly the same instant that the water level reached the level of the transducer. This indicates that the wetting front was moving very quickly through the embankment, at nearly the same rate the water was rising adjacent to the embankment. This was expected because hydraulic conductivity increases in proportion to the ratio of centrifugal to gravitational acceleration, i.e. 165 times greater.

4.7 One-dimensional Settlement Prediction

Assuming one-dimensional strain conditions prevailed beneath the embankment centerlines and a comparable degree of saturation is achieved between the models and the oedometer samples, the double-oedometer test results presented in Figure 4.3 were used to predict self-weight and collapse settlements in the prototype embankments. The step-by-step procedure for the prediction is as follows:

1. The model was divided into ten layers of equal thickness.
2. The model dimensions were converted into prototype scale using the appropriate centrifuge scaling law. Prototype dimensions were obtained by multiplying model dimensions by 165.
3. The overburden stress below the centerline in each layer of the prototype embankment was assumed one-dimensional and approximated by the weight of overlying soil.
4. The self-weight settlement strain of each layer in the prototype was determined graphically from the as-compacted compression curve. The collapse strain was determined from the double-oedometer compression curves; the collapse strain is the difference between the as-compacted and soaked compression curves.
5. The self-weight settlement of each layer in the prototype is the product of the self-weight settlement strain and the thickness of the layer. The collapse settlement of each layer is the product of the collapse strain and the thickness of the layer.

6. The summation of both components of settlement for each layer gives the total predicted settlement at the centerline.
7. Predicted prototype settlements are compared to the measured prototype centerline settlements in Table 4.3. To obtain prototype settlements, the model LVDT and tracing measurements are multiplied by 165 in accordance with centrifuge scaling laws.

4.8 Comparison of Predicted & Measured Centerline Settlements

Comparing the measured and predicted centerline settlements shown in Table 4.3 reveals several significant observations. First, measurements of total settlement for each model are significant, in a range of 0.5 to 0.7 m, from tracings and LVDT readings. These results emphasize the importance of quality control and stringent compaction requirements during embankment construction. For example, Model No. 1 was compacted to 95 percent relative compaction at 2 percent dry of the OMC and, based on the tracings experienced a total settlement on the order of 0.5 m, which was the smallest in the three tests.

Second, measured self-weight settlements are substantial for Model Nos. 2 and 3, although most settlement would be expected to occur during construction of actual embankments. Of greater concern may be the very large collapse settlements, on the order of 0.5 m. In reality, an embankment may not experience complete wetting, unless flooded, and may rarely approach 20 m in height; however, settlements of even half those observed in the models would be considered substantial (see Table 4.2). Thus, it could be expected that even partial wetting in smaller embankments may result in substantial settlement. Furthermore, many soils exhibit far greater collapse susceptibility than the test soil, which is classified as having a slight degree of collapse based on ASTM D 5333.

In Oklahoma, embankments vary in height with many exceeding 20 m (Laguros et al. 1990). Of particular relevance to collapse settlement are the numerous approach embankments that were built for bridge crossings over reservoirs. Many of these embankments exceed 30 m in height, exhibit extensive settlement, and were completely flooded to over half their structural

height during filling of reservoirs. A field study carried out in this research, that is presented in next chapter, showed an average increase in moisture content of 3 to 4 percent above the OMC for an approach embankment crossing a lake that experienced more than 0.61 m of settlement.

For highway embankments above water, partial wetting may occur over long periods. Data showing post-construction wetting of these embankments are not readily available; however, one unpublished case study from the ODOT revealed an average increase in moisture content of about 4 to 5 percent above the OMC in a 13-year old embankment. This particular embankment, along Interstate I-235 in Oklahoma City, was 14 m high and had experienced settlements on the order of 0.12 to 0.24 m. In another study, Laguros et al. (1990) report a similar average increase in moisture content in a 25-year old embankment above water. Although partial wetting may prevail in field situations, sometimes degree of saturation attained in the soil may be very close to complete saturation. Moisture content increases of 3 to 4 percent above the OMC represent near complete saturation of soil; thus, fully wetted oedometer specimens may be a reasonable approximation.

Third, predictions of self-weight settlement based on one-dimensional double-oedometer test results agreed reasonably well with measured prototype settlements. These results are consistent with the U.S. Bureau of Reclamation embankment compression measurements of more than 20 large dams (Gould 1953 and 1954, as cited by Sherard et al. 1963). Gould reports that the self-weight compression during construction in the centerline of earth dams, where the measuring devices were installed, was essentially one-dimensional. Collapse settlements, on the other hand, were under-predicted by a factor of 1.4 for Model No. 2 and by a factor between 2.3 and 2.6 for each wetting sequence of Model No. 3. Two factors can be identified as having significant effects on the quality of prediction. Firstly, it appears that the one-dimensional model did not properly account for the two-dimensional nature or shear-induced deformation of collapse settlements for Model Nos. 2 and 3. As both models were prepared at comparable moisture content, it is speculated that the higher compaction dry unit weight of Model No. 3 was

responsible for the larger difference between predicted and measured collapse settlement. In other words, more lateral expansion accompanying vertical compression would be expected for embankments compacted at higher unit weights for a given moisture condition. From a soil mechanics standpoint, soils compacted at a higher dry unit weight tend to dilate more than soils that are compacted at a lower dry unit weight during shear resulting more lateral expansion accompanying vertical compression. Secondly, differences in prewetting moisture contents between the models and the corresponding oedometer samples may have affected the quality of prediction. To reduce the possible soil fabric difference between the models and the oedometer samples, the oedometer samples were compacted at the compaction moisture contents of the corresponding models. Although some water loss from the samples to the top and bottom porous stones occurred when the samples were tested in the as-compacted condition, the post-compaction drying of the models was not effectively simulated in the double-oedometer tests. Prewetting moisture contents of the oedometer samples were between 0.5 and 1 percent lower than compaction moisture contents, based on moisture content determinations on the as-compacted samples at the end of loading. On the other hand, prewetting moisture contents for Model Nos. 1 and 2 were 1.1 to 1.7 percent lower than compaction moisture contents. Referring to Table 4.1, the differences in prewetting moisture content between the oedometer samples and models are in the order of 0.2 to 1.2 percent. These differences in prewetting moisture content would amount to 0.05 to 0.12 percent difference in collapse index, as suggested by Figure 3.2 of Chapter 3, or 0.4 to 1 cm difference in predicted collapse settlement. Thus, it seems that prewetting moisture content differences can not fully account for the difference in predicted and observed collapse settlements shown in Table 4.3.

These results demonstrate that oedometer testing can give a good indication of collapse potential; however, observations from this study suggest that predicted settlements based on one-dimensional analysis should be considered a lower bound for embankments. As the one-dimensional model is inadequate for the prediction of strain conditions in the centerline of the

embankments, more sophisticated techniques can be employed. Lourens and Czapla (1987) report the successful use of finite element techniques for analysis of collapse deformations in a highway embankment.

Prediction made using the settlement charts presented in Figure 3.14 gives a collapse settlement at the embankment centerline of 0.28 m for Model No. 3 versus a measured total collapse settlement of 0.495 m. Again, this one-dimensional oedometer-based method under-predicted collapse settlement, in this case by a factor of 1.7 or 0.21m.

Table 4.1: Average moisture content measurements from each model and the corresponding single-oedometer tests

Source of sample	Moisture Content (%)		
	Model No. 1	Model No. 2	Model No. 3
Prior to Compaction	12.2	11.2	9.5
Trimmings during Model Preparation	12.6	---	---
Drilled Sample before Test	11.1	9.5	---
End of Test	20.1	22.0	20.8
Single-Oedometer (Before Soaking) [a]	12.0	10.0	9.0
Single-Oedometer (End of Soaking)	16.6	18.5	16.8

[a]Values for single-oedometer samples before soaking are estimated from limited moisture content measurements.

Table 4.2: LVDT readings for each model

Event	Model No. 1		Model No. 2					Model No. 3				
	RH LVDT	LH LVDT	CL LVDT	RV LVDT	LV LVDT	RH LVDT	LH LVDT	CL LVDT	RV LVDT	LV LVDT	RH LVDT	LH LVDT
165 g	0.033	-0.025	0.304	-0.396	-0.116	0.050	0.050	0.132	-0.330	-0.198	0.099	0.066
WL 1	0.038	-0.025	0.417	-0.396	-0.033	0.050	0.050	0.279	-0.247	-0.165	0.116	0.083
WL 2	0.050	0.012	0.618	-0.380	0.099	0.060	0.060	0.495	-0.198	-0.033	0.124	0.099
WL 3	0.071	0.107	---	-0.380	0.099	0.060	0.060	0.627	-0.165	-0.033	0.099	0.083

Notes: (1) Positive values denote downward or outward movements and negative values denote upward or inward movements for vertical and horizontal LVDTs, respectively.

(2) WL = water level.

(3) WL 1 and 2 were at 2 and 6 cm, respectively for all models; WL 3 was at 13, 14, and 12 cm for Model Nos. 1, 2, and 3, respectively.

(4) LVDT readings are in meters.

(5) Only readings for LVDTs that responded correctly are given.

Table 4.3: Measured and predicted centerline settlement of prototype embankments

Model No.	Event	Self-Weight Settlement (m)		Collapse Settlement (m)		Total Settlement (m)		
		CL LVDT	Predicted	CL LVDT	Predicted	CL LVDT	Tracings	Predicted
1	At 165 g	---	0.25	---	---	---	0.46	0.34
	WL 1 [a]	--- [c]	---	--- [c]	0.08			
2	At 165 g	0.304	0.30	---	---	---	0.69	0.59
	WL 1 [a]	---	---	0.113	0.08			
	WL 2 [a]	---	---	0.314	0.23			
	WL 3 [b]	--- [d]	---	--- [d]	0.29			
3	At 165 g	0.132	0.19	---	---	0.627	0.66	0.38
	WL 1 [a]	---	---	0.147	0.06			
	WL 2 [a]	---	---	0.363	0.16			
	WL 3 [b]	---	---	0.495	0.19			

Notes: Prototype settlement calculated by multiplying LVDT measurements by N=165.
[a]WL 1 and 2 were at 2 and 6 cm, respectively for all models.
[b]WL 3 was at 13, 14, and 12 cm for Model Nos. 1, 2, and 3, respectively.
[c]CL LVDT measurements for Model No. 1 were not obtained due to faulty LVDT.
[d]CL LVDT measurement for Model No. 2 was not obtained at the third water level due to faulty LVDT readings.

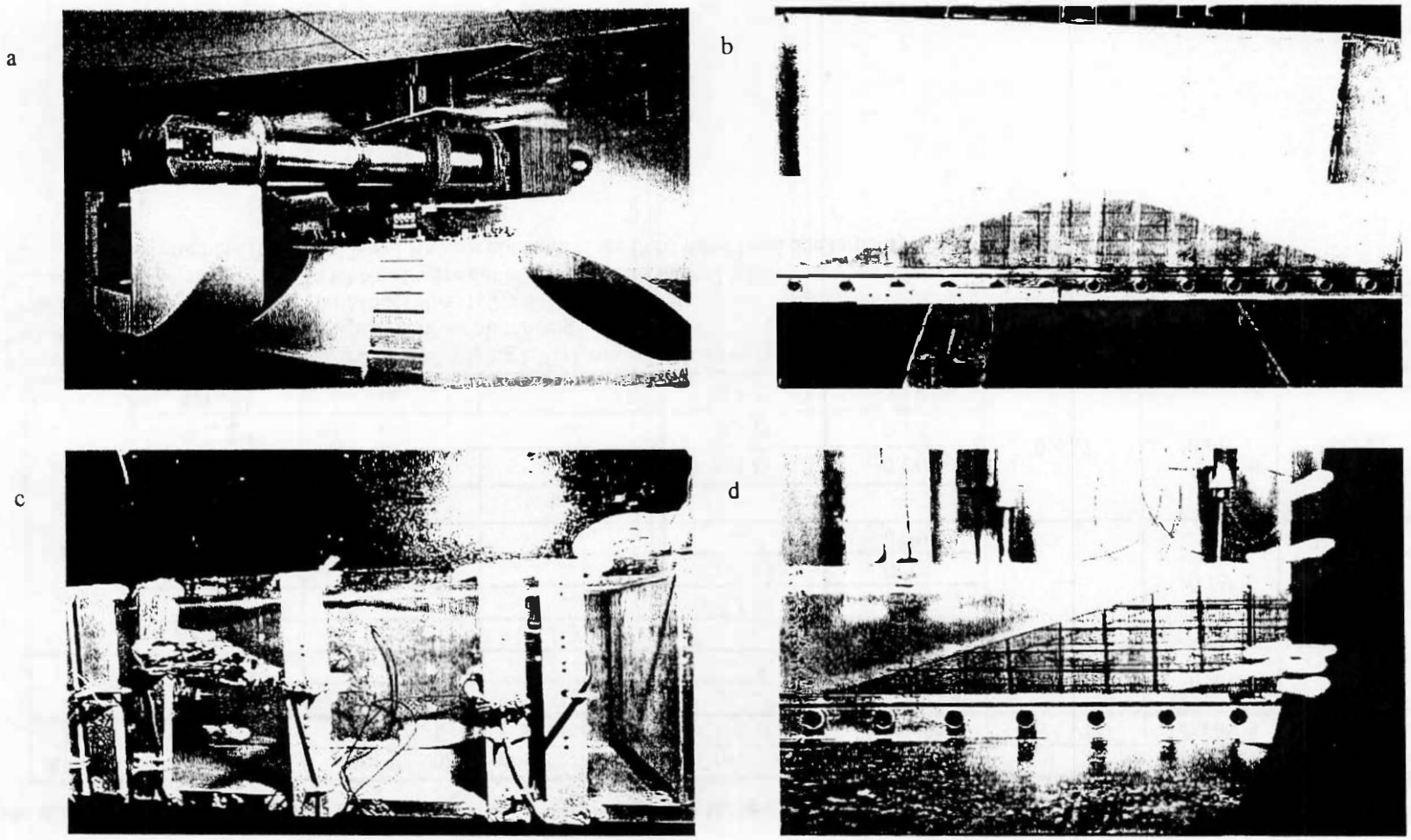

Figure 4.1: (a) The centrifuge at Army Corps of Engineers Centrifuge facility (b) Polystyrene strips to minimize friction and wet paper towels to minimize moisture loss (c) Completed installation of PDCR 81s and LVDTs (top view) (d) Flooding of a model

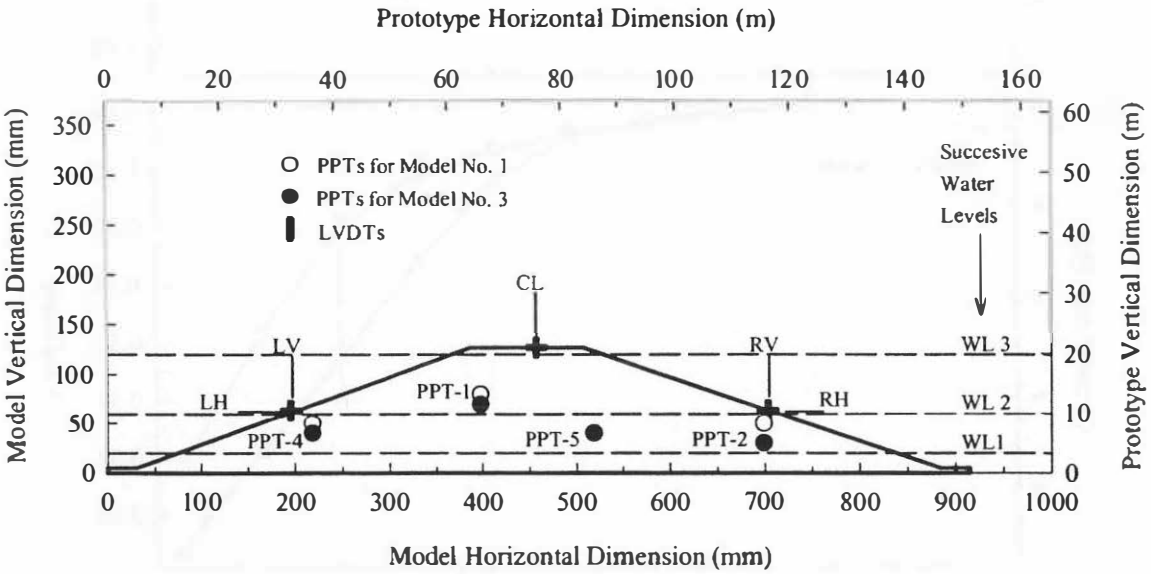

Figure 4.2: Model and prototype dimensions and locations of sensors

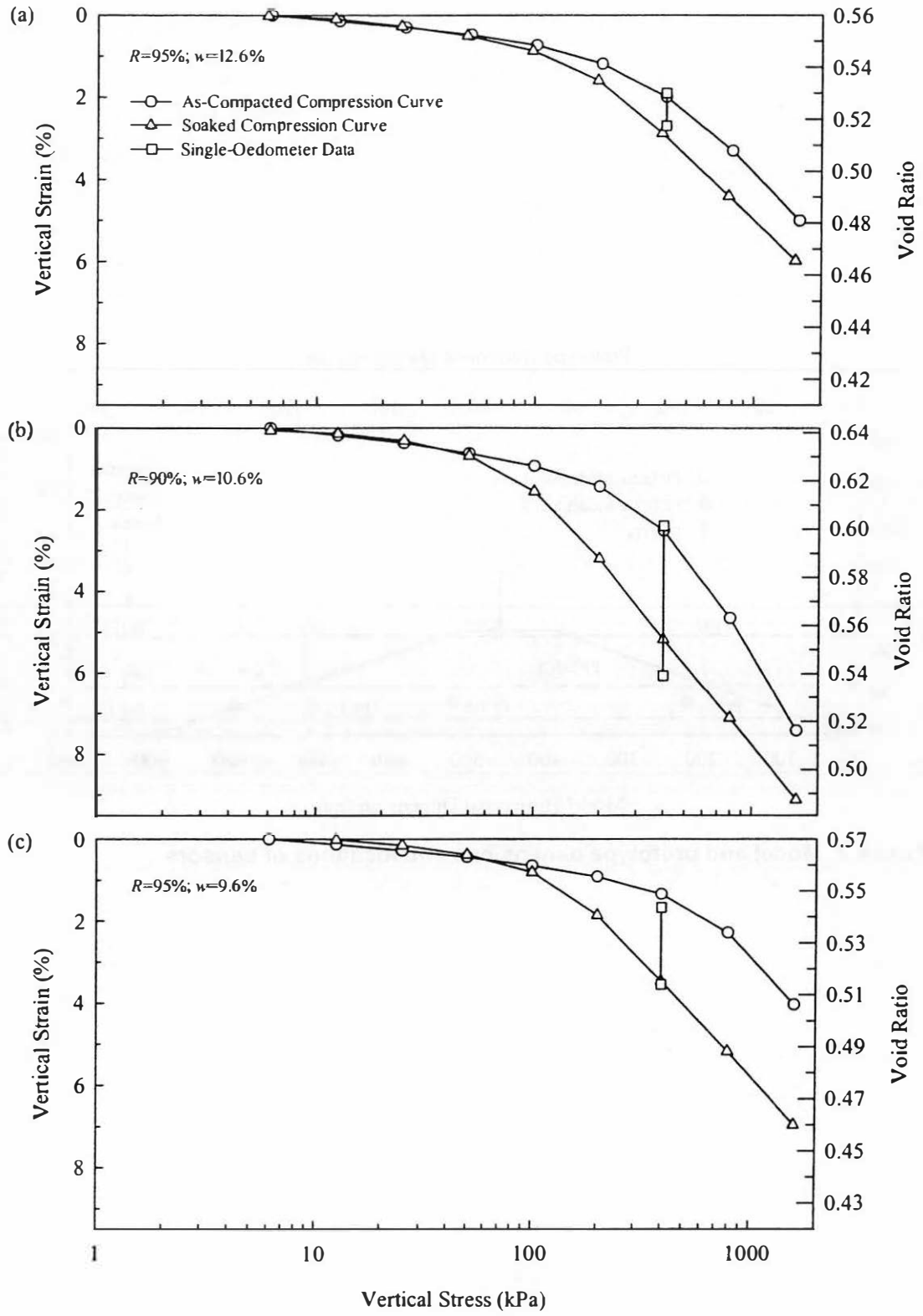

Figure 4.3: Single- and double-oedometer results for model embankment soil, average of three tests

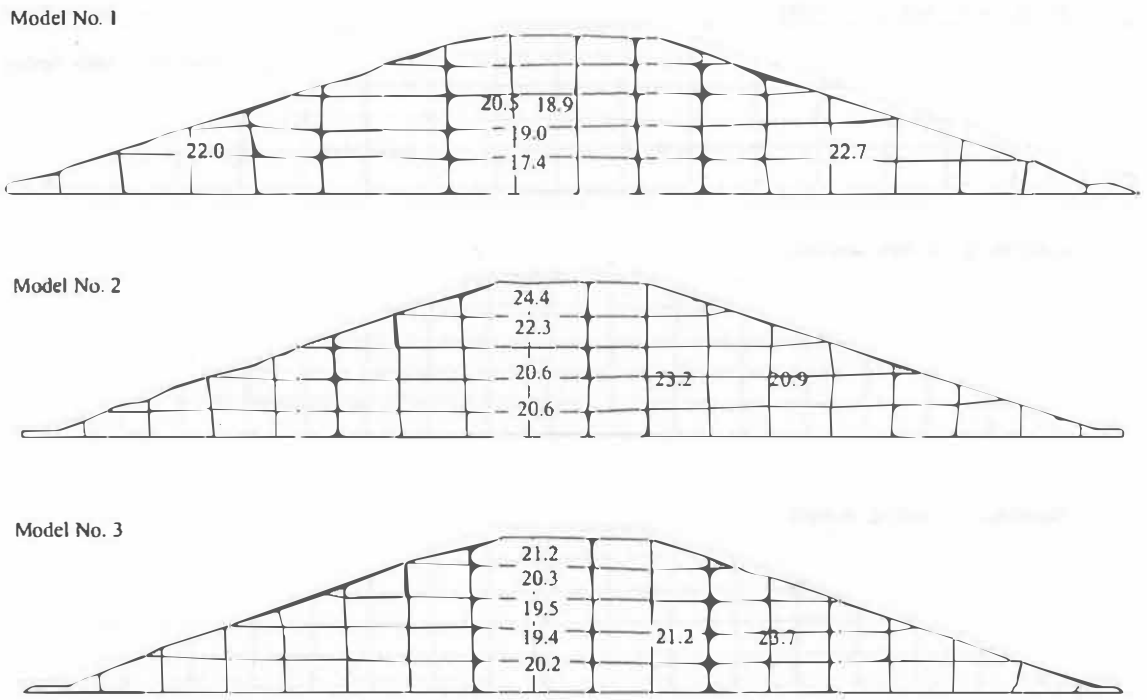

Figure 4.4: Moisture content (percent) determinations at various positions in models after testing

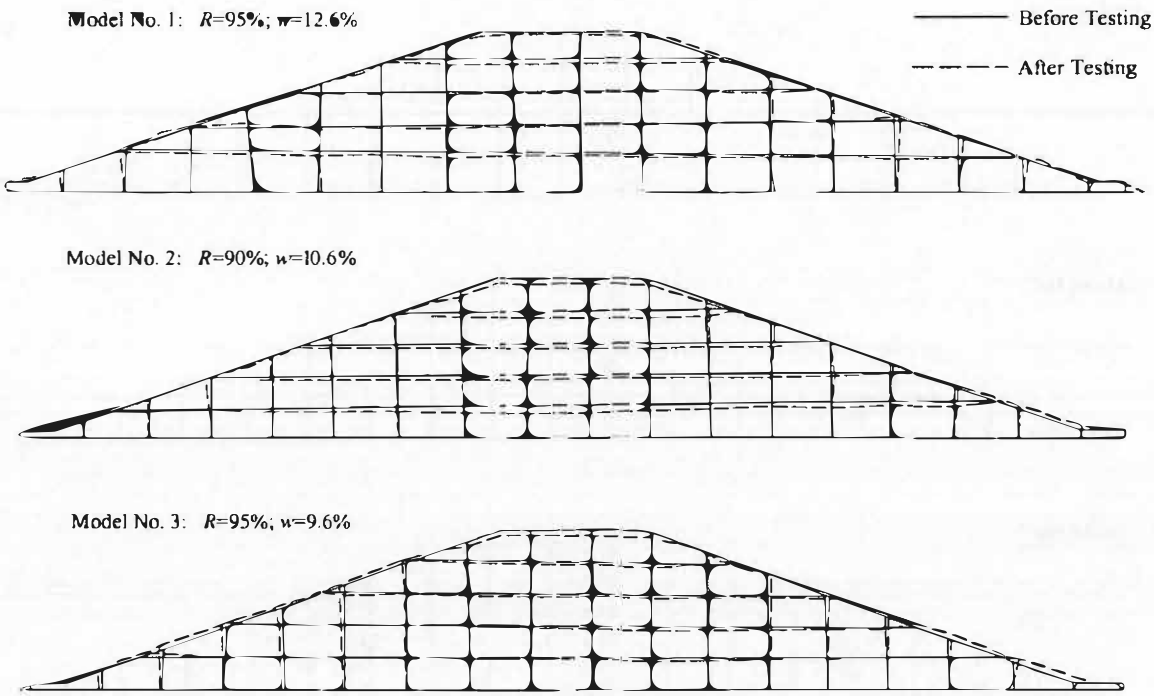

Figure 4.5: Side tracing of centrifuge model embankments before and after testing

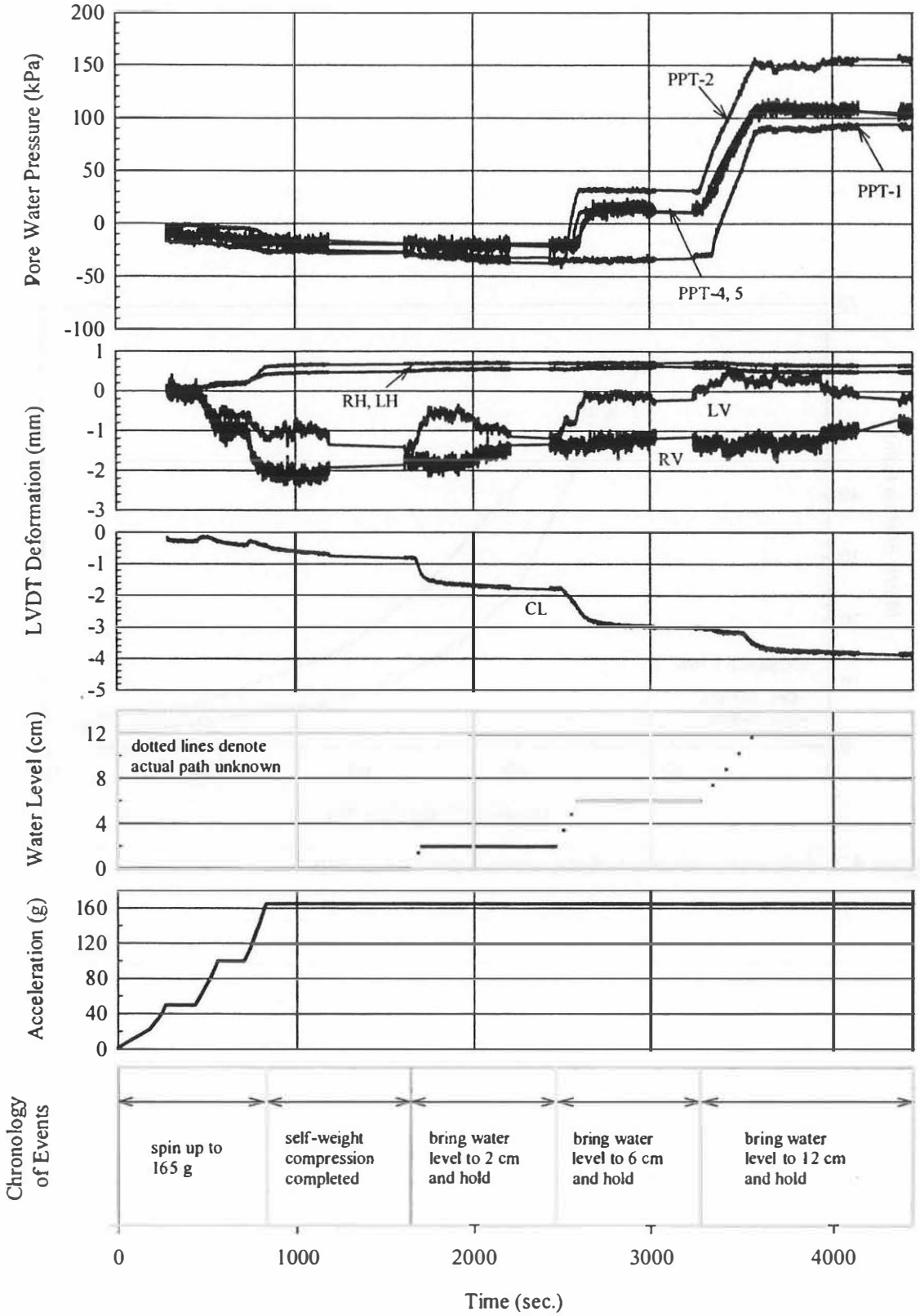

Figure 4.6: Results of centrifuge testing on Model No. 3

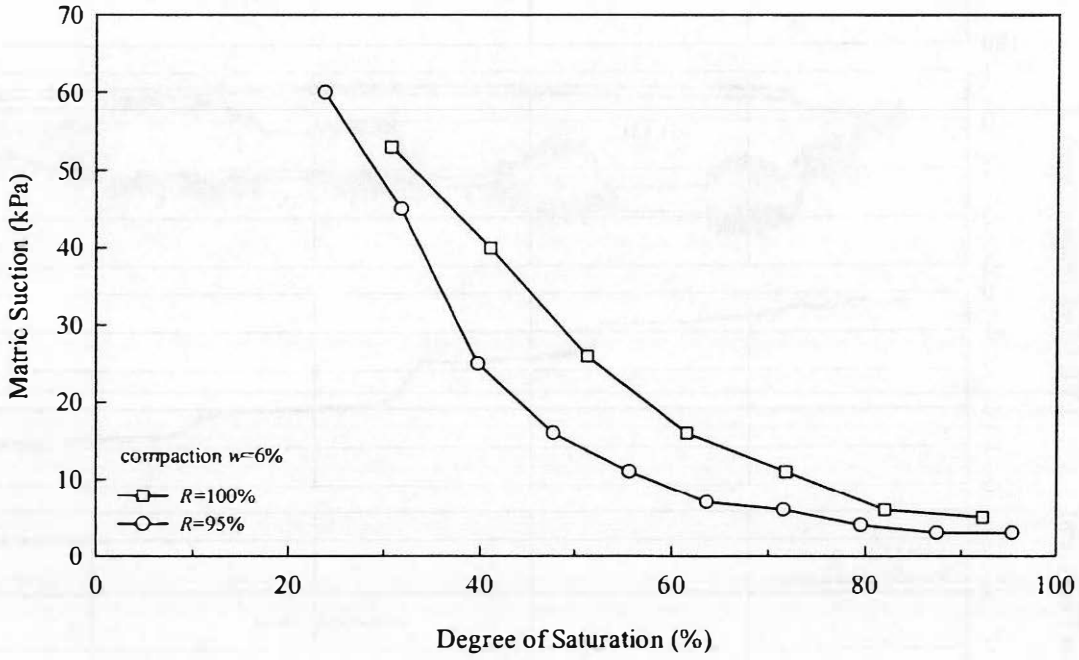

Figure 4.7: Soil-water characteristic curves for Minco Silt

Chapter 5: Field Study

5.1 Introduction

Further evaluation of the one-dimensional oedometer-based analysis was accomplished by comparing predictions with the settlement of an existing embankment. In this respect, the post-construction settlement of the Gaines Creek Bridge approach Embankment No. 2 was investigated. This embankment was selected as a case study because it was subjected to post-construction wetting following impoundment of a reservoir in which it is located. Thus, it is ideal for comparison to predictions based on fully wetted oedometer tests. This chapter will describe available information regarding the structural features of the abutment and associated approach embankment, subsoil conditions, as well as construction and maintenance records. A thorough field investigation of the fill materials and subsoil via a series of in-situ and laboratory tests is presented.

5.2 Structural Features & Subsoil Conditions

The embankment was located near Crowder, Oklahoma, as shown in Figure 5.1. It was constructed with a maximum height of 19.8 m above the natural ground surface and a side slope of 2.5:1 on the upper-half and 3:1 on the lower-half, as shown graphically in Figure 5.2. The embankment was compacted with materials obtained from adjacent flood plain borrow areas. Auger borings indicate that the top 3.7 m of borrow areas consist of predominately lean clays, fat clays, silts, and sands (U.S. Army Corps of Engineers 1960).

Construction records indicate that the average values of maximum dry unit weight and OMC were approximately 15.4 kN/m^3 and 23 percent, respectively. In-place unit weight measurements of soils compacted along the project alignment indicate that the embankment was compacted at dry unit weights higher than required by the U.S. Army Corps of Engineers embankment specifications, with an average relative compaction of 99 to 100 percent of AASHTO T-99. Compaction moisture contents for the embankment did not meet the specifications; they were on

average 5 percent below the OMC (Kellner and Rose 1971). The specifications call for compaction to at least 95 percent of the maximum dry unit weight, as determined by AASHTO T-99 (standard Proctor procedure), and to moisture content within 2 percent of the OMC.

The embankment was built on relatively flat flood-plain deposits with an average thickness of 12 m, composed primarily of moderately plastic clays interspersed with permeable lenses of silty sands, gravels, and sandstone boulders. The underlying bedrock strata are shales, sandstones, and siltstones of the Boggy Formation. The sandstones vary from soft to hard and from a few centimeters up to 12 m in thickness. The shales are mostly fissile and range from sandy to clayey shales (Kellner and Rose 1971). The pre-impoundment water table existed at a depth of about 3 m below ground surface (U.S. Army Corps of Engineers 1960).

The bridge., as depicted in Figure 5.2, is a 3-span, 165-m long, 8.2-m wide concrete deck constructed on a superstructure of four 2.3-m deep continuous plate girders. The two central piers are founded on firm, moderately hard shale, and 13 H-piles driven to the shale support the abutments, of which 8 are vertical and 5 are battered (Kellner and Rose 1971).

5.3 Deformation Records

This particular 19.8-m high embankment had experienced an estimated 0.61-m of settlement since construction as a result of post-construction lake impoundment (Kellner and Rose 1971). The construction work was initiated in 1956 and completed in August of 1962. Reservoir impoundment began about 2½ years after completion of the approach embankment and flooded to over half of the embankment's structural height approximately six months later.

To measure the horizontal and vertical earth movements, a slope indicator was installed in the embankment in August 1968 (Kellner and Rose 1971). Vertical movements on the order of 0.16 m were registered at the top of the slope indicator since installation and most continuing settlements recorded by the slope indicator were occurring in the unsaturated portion of the fill. Prior to installation of the slope indicator, additional vertical settlement on the order of 0.46 m was estimated from measurements of the differential movement between embankment soil and

the abutment backwall. Figure 5.3 depicts the deformation records from the time construction was completed until 1971.

5.4 Forensic Investigation Procedure

In 2001, a forensic investigation was initiated jointly by the University of Oklahoma and ODOT. Four conventional test borings, of which three utilized the continuous sample tube system (ASTM D 6282) and one used the thin-walled tube sampling technique (ASTM D 1587), were conducted as part of this investigation. In addition, three friction cone penetration tests (CPT) (ASTM D 5778) were conducted. Drilling was conducted on the pavement using hollow-stem augers in each case. The locations of the test borings and CPT soundings are depicted in Figure 5.4.

In the continuous tube sampling procedure, a 8.25-cm inner diameter and 1.52-m long split sample barrel was advanced into the soil to obtain disturbed samples. Of the three borings conducted using this procedure, one boring was advanced down to the top of the bedrock, while the remaining borings were terminated at the top of the underlying subsoil. In the thin-walled tube sampling procedure, a 6.3-cm inner diameter thin-walled seamless tube was pushed into the soil to obtain relatively undisturbed samples. Thin-walled tube samples were obtained at 1.52-m intervals through the fill into the underlying subsoil. A 3.57-cm diameter and 60° apex friction cone was used in the CPT sounding. Of the three CPT soundings, one was terminated within the fill, while the remaining were continued down to the underlying subsoil.

5.5 Laboratory & Field Tests

Because the focus of this study is on the evaluation and prediction of settlement of the embankment, compressibility and collapse characteristics of fill materials are mainly considered. Single-oedometer tests (ASTM D 5333) were conducted on the unsaturated, undisturbed samples at their corresponding overburden stress to quantify the collapse susceptibility of the existing fill materials. Consolidation tests (ASTM D 2435) were conducted on undisturbed specimens collected below the normal pool level for evaluation of compression behavior. Representative fill materials were composited and subjected to the single- and double-oedometer tests for later use in

the prediction of embankment settlement. In addition to these tests, selected disturbed samples were subjected to standard tests, including tests for grain-size distribution (ASTM D 422), Atterberg limits (ASTM D 4318), and natural moisture content. The undisturbed samples were subjected to various tests, including unit weight, natural moisture content, and unconfined compression (ASTM D 2166). Table 5.1 shows a summary of laboratory tests conducted in this study.

5.6 Results & Discussion of Laboratory & Field Tests

Soil Types & Index Properties

Index properties of the fill materials and/or subsoil for Boring Nos. 1, 2, and 3 are summarized in Figure 5.5. Results for individual test borings are given in Figures C-1 through C-3 of Appendix C. Table 5.2 summarizes the average fill characteristics determined from Figures C-1 through C-3. Referring to Figure 5.5 and Table 5.2, the fill materials are fairly homogeneous with predominantly moderate to high plasticity clay with occasional silt and sand layers and generally similar in the three test borings. Boring No. 3 tends to have more fines over its entire depth than other test borings, as indicated by the average plasticity index, clay-size fraction, and fines fraction. Also, fat clay is present at depths of between 13 m and 19 m in Boring Nos. 1 and 2.

Typical CPT results, along with the soil behavior type, are presented in Figure 5.6, and the remaining CPT results are included in Figures C-4 and C-5 of Appendix C. Soil behavior type from the CPT is defined using the soil behavior type chart proposed by Robertson et al. (1986). Comparing results from the conventional test borings and CPT sounding side-by-side reveals that they are in general agreement.

Field Dry Unit Weight & Moisture Content

Moisture content measurements in the fill are indicated in Figures 5.5 and 5.7, and dry unit weight values in the fill are given in Figure 5.7. Referring to these figures, the following observations are made:

1. The values of dry unit weight in the fill vary considerably; they are between 14.1 and 17.5 kN/m^3. The average dry unit weight is about 15.3 kN/m^3, which coincides with the in-situ unit weight measurements taken during field compaction.
2. There is no discernible difference in dry unit weight above and below the normal pool level; the dry unit weights are 15.5 and 15.3 kN/m^3, respectively. Using the double-oedometer test results presented in Figures 5.10 (a) and (b) as a guide, swell is estimated to occur above a depth of 5 m, while collapse at a depth greater than 5 m. It is well known that specimens undergoing swell experience a reduction in dry unit weight, while specimens undergoing collapse experience an increase in dry unit weight. However, such a trend is not observed. It is likely that the variability in dry unit weight during field compaction prevents any meaningful quantification of changes in dry unit weight after wetting. Consider that typical change in dry unit weight during inundation in a single-oedometer test is about 0.8 kN/m^3 for a measured vertical strain of 5 percent.
3. The values of dry unit weight of the subsoil are higher than in the fill, with an average of 16.5 kN/m^3. Furthermore, they fall within a tighter range than the fill, between 16.2 and 16.8 kN/m^3.
4. Natural moisture contents were high and relatively uniform within the fill, averaging about 26.6 percent, which is about 8 to 9 percent higher than the placement moisture content or 3 to 4 percent above the OMC of the fill.
5. There is no distinguishable difference in natural moisture content in the fill materials above and below the reservoir pool level, which is an indication of severe wetting throughout the embankment soil. Average moisture content above and below pool level is 27.1 and 26.3 percent, respectively. These data suggest wetting-induced deformation as a main mechanism of settlement for these embankments. Precipitation drained to the roadway shoulder (Pagen et al. 1968) and capillary effects are responsible for the moisture increase above the pool level.

6. The natural moisture contents of the subsoil fall in a tighter range than that of the fill, between 20.5 and 22.5 percent, with an average of 21.8 percent.

Collapse Potential

Three single-oedometer collapse tests were conducted on the undisturbed samples (collected above the normal pool level) at their corresponding overburden stress. Sample preparation consisted of carefully trimming an extruded thin-walled tube sample to fit into a greased oedometer ring. These specimens were then tested in a manner similar to compacted specimens discussed in Section 3.4. Test results demonstrated that these samples are not collapsible, as depicted in Figure 5.8. Specimens from a depth of 1.1 m exhibited negligible swell of 0.1 percent, while specimens from a depth of 6.4 and 8.0 m registered collapse potential less than 0.1 percent when inundated at vertical stress of 100 and 200 kPa, respectively. On the other hand, using the double-oedometer test results given in Figures 5.10 (a) and (b), collapse strain between 2 to 4 percent at stress levels of 150 to 200 kPa would be expected for samples at their as-compacted moisture conditions. The negligible collapse potential observed in single-oedometer tests on the undisturbed samples is a result of severe post-construction wetting that has occurred in the field.

Consolidation Properties

Results of one-dimensional consolidation tests conducted on undisturbed specimens collected below the pool level are given in Figure 5.9. The compression ratio after adopting Schmertmann's reconstruction technique (1953) and the saturated prestress (or preconsolidation pressure) in conjunction with the overburden stress are plotted in Figure 5.7. The compression ratio, $C_{\varepsilon c}$, values determined from the consolidation test vary between 0.10 to 0.18 in the fill and subsoil. Hence, fill materials and subsoil can be considered moderately compressible beyond the saturated prestress according to Coduto (1994). The recompression ratio, $C_{\varepsilon r}$, values estimated

from the consolidation test is 0.02, which indicates very slightly compressible soil below the saturated prestress.

With one exception, all saturated prestresses in the fill calculated from the one-dimensional consolidation tests compare fairly well to the overburden stresses. These results are consistent with the findings of Nwabuokei and Lovell (1985). Nwabuokei and Lovell report, that for moderately plastic clay compacted to or less than the standard Proctor effort, the saturated prestress equals or slightly exceeds the confining pressure during saturation.

There are two possible reasons for the large difference between soaked prestress and the overburden stress at a depth of 15.4 m. First, Casagrande's method is subjective and can be difficult in getting a good estimate of saturated prestress especially when there is no well-defined break in the stress versus logarithm of strain curves. Second, the large difference between soaked prestress and the overburden stress may be due to extremely high compaction prestress induced during field compaction for the layer in question. Nwabuokei and Lovell (1985) report that for a given confining pressure during inundation, the clay compacted at modified Proctor effort has a higher soaked prestress than the same clay compacted at standard Proctor or lower effort. As depicted in the CPT-1 and CPT-3 profiles, there is a noticeable increase in tip resistance at the depth in question.

Undrained Shear Strength

The undrained shear strength, s_u, values determined from the unconfined compression test are highly scattered in the fill and scattered to a lesser extent in the underlying subsoil, as depicted in Figure 5.7. The values are between 15 and 99 kPa, and 68 and 117 kPa in the fill and subsoil, respectively. Acknowledging that that the unconfined compression test data are generally unreliable (DeGroot and Sheahan 1995), the fill materials vary from soft to very stiff clay, and the underlying soil is of very stiff clay (Das 1998).

5.7 Results & Discussion of Oedometer Tests

Three representative composite samples were selected on the basis of the index properties and subjected to the oedometer tests. Sample Nos. 1 and 2 consisted of material from Boring No. 1 from depths of 6.4 to 10.7 and 13.7 to 18.5 m, respectively. Sample No. 3 was composed of material from boring No. 2 from depths of 5.1 to 8.6 m. To assess the heterogeneity of the fill materials with depth, material at 1.5 m intervals was combined and subjected to classification as well as compaction tests; Sample Nos. 4 and 5 are composed of material from 0 to 9.1 m and 9.1 to 18.2 m, respectively. The properties of the test soils are listed in Table 5.3. It is noted that the dry unit weight range for the embankment soils (see Table 5.3) is overall, higher than those determined previously in the compaction-control laboratory tests. This may have resulted from physicochemical changes of the embankment soils since being excavated from the borrow area.

Double-oedometer specimens were compacted at a dry unit weight and a moisture content corresponding to that of the average value for the embankment as determined from the compaction-control tests. An additional single-oedometer test inundated at 400 kPa was performed to use for comparison with the double-oedometer test results. Test results are depicted in Figure 5.10 and tabulated in Table C-1 through C-3 of Appendix C. Referring to the results, several important observations are made as follows:

1. Single- and double-oedometer data are in reasonably good agreement.
2. Complete saturation prevailed in the single-oedometer test specimens. These samples attained an average degree of saturation of 100 percent at the end of a 24-hour soaking period.
3. Sample Nos. 1 and 2 show similar collapse potential, as well as as-compacted and soaked compression over stress levels investigated. This is partly attributed to their similar soil properties and partly because they were tested under similar conditions, i.e., molding moisture content and dry unit weight.

4. The fill exhibits swelling behavior based on the double-oedometer results. Swelling occurs to a lesser extent for Sample Nos. 1 and 2 compared to Sample No. 3 because of the lower clay-size fraction of Sample Nos. 1 and 2.
5. All samples have considerable collapse potential when they were compacted dry of the OMC.
6. The point at which the as-compacted and soaked curves diverge, as given in Figure 5.10, is near 80 kPa for Sample Nos. 1 and 2 and near 180 kPa for Sample No. 3. These data indicate that collapse may occur in soil in which the overburden depth exceeds about 4.4 to 10 m. Hence, the embankments are sufficiently high for collapse to occur in the lower ½ to ¾ of the embankments.

5.8 One-Dimensional Settlement Prediction

The collapse settlement at the centerline of the embankment was predicted using the double-oedometer test results in Figure 5.10 in a manner similar to that used with the results of the centrifuge tests presented in Section 4.7. Predictions of centerline settlement are made from the time construction was completed until 1968 and 1971. It is assumed that complete wetting prevails in the embankment just below the normal pool level, i.e. 10.7 m below the top of the embankment in 1968 and by 1971 the entire embankment is completely wetted.

As indicated in Section 5.5.1, fat clay is predominant at greater depths and moderately plastic clay is generally found at shallow depths in the embankment. Hence, double-oedometer test results for moderate plastic clay as given in Figures 5.10 (a) and (b) were used for the prediction of collapse settlement for the upper 13 m of the fill. On the other hand, double-oedometer test results for fat clay, given in Figure 5.10 (c), were used for the prediction at depths greater than 13 m.

5.9 Comparison of Predicted & Measured Centerline Settlements

Comparing the measured and predicted centerline settlements reveals that the one-dimensional oedometer-based method under-predicted the centerline collapse settlements of the embankment by a factor of between 1.4 and 1.6. The predicted centerline collapse settlements were 0.32 and

0.39 m in 1968 and 1971, respectively; while estimated centerline collapse settlements were 0.46 and 0.61 m in 1968 and 1971, respectively. This coincides with predictions of collapse settlement at the centerline of the centrifuge model embankments presented in Chapter 4, in that collapse settlements in these models were under-predicted by a factor between 1.4 and 2.6. Several factors can be identified as having significant effects on the quality of prediction:

1. The one-dimensional model does not properly account for the two-dimensional nature or shear-induced deformation of collapse settlements in embankments (see Section 4.8).
2. The variability in fill materials with respect to soil type, compaction dry unit weight, and moisture content as evidenced in the field construction records and index properties results may also contribute to prediction discrepancy. Based on a comparison of U.S. Bureau of Reclamation laboratory consolidation test results and embankment compression measurements, Sherard et al. (1963) report that laboratory compression tests roughly approximated the measured field compressions because of the variability in fill materials.
3. Significant fabric differences between laboratory- and field-compacted clays, as suggested by Barden (1974), may also impact the quality of prediction. White (1980) stated that extrapolation of laboratory results to field situations is questionable based on published results in the literature.
4. Consolidation of foundation soil that was neglected in the settlement prediction may have contributed to the overall settlement of the embankment. Consolidation settlement of the subsoil was estimated from a consolidation test (presented in Section 5.5.4) by means of the Terzaghi consolidation theory. It was estimated that a 0.20-m settlement would occur, most of it during construction.

Other uncertainties associated with field settlement measurements may also have contributed to the quality of prediction. Given the many uncertainties, predictions based on the one-dimensional oedometer data are quite reasonable.

The substantial collapse settlement of the embankment reveals the importance of using quality fill materials and/or stringent quality control during embankment construction. This is especially true in light of the severe damage to the bridge abutments that has directly resulted from embankment soil deformation. As most of the fill materials for the embankment are classified as the AASHTO designated A-6 and A-7 soils, they are generally regarded as being less desirable for embankments because of the collapse susceptibility mentioned in Section 3.7.1. Sherard et al. (1963) report that even though some U.S. Bureau of Reclamation dams were compacted at moisture contents as low as 3 percent below the standard Proctor OMC, none of them experienced any swell or collapse because none of these dams was constructed of soils with large percentage of high plasticity fines. In situations where quality fill materials are not available within a reasonable haul distance, good quality control, more stringent compaction requirements, and/or utilization of chemical stabilizers may be needed for embankment construction, particularly for large embankments and embankments susceptible to flooding.

Prediction of settlement at the embankment centerline was also made using the settlement charts presented in Figure 3.14. Prediction gives a value of 0.60 m, which compares well with the measured settlement of 0.61 m as of 1971.

Table 5.1: Summary of laboratory tests conducted on fill materials

Type of test	Field samples				Composite samples				
	B-1	B-2	B-3	B-4	No. 1	No. 2	No. 3	No. 4	No. 5
Atterberg Limits	12	12	18	---	1	1	1	1	1
Grain-Size Distribution	12	12	18	---	1	1	1	1	1
Field Dry Unit Weight	---	---	---	37	---	---	---	---	---
Natural Moisture Content	12	12	19	37	---	---	---	---	---
Single-Oedometer	---	---	---	3	1	1	1	---	---
Double-Oedometer	---	---	---	---	2	2	1	---	---
Consolidation	---	---	---	7	---	---	---	---	---
Unconfined Compression	---	---	---	18	---	---	---	---	---
Standard Proctor	---	---	---	---	1	1	1	1	1

Note: Numbers indicate number of tests conducted.

Table 5.2: Average soil properties of the fill materials from Boring No. 1, 2, and 3

Boring No.	Plasticity index	Fines fraction (%)	Clay-size fraction (%)	Dominant Soil Types
1	27	87	49	Fat clay, Lean clay, Sandy lean clay
2	26	84	46	Fat clay, Fat clay with sand, Lean clay with sand, Sandy lean clay
3	32	92	55	Fat clay

Table 5.3: Properties of the composite samples

Composite sample No.	AASHTO classification	USCS classification	Liquid limit	Plasticity index	Fines (%)	Clay-size fraction (%)	Max. dry unit wt. (kN/m^3)	OMC (%)
1 [a]	A-7-6 (18)	CL	48	28	69	50	16.5	19.1
2 [a]	A-7-6 (19)	CL	49	30	68	51	16.3	19.3
3 [b]	A-7-6 (32)	CH	57	35	85	64	15.4	21.2
4 [c]	A-7-6 (17)	CL	45	26	70	52	16.5	19.6
5 [c]	A-7-6 (14)	CL	46	23	67	52	16.4	19.5

[a]Sample Nos. 1 and 2 consisted of material from Boring No. 1 from depths of 6.4 to 10.7 m and 13.7 to 18.5 m, respectively.
[b]Sample No. 3 was composed of material from boring No. 2 from depths of 5.1 to 8.6 m.
[c]Sample Nos. 4 and 5 were composed of material from 0 to 9.1 m and 9.1 to 18.2 m, respectively.

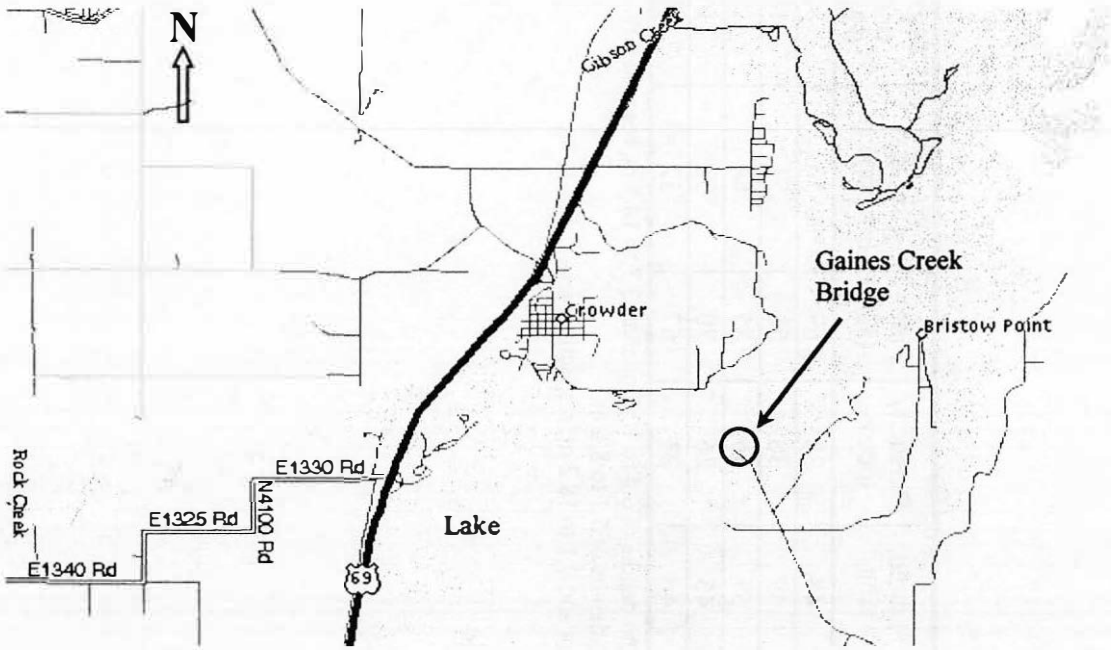

Figure 5.1: Location of the Gaines Creek Bridge approach embankments

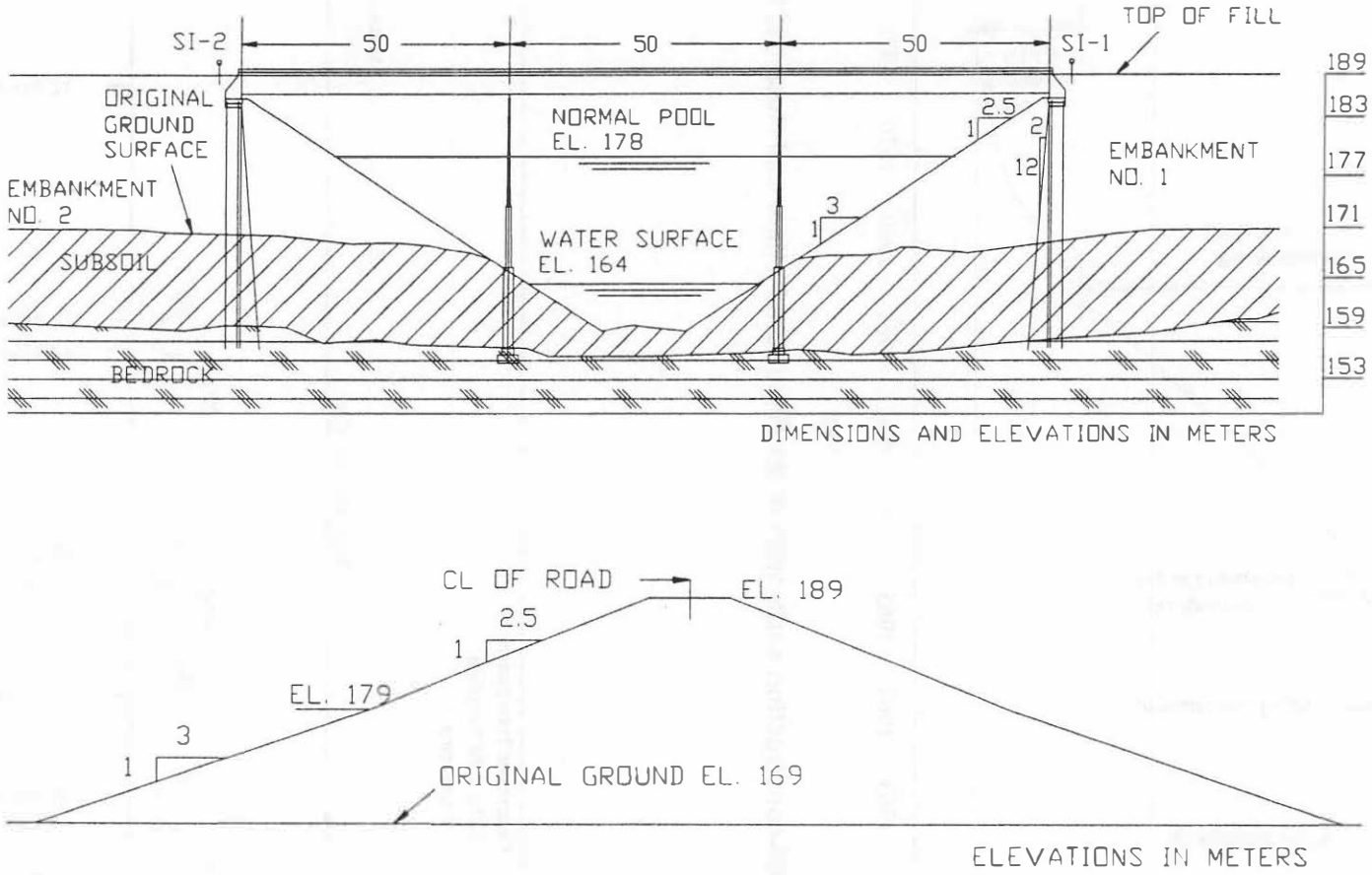

Figure 5.2: Elevation and section view of the approach fills (from Kellner and Rose 1971)

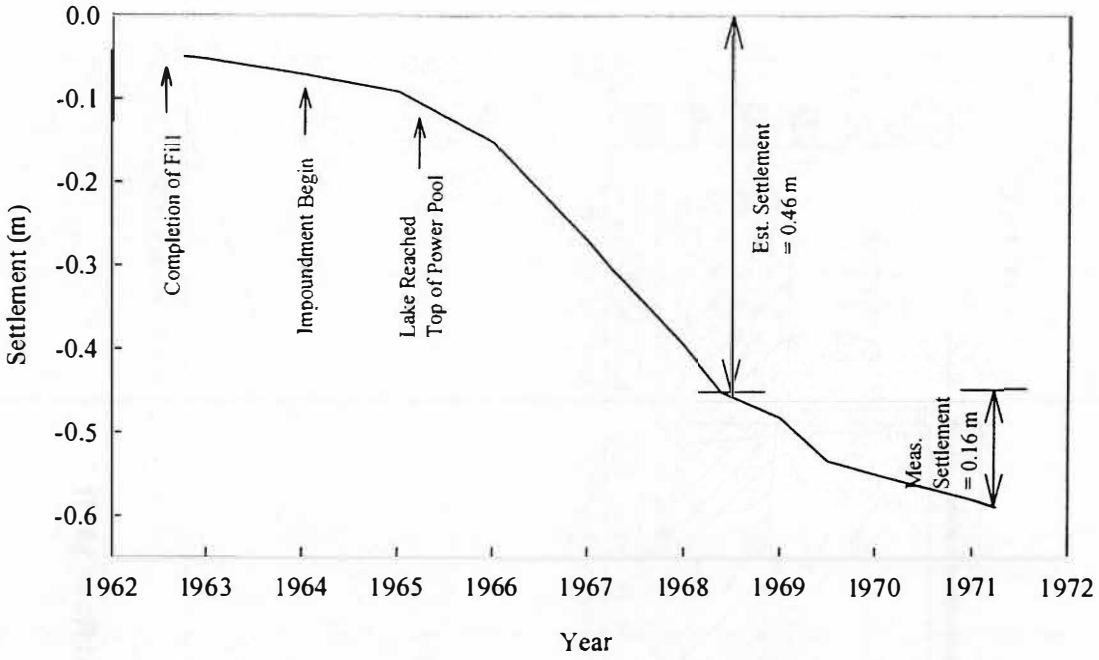

Figure 5.3: Post-construction settlement of the fills (from Kellner and Rose 1971)

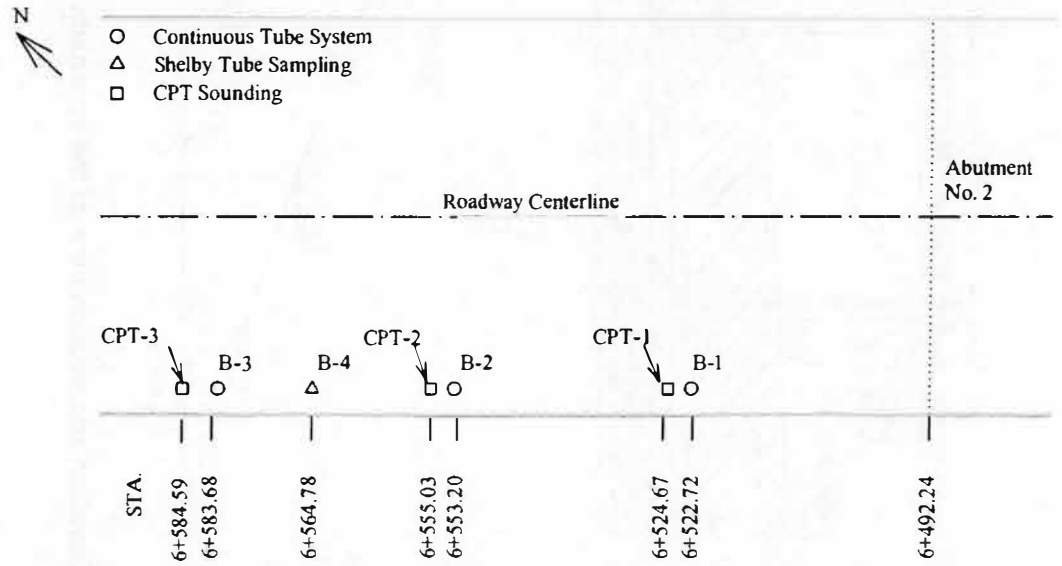

Figure 5.4: Locations of test borings and CPT soundings at the embankment

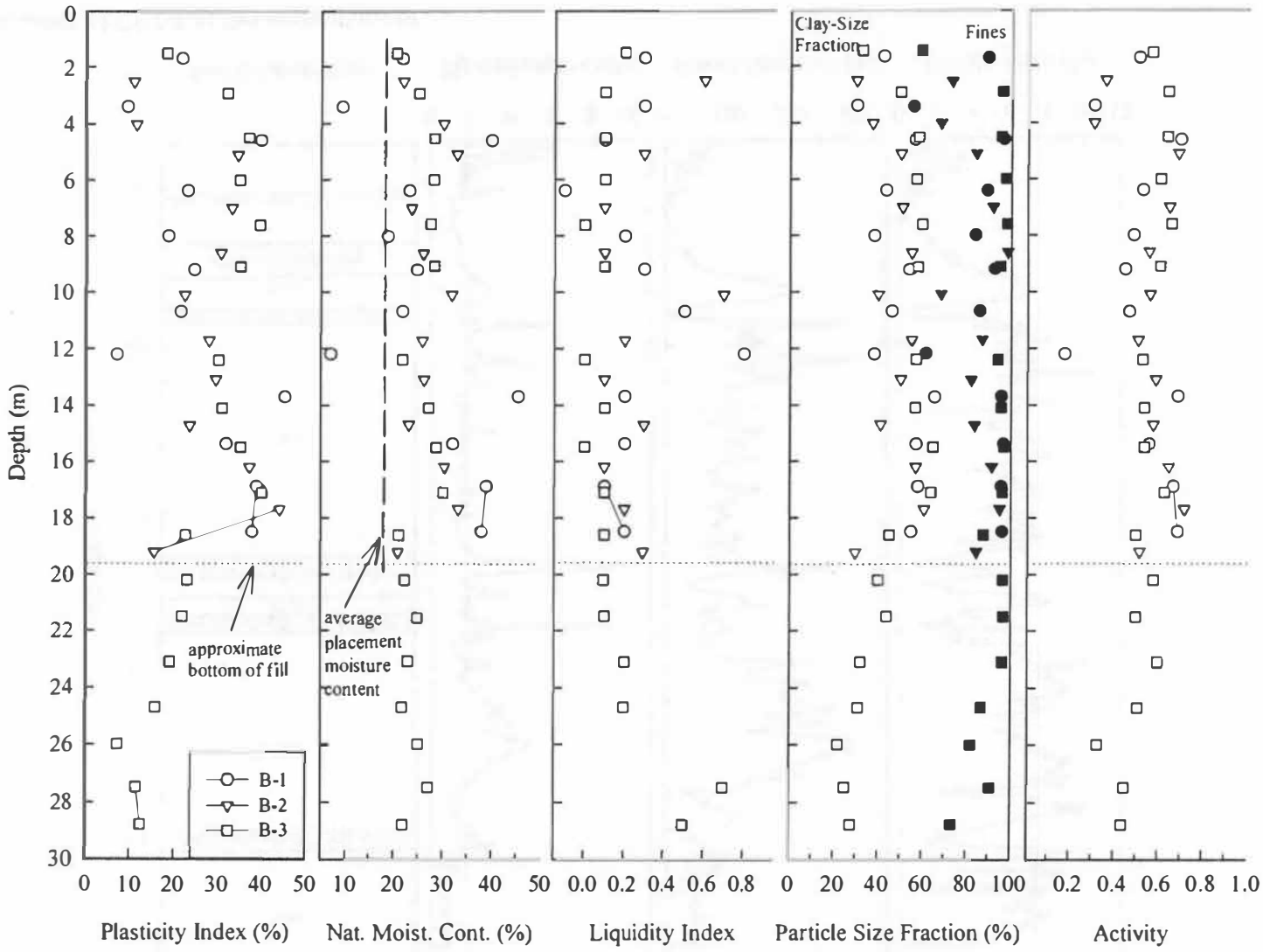

Figure 5.5: Index properties and natural moisture content

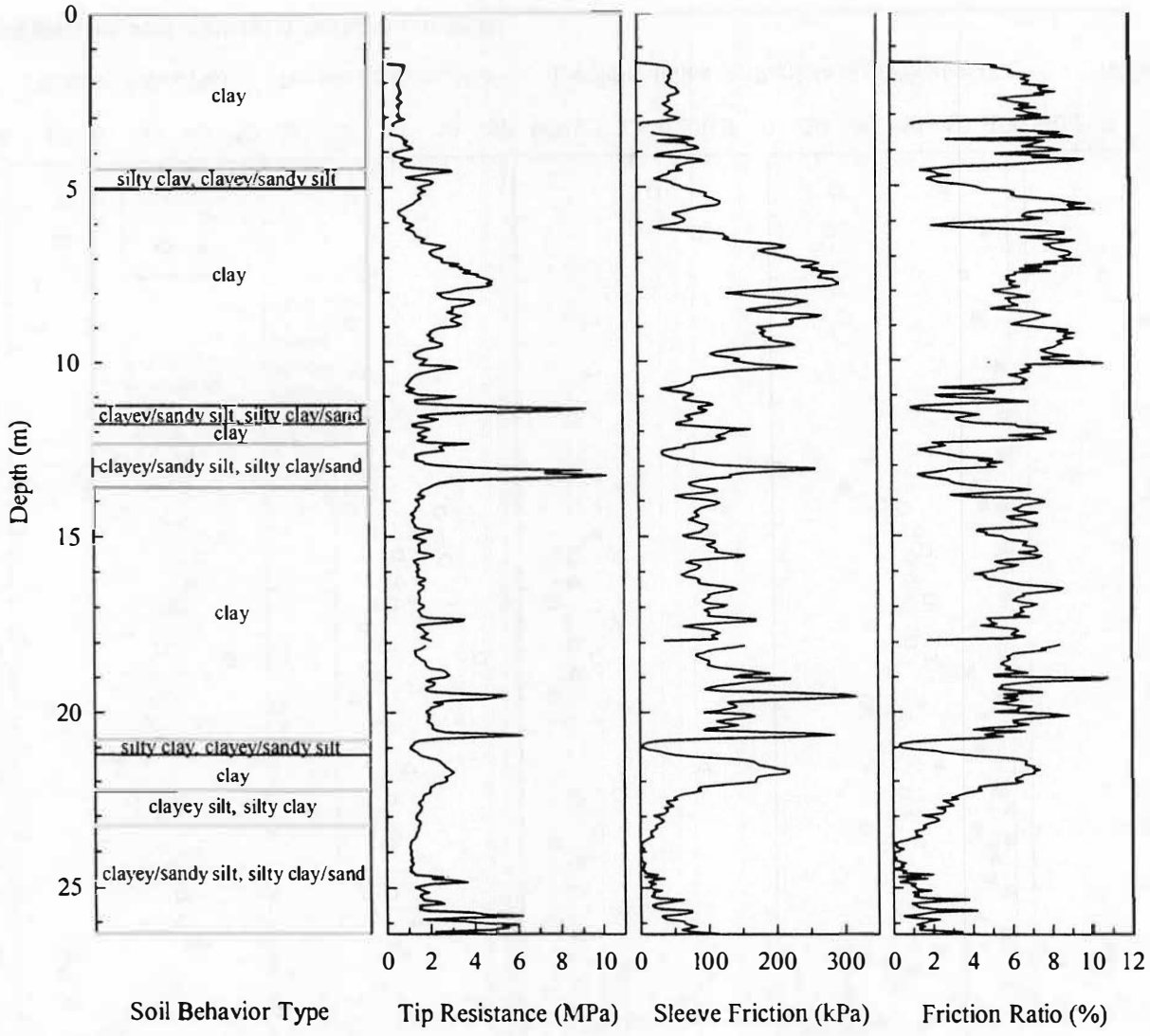

Figure 5.6: Results of CPT-1 at the embankment

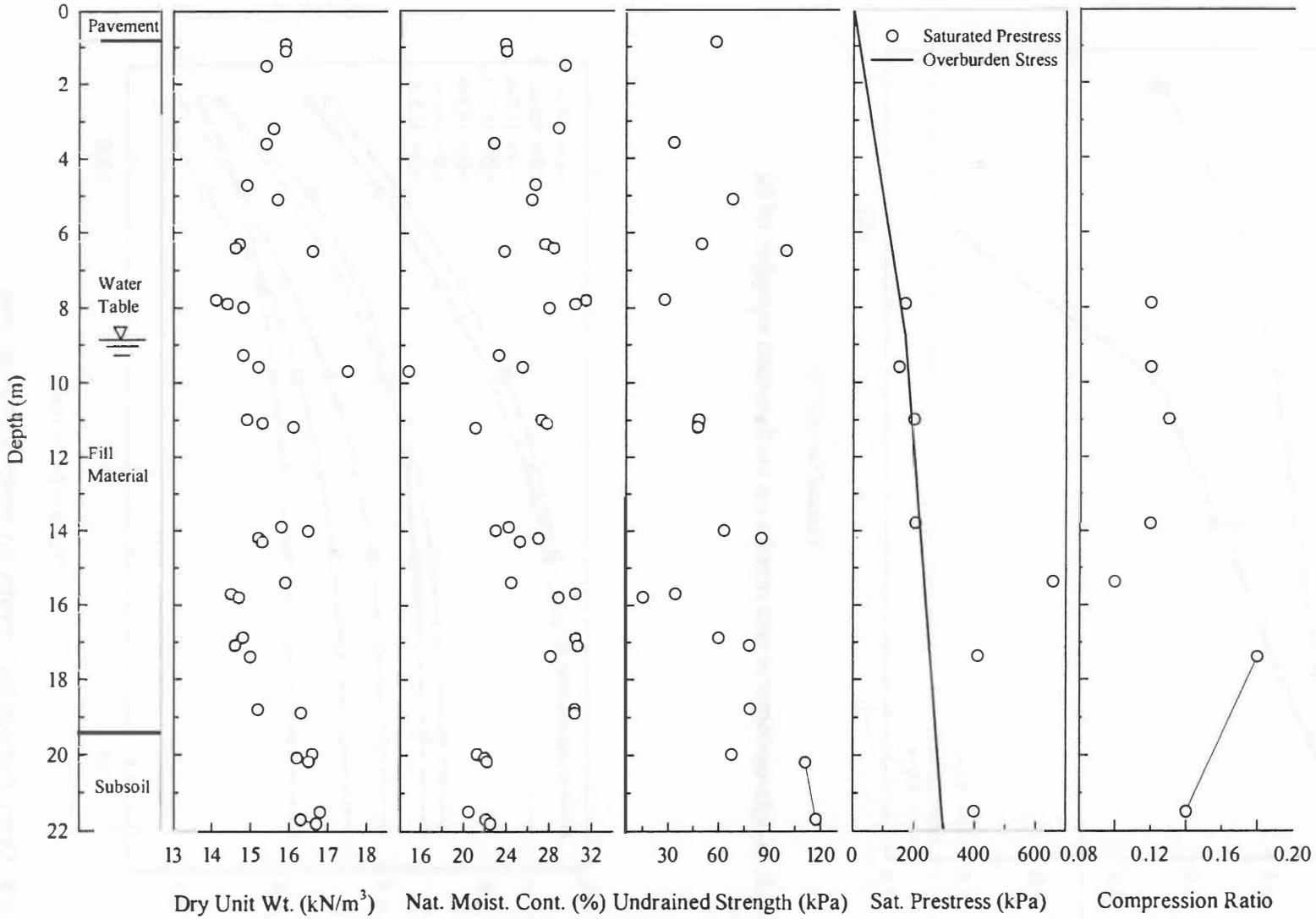

Figure 5.7: Soil characteristics for Boring No. 4 at the embankment

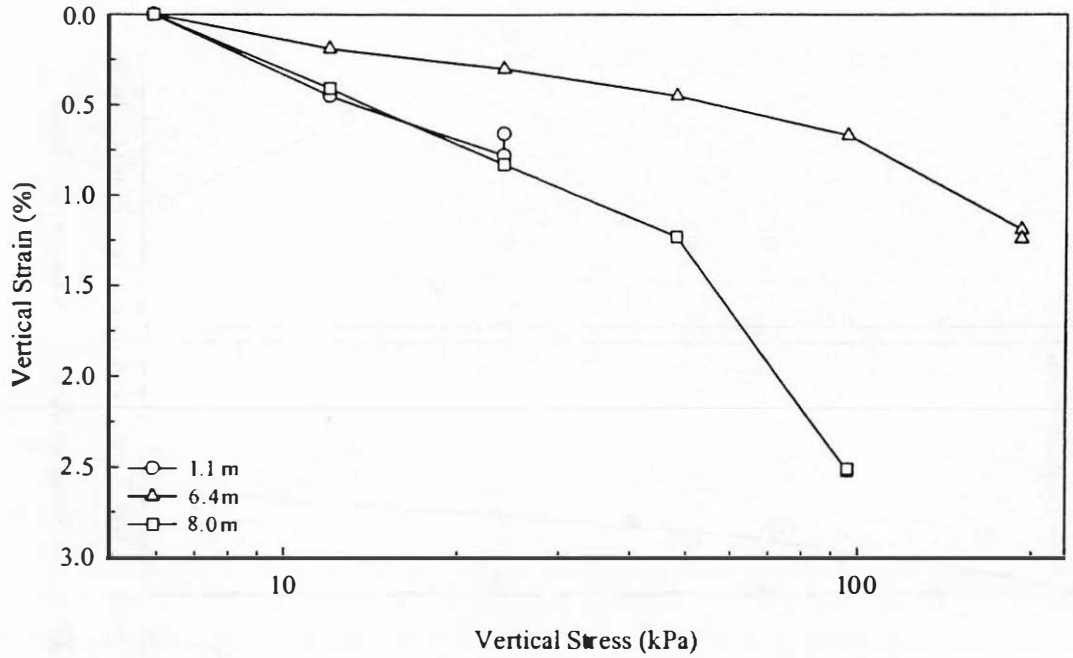

Figure 5.8: Single-oedometer test results on undisturbed samples of fill

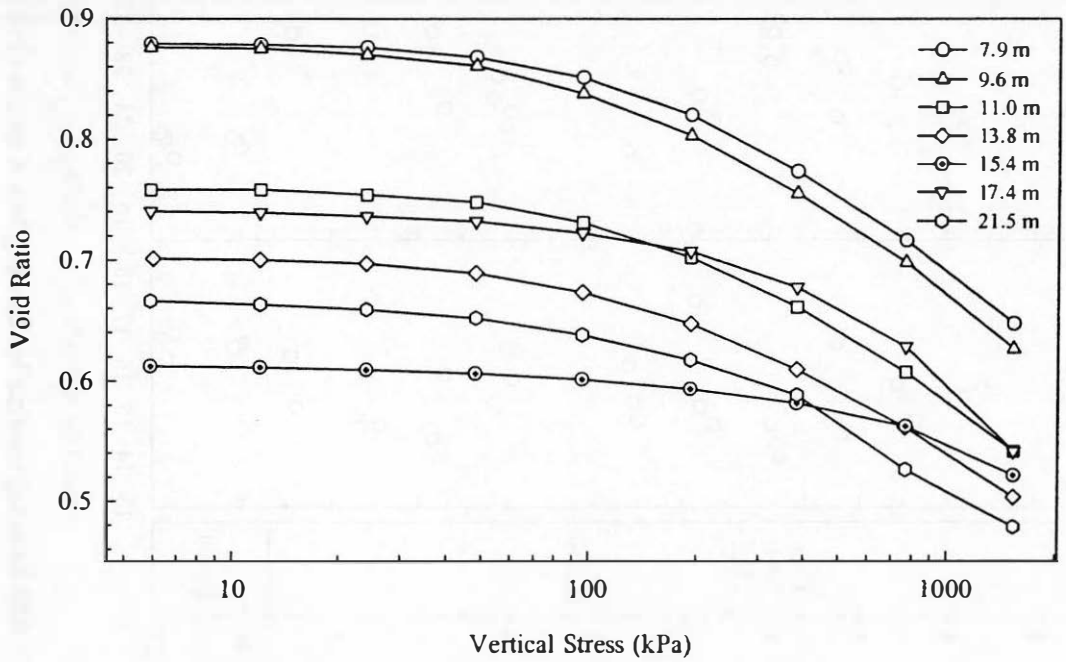

Figure 5.9: Consolidation test results on undisturbed samples

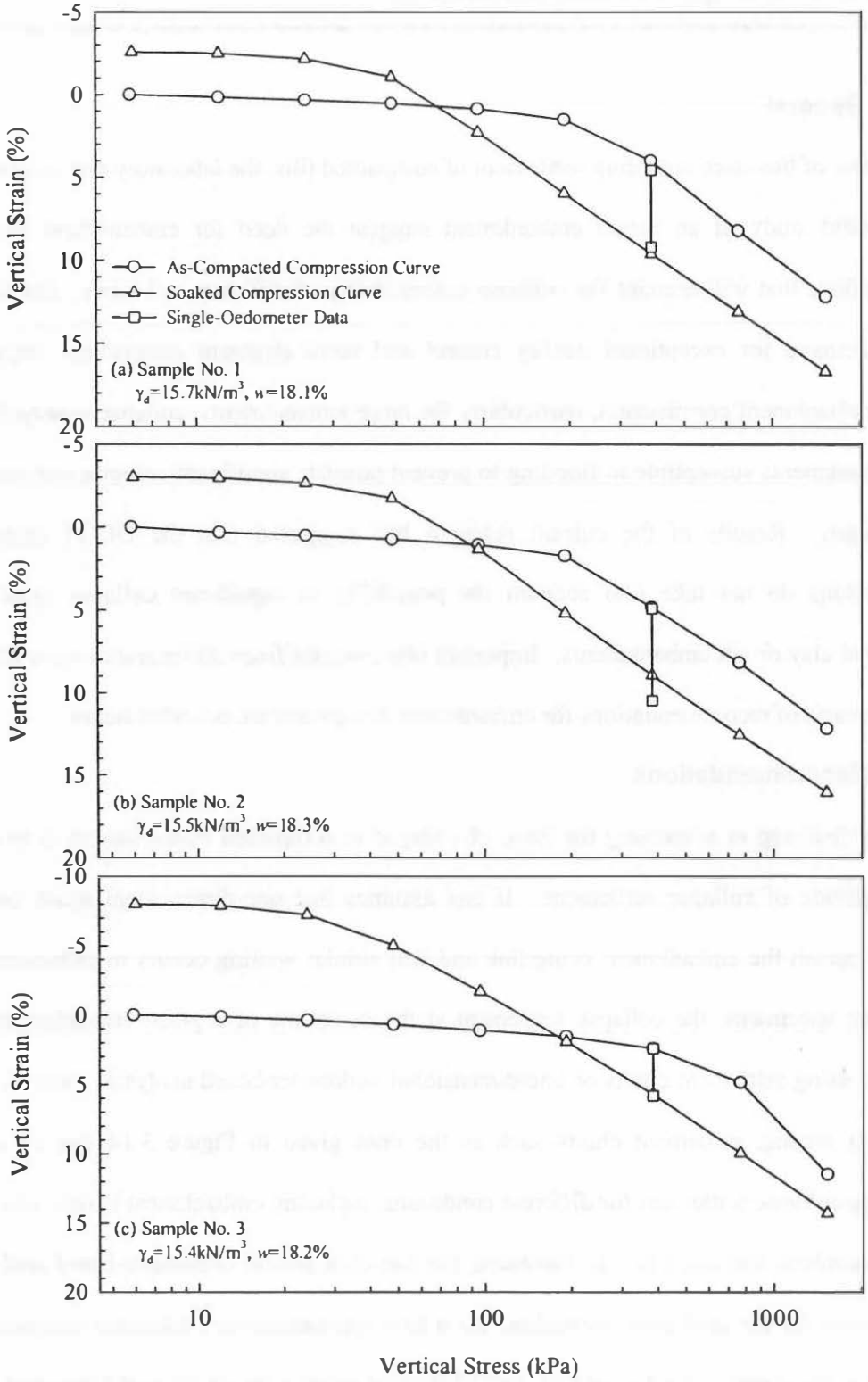

Figure 5.10: Single- and double-oedometer test results for composite compacted Sample Nos. 1, 2, and 3

Chapter 6: Design Recommendations

6.1 General

The review of literature regarding settlement of compacted fills, the laboratory test results, as well as the field study of an actual embankment suggest the need for embankment design and specifications that will account for collapse susceptibility of different soil types. Specifications should demand for exceptional quality control and more stringent compaction requirements during embankment construction, particularly for large embankments, collapse-susceptible soils, and embankments susceptible to flooding to prevent possible significant collapse settlement after construction. Results of the current research has suggested that the ODOT embankment specifications do not take into account the possibility of significant collapse settlement in compacted clay or silt embankments. Important observations from this research were adopted to form the basis of recommendations for embankment design and are provided below.

6.2 Recommendations

The very first step in addressing the issue of collapse in compacted embankments is to estimate the magnitude of collapse settlement. If one assumes that one-dimensional strain conditions prevail beneath the embankment centerline and that similar wetting occurs in embankment and oedometer specimens, the collapse settlement at the centerline of a given embankment can be predicted using settlement charts or one-dimensional oedometer-based analysis. Prior to double-oedometer testing, settlement charts such as the ones given in Figure 3.14 can be used for estimating collapse settlement for different conditions, including embankment height, compaction moisture content, and soil type. If warranted, the one-dimensional oedometer-based analysis can be employed for the settlement estimates. As a first approximation, oedometer samples can be prepared at the expected field condition, i.e., 95 percent relative compaction and moisture content of between 4 percent below and 2 percent above the OMC. Lower moisture contents are more conservative and should be based on local construction practice. Partial wetting may occur in

embankments above water, i.e., typical highway embankments not in reservoirs; however, even in such embankments the degree of saturation may eventually become significant, as indicated in Section 4.8. Thus, assuming similar wetting is prevalent in embankments above water and in oedometer specimens may be reasonable and is conservative. For embankments with direct contact with water, such an assumption would be even more appropriate.

If predicted settlement suggests the likelihood of excessive differential settlement between the approach embankment and the bridge structure, the following suggestions may be appropriate during construction. Because swelling is nonexistent in silts, the use of a dry unit weight corresponding to greater than 95 percent relative compaction to reduce collapse settlement in compacted silt embankments is legitimate. Adopting a compaction moisture content equal to the OMC or above will help to reduce collapse potential. The selection of an appropriate combination of dry unit weight and moisture content that will result in negligible collapse potential for the expected stress level can be performed with the aid of the double-oedometer test. In the case of clayey soils, collapse potential can be reduced by compacting at a higher dry unit weight, keeping in mind that swelling increases with increasing dry unit weight; hence, selection of an appropriate placement dry unit weight for clayey soils may be more complicated. For compacted clay embankments, the use of greater relative compaction to reduce collapse settlement may be appropriate if excessive swelling can be prevented, such as at greater depths where collapse is possible. It is recommended that the placement moisture content be adjusted to the OMC to reduce collapse and swell movement resulting from wetting. As before, the selection of an appropriate combination of compaction parameters can be performed using the double-oedometer test. Obviously, the success of the preceding suggestions greatly depends on how well compaction requirements are enforced in the field.

Although the recommendations in the current research primarily deal with adopting more stringent compaction requirements to reduce collapse settlement in compacted fills, it is important to point out that there are other methods of achieving this goal. For example, select fill materials

could be used to reduce collapse settlement in compacted fills. In addition, the use of chemical stabilizers has been shown to reduce collapse potential (Miller et al. 1997, Lawton et al. 1993). To optimize cost-efficiency, these methods for reducing collapse deformations can be applied to critical zones within the embankment, i.e., at centerline depths where stresses are sufficient to cause collapse.

Chapter 7: Conclusions & Recommendations

This chapter presents conclusions from the current study on the evaluation of settlement potential of various Oklahoma soils and the development of a design and construction method to overcome settlement problems of embankments. In addition, the suggestions for future research are discussed.

7.1 Conclusions

Results of oedometer testing on 22 Oklahoma soils that represent most of the AASHTO soil classes led to the following conclusions:

1. Considerable amount of collapse can occur in silts and clays compacted within ODOT embankment specifications suggesting the specifications require modification to properly address collapse settlement in embankment design and construction.
2. Collapse can occur over a wide range of dry unit weights depending on soil type. Dry unit weight alone cannot be used to assess collapse susceptibility, because different soils may be stable for different ranges of dry unit weight, stress state, and moisture condition.
3. Satisfying the dry unit weight criterion alone (for instance, for a relative compaction of 95 percent) is not sufficient to prevent collapse settlement in compacted embankments, because compaction moisture content can influence collapse index in addition to dry unit weight.
4. Collapse index can be significant for some cohesive soils (for instance, Hennessey Shale 2, Boggy Shale, Heiden Clay, Lomill Clay, Bosville Clay, and Dennis Clay) compacted at optimum and/or 2 percent wet of optimum moisture content for a relative compaction of 95 percent.
5. Cohesionless soils compacted within ODOT embankment specifications were not collapse-susceptible. Silty soils from the AASHTO designated A-4 group compacted within ODOT embankment specifications exhibited a slight degree of collapse with collapse index of less than 2 percent at a vertical stress of 200 kPa. Clayey soils from the AASHTO designated A-6

and A-7 groups exhibited considerable collapse index, on the order of 0.5 to 7.1 percent at a vertical stress of 200 kPa. These soils, which most compacted fills are constructed from, are less desirable for embankments because of the collapse susceptibility.

6. Collapse index decreases approximately linearly with degree of saturation and moisture content for a given relative compaction. Depending on soil type, this reduction in collapse index varied from negligible in cohesionless soils to substantial (between 1.2 to 4.4 percent) in clays.
7. Factors related to fines composition can be used for identification of collapsible soils. Collapse index increases with increasing plasticity index, liquid limit, activity, and clay-size fraction for a given molding moisture content and compaction effort.
8. Collapse index is observed to increase with increasing AASHTO group index for a given molding moisture content and compaction effort.
9. Slake durability index did not correlate with collapse index of non-durable soil-like shales.
10. Statistical analysis of the single-oedometer data enabled the development of a predictive model for estimating collapse index. Variables that have the most impact on collapse index are the moisture content, dry unit weight, plasticity index, and clay-size fraction.
11. In general, specimens prepared at a moisture content 4 percent dry of the OMC had comparable compressibility at applied stresses less than 200 kPa regardless of soil type. Compressibility at higher moisture contents, on the contrary, varied over a wider range.
12. Time rate of collapse for cohesionless soils was faster than that of cohesive soils based on oedometer testing. The majority of collapse measured in cohesionless samples was completed in less than 30 minutes. A significant difference in time was observed for collapse to be completed for cohesive samples. Some cohesive soils require considerably longer times, up to 24 hours, for collapse to be completed as a result of low permeability in these soils.

Results of oedometer testing, centrifuge modeling, and predictions of embankment settlement for compacted Minco Silt led to the following conclusions:

1. Centrifuge modeling of compacted embankments proved valuable for discerning between self-weight and collapse settlements.
2. Substantial self-weight settlement occurred in model embankments compacted dry of the OMC to relative compactions of 90 and 95 percent. A majority of self-weight settlements occurred nearly simultaneously with application of load. Using oedometer test results and assuming one-dimensional conditions, predicted centerline settlements resulting from self-weight compression compared favorably to measured settlements.
3. Large collapse settlements in model embankments occurred during complete wetting. Using oedometer test results and assuming one-dimensional conditions, collapse settlement at the centerline was under-predicted by a factor of between 1.4 and 2.6.
4. While the test soil is classified as exhibiting a slight degree of collapse based on oedometer test results and ASTM D 5333, actual collapse settlement was substantial in the model embankments. Thus, the categorization of collapsible soils according to collapse index given in ASTM D 5333 should be applied with care.

Results of oedometer testing, field study of an actual embankment, and predictions of embankment settlements led to the following conclusions:

1. The one-dimensional oedometer-based method under-predicted the centerline settlement of the embankment by a factor of between 1.4 and 1.6. The predicted centerline settlements were 0.32 and 0.39 m in 1968 and 1971, respectively. Estimated centerline settlements based on field measurements were approximately 0.46 and 0.61 m in 1968 and 1971, respectively.
2. Given the many uncertainties associated with field settlement measurements, variability of embankment soils, and the two-dimensional nature of embankments, predictions based on one-dimensional oedometer data are quite reasonable.

7.2 Recommendations for Future Study

Based on this current research, several recommendations can be made with regard to furthering the understanding of collapse behavior in compacted soils.

1. This research has demonstrated that collapse index increases with increasing plasticity index, liquid limit, activity, and clay-size fraction for a given molding moisture content and compaction effort. These single-oedometer tests were conducted on soil samples prepared at 95 percent relative compaction. It is, however, uncertain if such a trend holds true at higher dry unit weights. More research in this regard is required.
2. Centrifuge test results demonstrate that one-dimensional oedometer-based analysis can give a good indication of collapse potential at the embankment centerline; however, settlements were under-predicted by a factor between 1.4 and 2.6. As the one-dimensional model may be inappropriate for the prediction of strain conditions in the centerline of embankments, other techniques such as the finite element method should be employed to investigate this behavior.
3. Because only compacted silt embankments were analyzed in the current research, centrifuge testing should be extended to include sand and clay model embankments to study the effect of soil types on the two-dimensional nature of collapse settlement at the embankment centerline.
4. Because of significant fabric differences between laboratory- and field-compacted clays (Barden 1974), laboratory-compacted oedometer samples may exhibit different collapse behavior compared to field-compacted clays. A large diameter oedometer can be used to study the influence of fabric differences on the amount of collapse potential.

References

AASHTO, Standard Specifications for Transportation Materials and Methods of Sampling and Testing, Part I & II, American Association of State Highway Transportation Officials, Washington, D.C., 2000.

Alwail, T. A., Ho, C. L., and Fragaszy, R. J., "Collapse Mechanism of Compacted Clayey and Silty Sands," Proceedings of Settlement '94, American Society of Civil Engineers, Vol. 2, 1994, pp. 1435-1446.

ASTM, Annual Book of ASTM Standards, Sec. 4, Vols. 04.08 & 04.09, American Society for Testing and Materials, West Conshohocken, PA, 2000.

Barden, L, McGown, A., and Collins, K., "The Collapse Mechanism in Partly Saturated Soil," Engineering Geology, Vol. 7, No. 1, 1973, pp. 49-60.

Barden, L, "Consolidation of Clays Compacted "Dry" and "Wet" of Optimum Water content," Geotechnique, Vol. 24, No. 4, 1974, pp. 605-625.

Basma, A. A., and Tuncer, E. R., "Evaluation and Control of Collapsible Soils," Journal of Geotechnical Engineering, Vol. 118, No. 10, 1992, pp. 1491-1504.

Booth, A. R., Collapse Settlement in Compacted Soils, CSIR Research Report 324, 1977, Commonwealth Scientific Institute for Research, National Institute for Transport and Road Research, Pretoria, South Africa.

Brandon, T. L., Duncan, J. M., and Gardner, W. S., "Hydrocompression Settlement of Deep Fills," Journal of Geotechnical Engineering, Vol. 116, No. 10, 1990, pp. 1536-1548.

Briaud, J. L., James, R. W., and Hoffman, S. B., Settlement of Bridge Approaches (The Bump at the End of the Bridge), Synthesis of Highway Practice 234, 1997, Transportation Research Board, Washington D. C.

Clevenger, W. A., Placement Moisture Control Studies, Cachuma Dam Borrow Materials, Cachuma Project, Earth Laboratory Report No. EM-295, Apr. 1952, U.S. Department of Interior, Bureau of Reclamation, Denver, Colorado.

Coduto, P. D., Foundation Design Principles and Practices, Prentice Hall, New Jersey, 1994.

Das, M. B., Principles of Geotechnical Engineering, 4th Ed., PWS, Boston, 1998.

DeGroot, D.J. and Sheahan, T.C., "Laboratory Methods for Determining Engineering Properties of Overconsolidated Clays," Transportation Research Board, Record 1479, 1995, pp. 17-25.

de Miranda, A. N. and van Zyl, D., "Discussion on Prediction of Collapse Settlement of a High Embankment," Civil Engineer in South Africa, Vol. 30, No. 2, 1988, pp. 75-76.

DiBernardo, A. and Lovell, C. W., "Dependence of Compacted-Clay Compressibility on Compaction Variables," Transportation Research Board, Record 754, 1980, pp. 41-46.

DiMillio, A. F. and Strohm, W. E., "Technical Guidelines for the Design and Construction of Shale Embankments," 60th Annual Meeting of the Transportation Research Board, Jan. 1981.

Finn, F. N., "The Effect of Temperature on the Consolidation of Soils," Special Technical Publication No. 126, ASTM, 1951, pp. 65-72.

Fredlund, D. G. and Rahardjo, H., Soil Mechanics for Unsaturated Soils, Wiley, New York, 1993.

Fredlund, D. G. and Gan, J. K-M., "The Collapse Mechanism of a Soil Subjected to One-Dimensional Loading and Wetting," Genesis and Properties of Collapsible Soils, Kluwer Academic Publishers, Netherlands, 1995, pp. 173-205.

Gould, J. P., "The Compressibility of Rolled Fill Materials Determined from Field Observations," Proceedings of Third International Conference on Soil Mechanics and Foundation Engineering, Vol. 2, 1953, Zurich, pp. 239.

Gould, J. P., "Compression Characteristics of Rolled Fill Materials in Earth Dams," Technical Memorandum 648, U.S. Bureau of Reclamation, Denver, Mar. 1954.

Hilf, J. W., An Investigation of Pore-Water Pressure in Compacted Cohesive Soil, Technical Memorandum 654, U.S. Department of Interior, Bureau of Reclamation, Denver, Colorado, 1956.

Hodek, R. J. and Lovell, C. W., "A New Look at Compaction Processes in Fills," Association of Engineering Geology Bulletin, Vol. 16, No. 4, 1979, pp. 487-499.

Houston, S. L. and Houston, W. N., "Collapsible Soils Engineering," Unsaturated Soil Engineering Practices, ASCE Geotechnical Special Publication No. 68, 1992, pp. 199-237.

Huang, D., A Laboratory Investigation on the Behavior of Collapsible Soil, Master's Thesis, Colorado State University, Fort Collins, Colorado, 1989.

Jennings, J. E. and Knight, K., "The Additional Settlement of Foundations due to Collapse of Sandy Soils on Wetting," Proceedings of Fourth International Conference on Soil Mechanics and Foundation Engineering, Vol. 1, 1957, London, U.K., pp. 316-319.

Jennings, J. E. and Burland, J. B., "Limitations to the Use of Effective Stresses in Partly Saturated Soils," Geotechnique, Vol.12, No. 2, 1962, pp. 125-144.

Justo, J. L., Delgado, A., and Ruiz, J., "The Influence of Stress-Path in the Collapse-Swelling of Soils at the Laboratory," Proceedings of the Fifth International Conference on Expansive Soils, 1984, pp. 67-71.

Kellner, R. and Rose, W. D., "Post-Construction Performance of P-18 Bridge Abutments and Approach Fills, Eastern Oklahoma," Proceedings of the 22nd Annual Highway Geology Symposium, Oklahoma Geological Survey, 1971, pp. 53-67.

Laguros, J. G., Zaman, M., and Mahmood, I. U., Evaluation of Causes of Excessive Settlements of Pavements Behind Bridge Abutments and Their Remedies-Phase II Executive Summary, Report No. FHWA/OK 89 (07), Jan. 1990, Oklahoma Department of Transportation, Oklahoma City, Oklahoma.

Lambe, T. W., "The Structure of Compacted Clay," Journal of the Soil Mechanics and Foundation Division, 1958a, Vol. 84, No. SM2.

Lambe, T. W., "The Engineering Behavior of Compacted Clay," Journal of the Soil Mechanics and Foundation Division, 1958b, Vol. 84, No. SM2.

Lawton, E. C., Wetting-Induced Collapse in Compacted Soil, Ph.D. Thesis, Washington State University, Pullman, Washington, 1986.

Lawton, E. C., Fragaszy, R. J., and Hardcastle, J. H., "Collapse of Compacted Clayey Sand," Journal of Geotechnical Engineering, Vol. 115, No. 9, 1989, pp. 1252-1267.

Lawton, E. C., Fragaszy, R. J., and Hardcastle, J. H., "Stress Ratio Effects on Collapse of Compacted Clayey Sand," Journal of Geotechnical Engineering, Vol. 117, No. 5, 1991a, pp. 714-730.

Lawton, E. C., Fragaszy, R. J., and Hetherington, M. D., Significance and Control of Wetting-Induced Collapse in Compacted Soils, Report No. 91-01, 1991b, University of Utah, Salt Lake City, Utah.

Lawton, E. C., Fragaszy, R. J., and Hetherington, M. D., "Review of Wetting-Induced Collapse in Compacted Soil," Journal of Geotechnical Engineering, Vol. 118, No. 9, 1992, pp. 1376-1394.

Lawton, E. C., Chen, J., Larson, C. T., Perez, Y., and Bravo, A., "Influence of Chemical Admixtures and Pore Fluid Chemistry on Wetting Induced Collapse of Compacted Soil," Proceedings of the 29th of Engineering Geology and Geotechnical Engineering Symposium, Mar. 1993, Reno, Nevada, pp. 425-445.

Leonards, G. A., and Girault, P., "A Study of the One-Dimensional Consolidation Test," Proceedings of the 5th International Conference on Soil Mechanics and Foundation Engineering, Vol. 1, 1961, pp. 213-218.

McMahon, D. J. and Kropp, A. L., " Proposed Compaction Specification to Minimize Hydrocompression-Induced Settlements in Fills Supporting Residential Structures," Construction and Controlling Compaction of Earth Fills, ASTM STP 1384, American Society for Testing and Materials, West Conshohocken, PA, 2000, pp. 209-228.

Mellors, T. W., " The Influence of the Clay Component in Loess on Collapse of the Soil Structure," Genesis and Properties of Collapsible Soils, Netherlands, 1995, pp. 207-216.

Miller, G. A., Azad, S., and Dhar, B., "The Effect of Cement Kiln Dust on the Collapse Potential of Compacted Shale," Testing Soil Mixed with Waste or Recycled Materials, ASTM STP 1275, American Society for Testing and Materials, West Conshohocken, PA, 1997, pp. 232-245.

Mishu, L. P., Collapse in One-Dimensional Compression of Compacted Clay Upon Wetting, Master's Thesis, Purdue University, West Lafayette, Indiana, 1963.

Mitchell, J. K., Fundamentals of Soil Behavior, John Wiley & Sons, NY, NY, 1993, pp. 303.

Muraleetharan, K. K. and Granger, K. K., "The Use of Miniature Pore Pressure Transducers in Measuring Matric Suction in Unsaturated Soils," Geotechnical Testing Journal, Vol. 22, No. 3, 1999, pp. 226-234.

Noorany, I. and Stanley, J. V., "Settlement of Compacted Fills Caused by Wetting," Proceedings of Settlement '94, American Society of Civil Engineers, Vol. 2, 1994, pp. 1516-1530.

Nwaboukei, S. O. and Lovell, C. W., Compressibility and Shear Strength Characteristics of Impact Compacted Lacustrine Clay, Report No. JHRP-85-6, 1985, Purdue University, West Lafayette, Indiana.

Osipov, V. I. and Sokolov, V. N., "Factors and Mechanism of Loess Collapsibility," Genesis and Properties of Collapsible Soils, Kluwer Academic Publishers, Netherlands, 1995, pp. 49-63.

Paaswell, R. E., "Temperature Effects on Clay Soil Consolidation," Journal of the Soil Mechanics and Foundations Division, Vol. 93, No. SM3, 1967, pp. 9-22.

Pagen, C. A., Wang, C., and Jagannath, B. N., Effect of Compaction and Increase of Saturation after Compaction on the Engineering Properties of Compacted Clay, Report No. EES 248-6, Jul. 1968, Ohio State University, Columbus, Ohio.

Pereira, J. H. F., Numerical Analysis of the Mechanical Behavior of Collapsing Earth Dams during First Reservoir Filling, Ph.D.'s Thesis, University of Saskatchewan, Saskatchewan, Canada, 1996.

Poulos, H. G. and Davis, E. H., Elastic Solutions for Soil and Rock Mechanics, John Wiley & Sons, NY, NY, 1973.

Proctor, R. R., "Design and Construction of Rolled Earth Dams," Engineering News Record, Vol. 3, 1933.

Robertson, P. K., Campanella, R. G., Gillespie, D., and Grieg, J., "Use of Piezometer Cone Data," Proceedings of In-Situ '86, American Society of Civil Engineers, 1986.

Schmertmann, J. H., "Undisturbed Consolidation Behavior of Clay," Transactions 1201, ASCE, Vol. 120, 1953.

Seed, H. B., and Chan, C. K., "Structure and Strength Characteristics of Compacted Clays," Journal of the Soil Mechanics and Foundations Division, Vol. 85, No. SM5, 1959, pp. 87-128.

Sherard, J. L., Woodward, R. J., Gizienski, S. F., and Clevenger, W. A., Earth and Earth-Rock Dams, Wiley, New York, 1963.

Stark, T. D., Scott, M. O., and Long, J. H., Differential Movement at the Embankment/Structure Interface-Mitigation and Rehabilitation, Report IAB-HI, FY 93, Apr. 1995, Illinois Department of Transportation, Illinois.

Steadman, L., Collapse Settlement in Compacted Soils of Variable Fines Content, Masters Thesis, Washington State University, Pullman, Washington, 1987.

Strohm, W. E., Bragg, G. H., and Zeigler, T. W., Design and Construction of Compacted Shale Embankments, Report No. FHWA-RD-78-141, 1978, Federal Highway Administration, Washington, D.C.

Tadros, M. K. and Benak, J. V., Bridge Abutment and Approach Slab Settlement (Phase 1), Dec. 1989, Nebraska Department of Roads, Lincoln, Nebraska.

U.S. Army Corps of Engineers, Record Drawing: Relocation Pittsburg County Road P-18, 1960, Tulsa, Oklahoma.

Vicente, E. E., Diaz, G. M., and Yourman, A. M., "Settlement of Deep Compacted Fills in California," Proceedings of Settlement '94, American Society of Civil Engineers, Vol. 2, 1994, pp. 1124-1134.

Witsman, G. R. and Lovell, C. W., The Effect of Compacted Prestress on Compacted Shale Compressibility, Report No. FHWA/IN/JHRP-79-16, Sep. 1979, Purdue University, West Lafayette, Indiana.

White, D. M., The Fabric of a Medium Plastic Clay Compacted in the Laboratory and in the Field, Report No. FHWA/IN/JHRP-80/10, Aug. 1980, Purdue University, West Lafayette, Indiana.

Yoshimi, Y., One Dimensional Consolidation of Partially Saturated Soil, Ph.D. Thesis, Northwestern University, Evanston, Illinois, Aug. 1958.

Appendix A : Oedometer Test Data

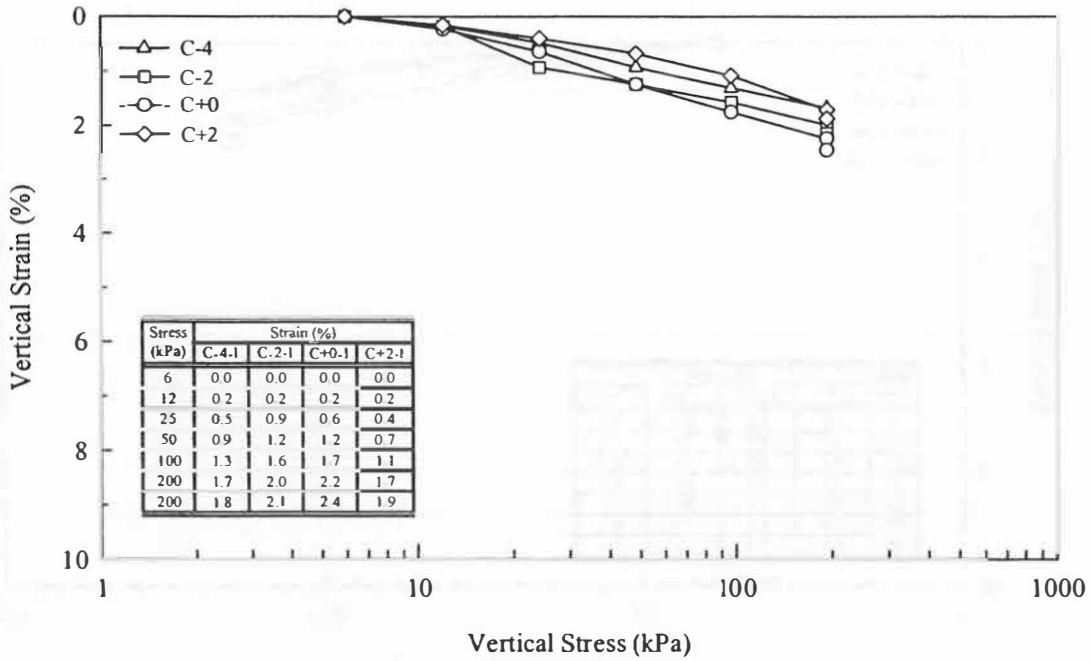

Stress (kPa)	Strain (%)			
	C-4-1	C-2-1	C+0-1	C+2-1
6	0.0	0.0	0.0	0.0
12	0.2	0.2	0.2	0.2
25	0.5	0.9	0.6	0.4
50	0.9	1.2	1.2	0.7
100	1.3	1.6	1.7	1.1
200	1.7	2.0	2.2	1.7
200	1.8	2.1	2.4	1.9

Figure A-1: Results of single-oedometer test for Gracemore Sand 1

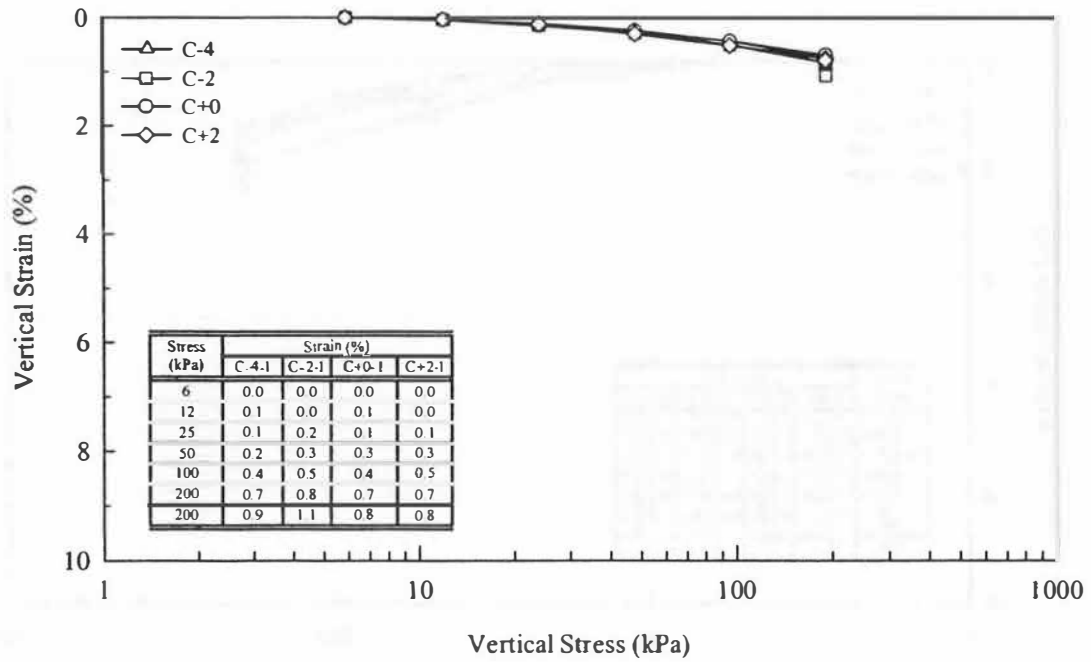

Stress (kPa)	Strain (%)			
	C-4-1	C-2-1	C+0-1	C+2-1
6	0.0	0.0	0.0	0.0
12	0.1	0.0	0.1	0.0
25	0.1	0.2	0.1	0.1
50	0.2	0.3	0.3	0.3
100	0.4	0.5	0.4	0.5
200	0.7	0.8	0.7	0.7
200	0.9	1.1	0.8	0.8

Figure A-2: Results of single-oedometer test for Gracemore Sand 2

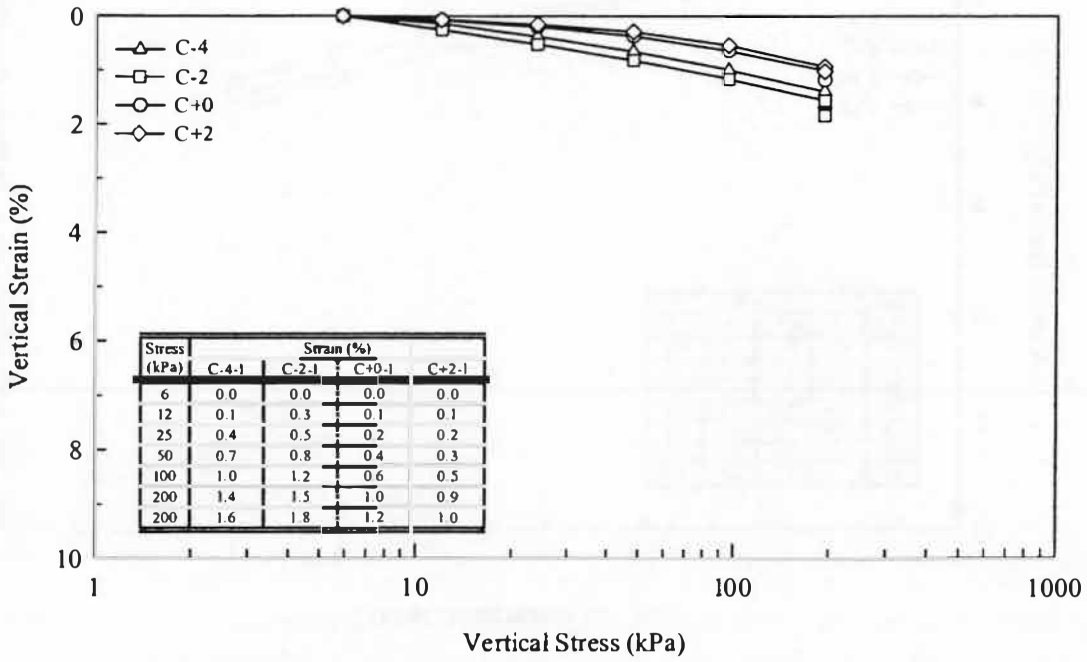

Stress (kPa)	Strain (%) C-4-1	C-2-1	C+0-1	C+2-1
6	0.0	0.0	0.0	0.0
12	0.1	0.3	0.1	0.1
25	0.4	0.5	0.2	0.2
50	0.7	0.8	0.4	0.3
100	1.0	1.2	0.6	0.5
200	1.4	1.5	1.0	0.9
200	1.6	1.8	1.2	1.0

Figure A-3: Results of single-oedometer test for Gracemore Sand 3

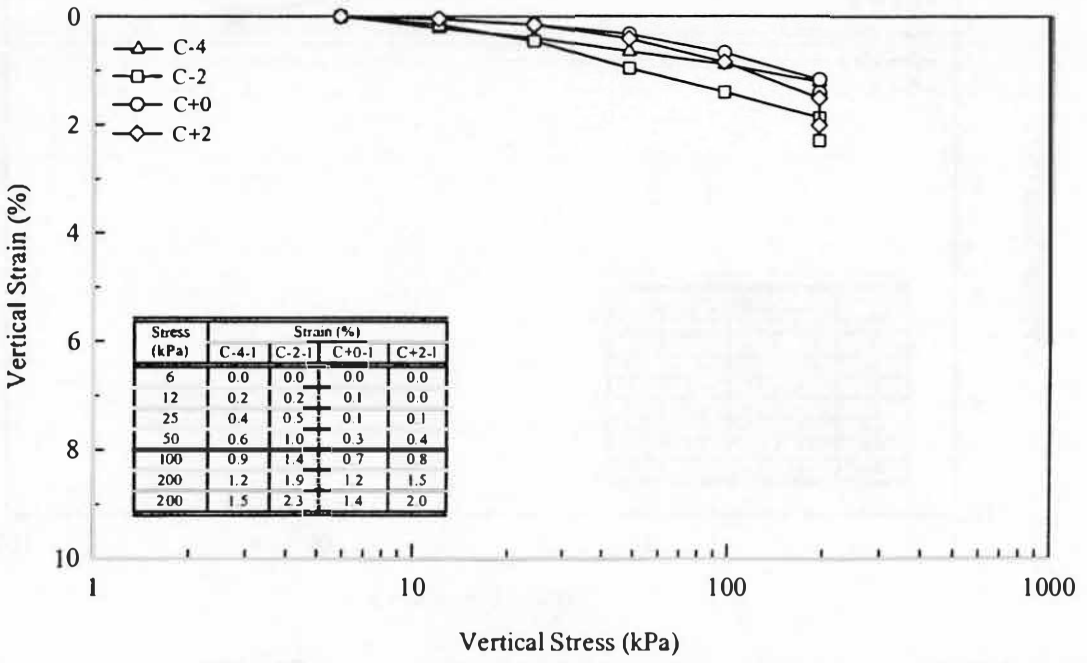

Stress (kPa)	Strain (%) C-4-1	C-2-1	C+0-1	C+2-1
6	0.0	0.0	0.0	0.0
12	0.2	0.2	0.1	0.0
25	0.4	0.5	0.1	0.1
50	0.6	1.0	0.3	0.4
100	0.9	1.4	0.7	0.8
200	1.2	1.9	1.2	1.5
200	1.5	2.3	1.4	2.0

Figure A-4: Results of single-oedometer test for Gracemore Sand 4

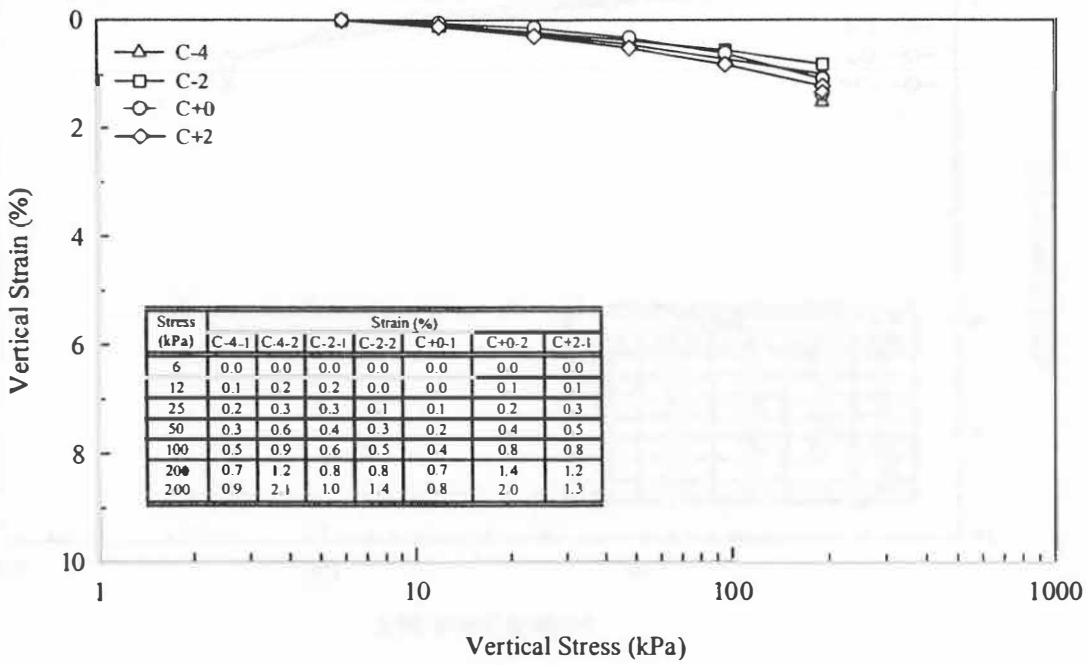

Stress (kPa)	Strain (%)						
	C-4-1	C-4-2	C-2-1	C-2-2	C+0-1	C+0-2	C+2-1
6	0.0	0.0	0.0	0.0	0.0	0.0	0.0
12	0.1	0.2	0.2	0.0	0.0	0.1	0.1
25	0.2	0.3	0.3	0.1	0.1	0.2	0.3
50	0.3	0.6	0.4	0.3	0.2	0.4	0.5
100	0.5	0.9	0.6	0.5	0.4	0.8	0.8
200	0.7	1.2	0.8	0.8	0.7	1.4	1.2
200	0.9	2.1	1.0	1.4	0.8	2.0	1.3

Figure A-5: Results of single-oedometer test for Vanoss Sand

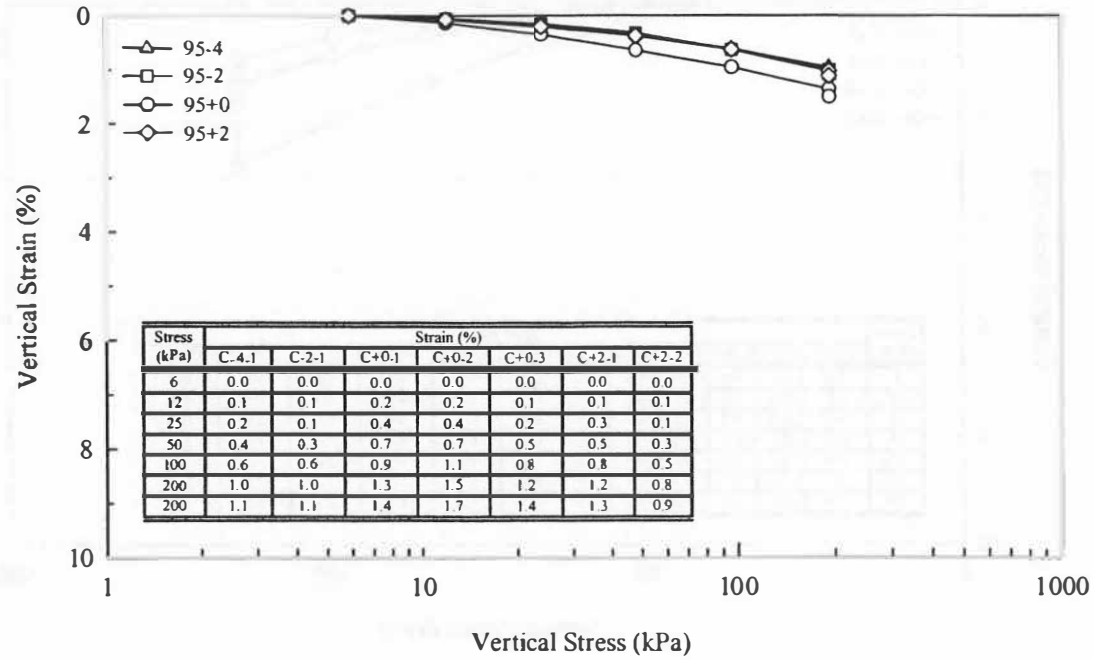

Stress (kPa)	Strain (%)						
	C-4-1	C-2-1	C+0-1	C+0-2	C+0-3	C+2-1	C+2-2
6	0.0	0.0	0.0	0.0	0.0	0.0	0.0
12	0.1	0.1	0.2	0.2	0.1	0.1	0.1
25	0.2	0.1	0.4	0.4	0.2	0.3	0.1
50	0.4	0.3	0.7	0.7	0.5	0.5	0.3
100	0.6	0.6	0.9	1.1	0.8	0.8	0.5
200	1.0	1.0	1.3	1.5	1.2	1.2	0.8
200	1.1	1.1	1.4	1.7	1.4	1.3	0.9

Figure A-6: Results of single-oedometer test for Darnell Sandstone

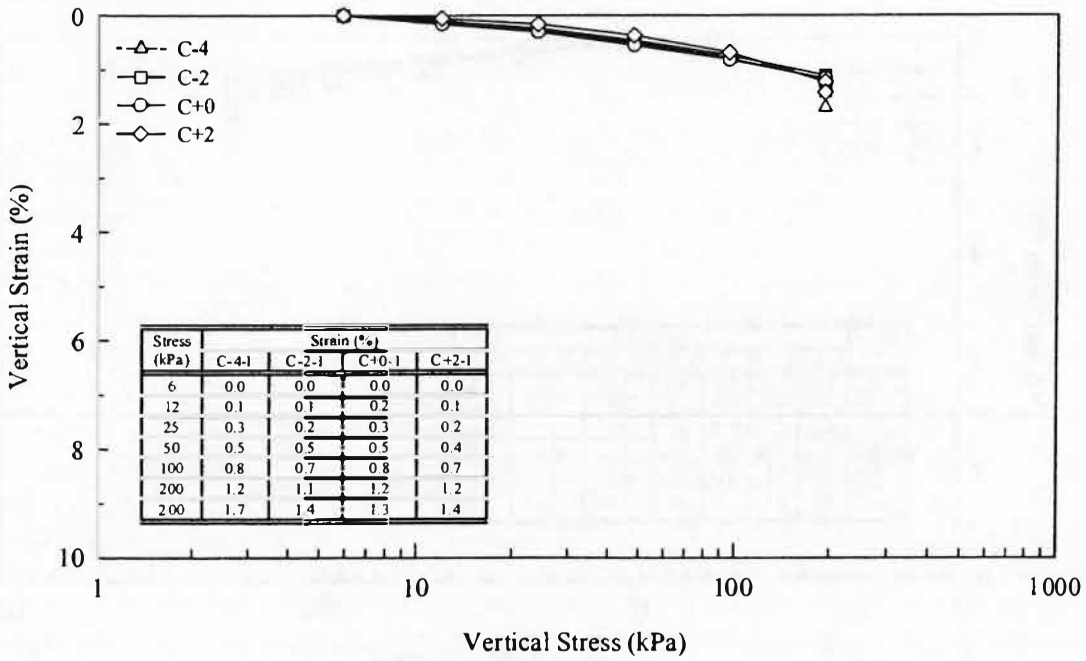

Stress (kPa)	Strain (%) C-4-1	C-2-1	C+0-1	C+2-1
6	0.0	0.0	0.0	0.0
12	0.1	0.1	0.2	0.1
25	0.3	0.2	0.3	0.2
50	0.5	0.5	0.5	0.4
100	0.8	0.7	0.8	0.7
200	1.2	1.1	1.2	1.2
200	1.7	1.4	1.3	1.4

Figure A-7: Results of single-oedometer test for Slaughterville Sand

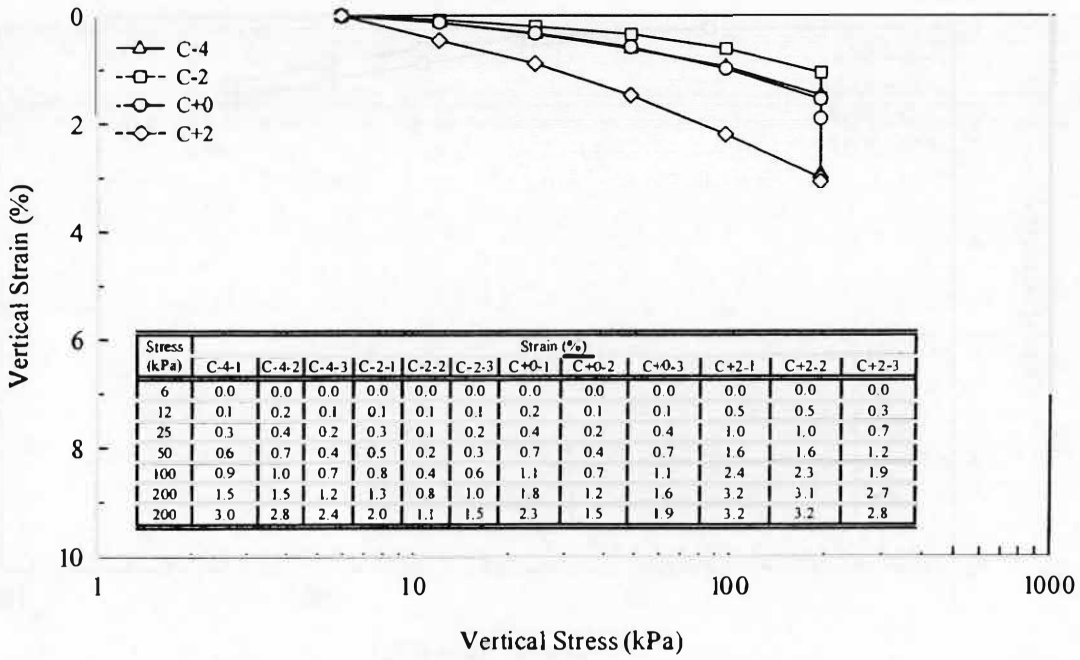

Stress (kPa)	Strain (%) C-4-1	C-4-2	C-4-3	C-2-1	C-2-2	C-2-3	C+0-1	C+0-2	C+0-3	C+2-1	C+2-2	C+2-3
6	0.0	0.0	0.0	0.0	0.0	0.0	0.0	0.0	0.0	0.0	0.0	0.0
12	0.1	0.2	0.1	0.1	0.1	0.1	0.2	0.1	0.1	0.5	0.5	0.3
25	0.3	0.4	0.2	0.3	0.1	0.2	0.4	0.2	0.4	1.0	1.0	0.7
50	0.6	0.7	0.4	0.5	0.2	0.3	0.7	0.4	0.7	1.6	1.6	1.2
100	0.9	1.0	0.7	0.8	0.4	0.6	1.1	0.7	1.1	2.4	2.3	1.9
200	1.5	1.5	1.2	1.3	0.8	1.0	1.8	1.2	1.6	3.2	3.1	2.7
200	3.0	2.8	2.4	2.0	1.1	1.5	2.3	1.5	1.9	3.2	3.2	2.8

Figure A-8: Results of single-oedometer test for Minco Silt

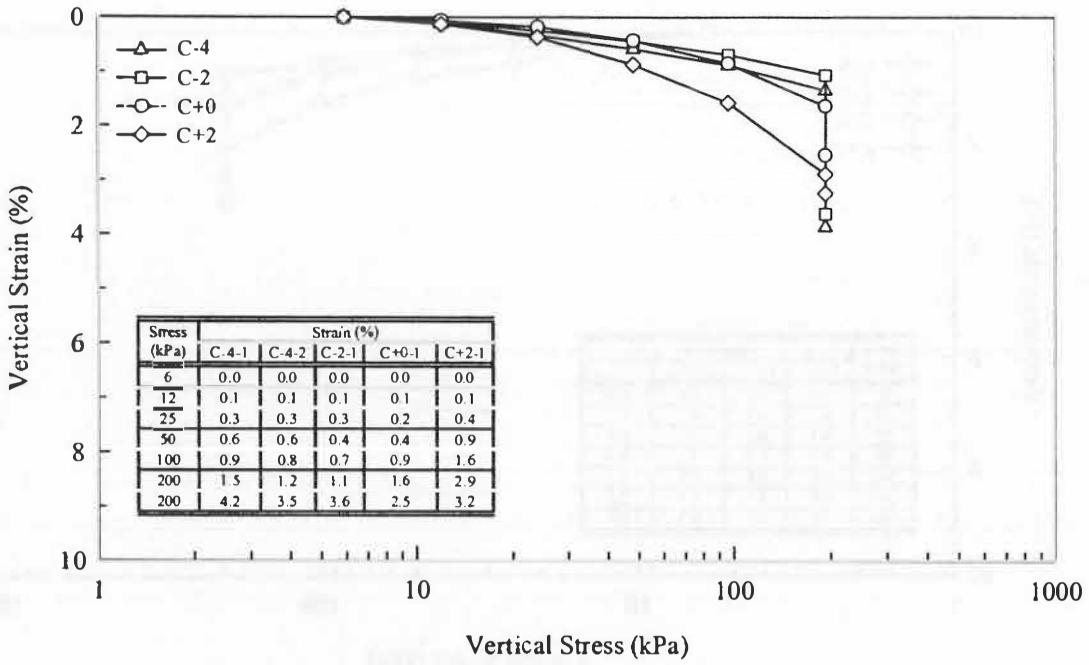

Stress (kPa)	Strain (%) C-4-1	C-4-2	C-2-1	C+0-1	C+2-1
6	0.0	0.0	0.0	0.0	0.0
12	0.1	0.1	0.1	0.1	0.1
25	0.3	0.3	0.3	0.2	0.4
50	0.6	0.6	0.4	0.4	0.9
100	0.9	0.8	0.7	0.9	1.6
200	1.5	1.2	1.1	1.6	2.9
200	4.2	3.5	3.6	2.5	3.2

Figure A-9: Results of single-oedometer test for Blaine Shale

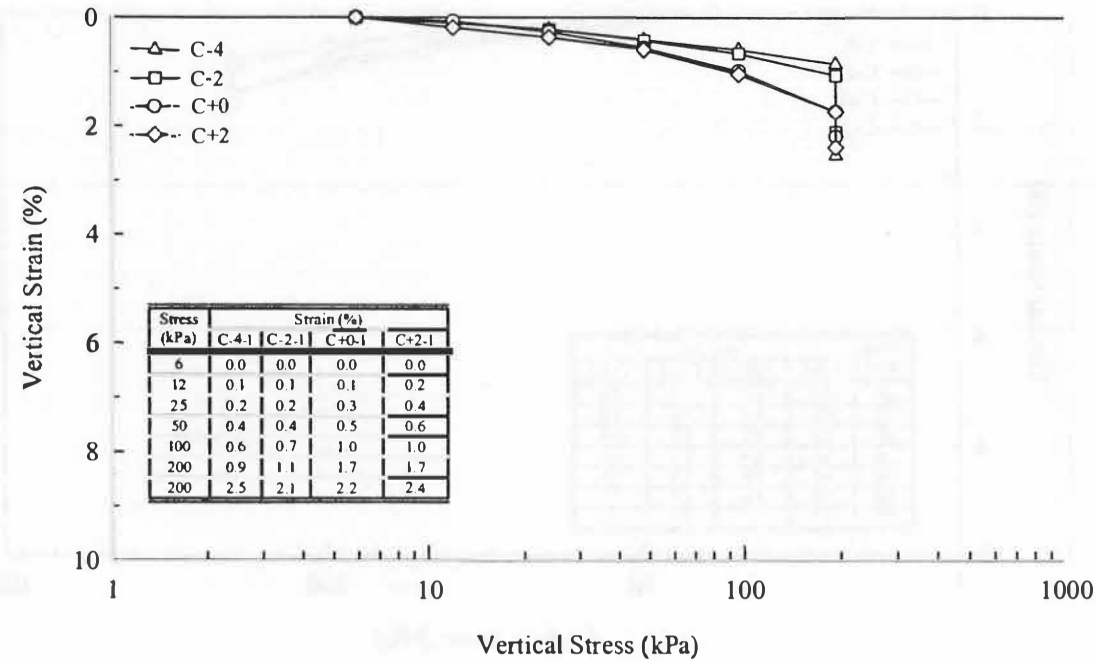

Stress (kPa)	Strain (%) C-4-1	C-2-1	C+0-1	C+2-1
6	0.0	0.0	0.0	0.0
12	0.1	0.1	0.1	0.2
25	0.2	0.2	0.3	0.4
50	0.4	0.4	0.5	0.6
100	0.6	0.7	1.0	1.0
200	0.9	1.1	1.7	1.7
200	2.5	2.1	2.2	2.4

Figure A-10: Results of single-oedometer test for Grainola Silt

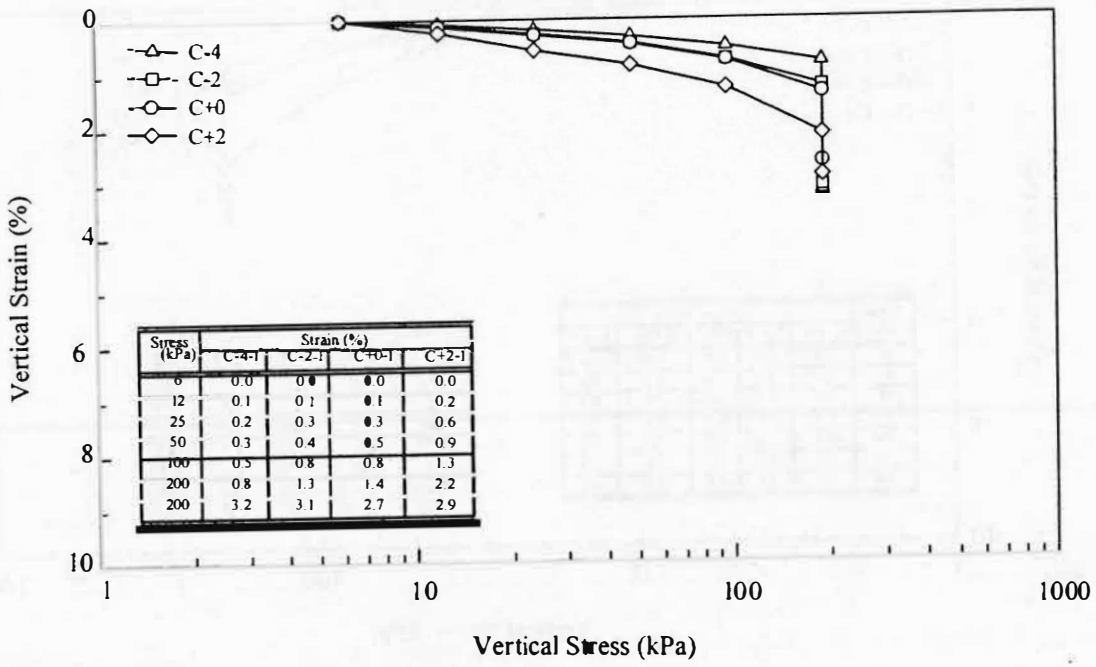

Stress (kPa)	Strain (%) C-4-1	C-2-1	C+0-1	C+2-1
6	0.0	0.0	0.0	0.0
12	0.1	0.1	0.1	0.2
25	0.2	0.3	0.3	0.6
50	0.3	0.4	0.5	0.9
100	0.5	0.8	0.8	1.3
200	0.8	1.3	1.4	2.2
200	3.2	3.1	2.7	2.9

Figure A-11: Results of single-oedometer test for Teller Silt

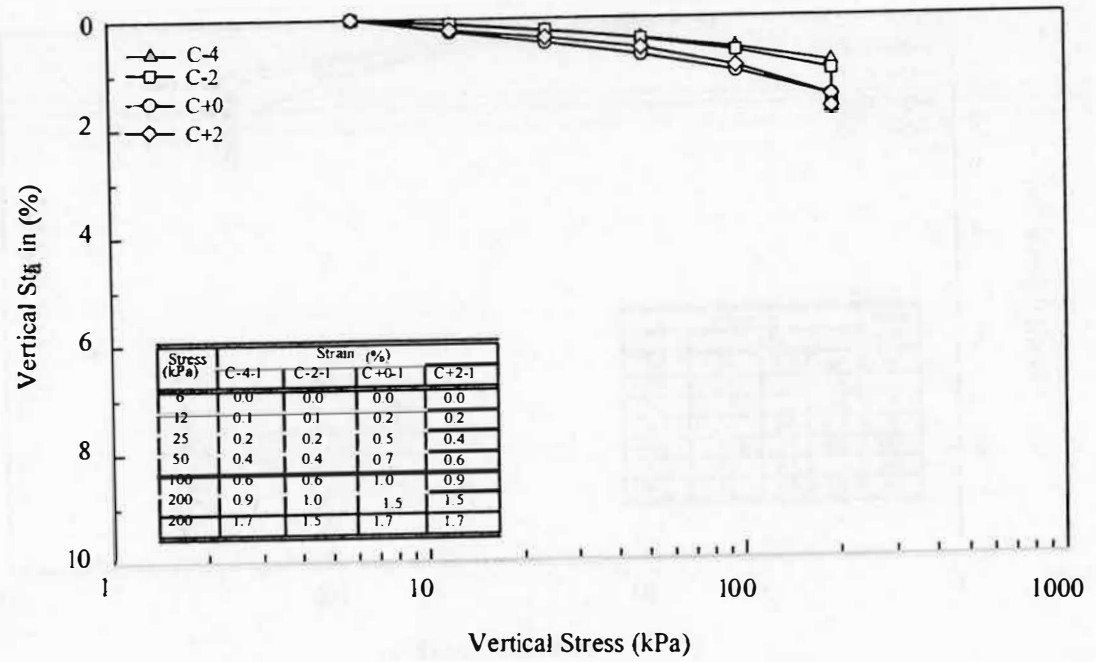

Stress (kPa)	Strain (%) C-4-1	C-2-1	C+0-1	C+2-1
6	0.0	0.0	0.0	0.0
12	0.1	0.1	0.2	0.2
25	0.2	0.2	0.5	0.4
50	0.4	0.4	0.7	0.6
100	0.6	0.6	1.0	0.9
200	0.9	1.0	1.5	1.5
200	1.7	1.5	1.7	1.7

Figure A-12: Results of single-oedometer test for Hennessey Shale 1

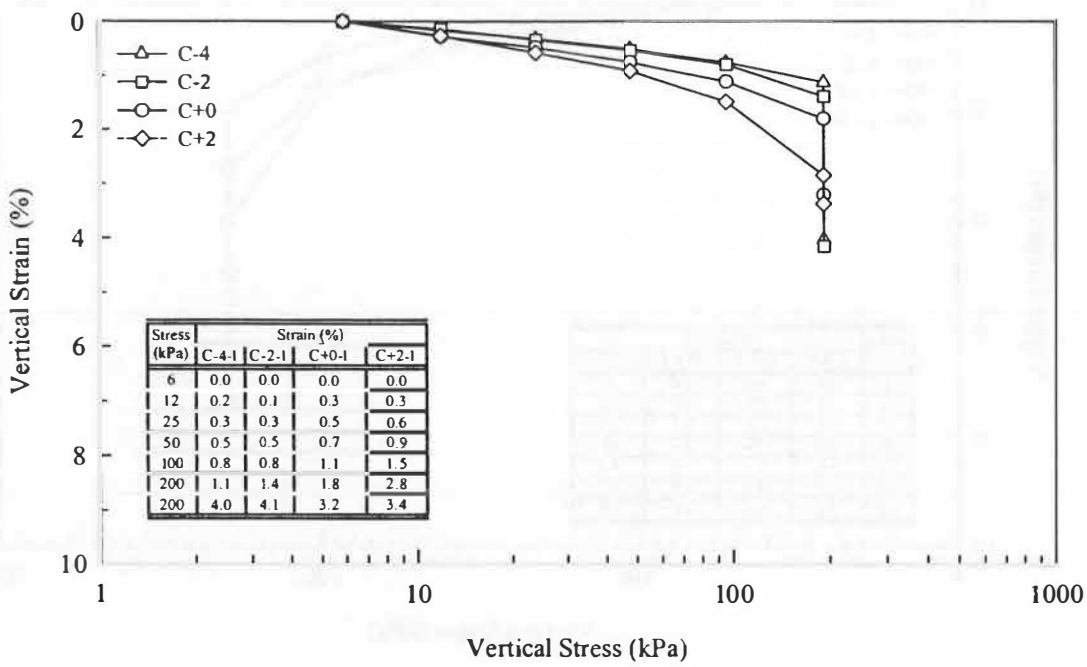

Stress (kPa)	Strain (%) C-4-1	C-2-1	C+0-1	C+2-1
6	0.0	0.0	0.0	0.0
12	0.2	0.1	0.3	0.3
25	0.3	0.3	0.5	0.6
50	0.5	0.5	0.7	0.9
100	0.8	0.8	1.1	1.5
200	1.1	1.4	1.8	2.8
200	4.0	4.1	3.2	3.4

Figure A-13: Results of single-oedometer test for Hennessey Shale 2

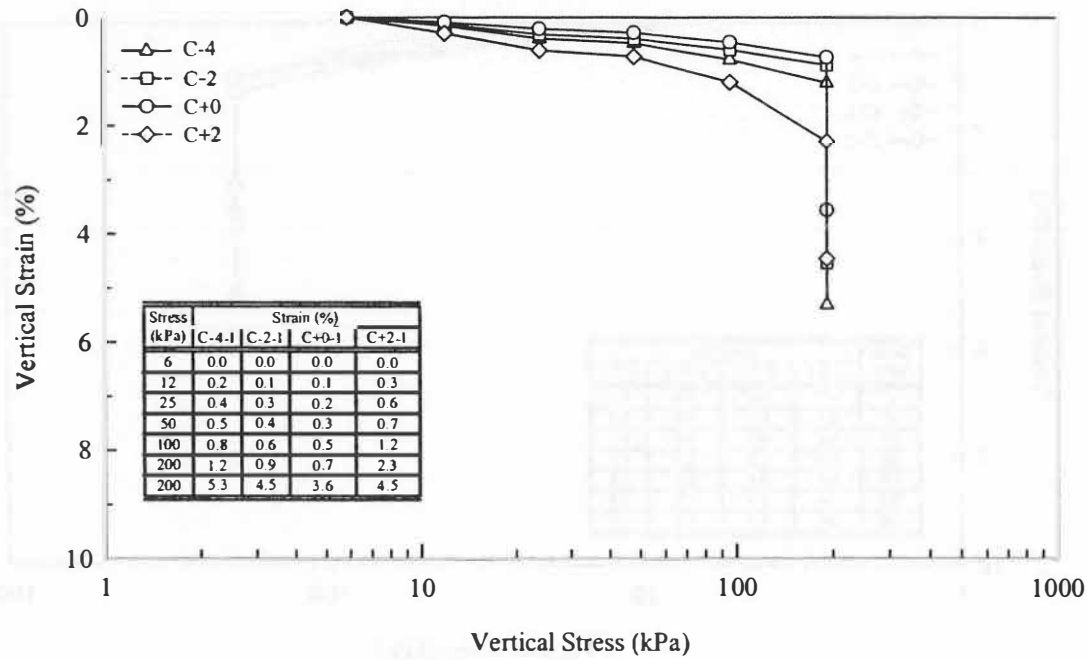

Stress (kPa)	Strain (%) C-4-1	C-2-1	C+0-1	C+2-1
6	0.0	0.0	0.0	0.0
12	0.2	0.1	0.1	0.3
25	0.4	0.3	0.2	0.6
50	0.5	0.4	0.3	0.7
100	0.8	0.6	0.5	1.2
200	1.2	0.9	0.7	2.3
200	5.3	4.5	3.6	4.5

Figure A-14: Results of single-oedometer test for Vanoss Clay

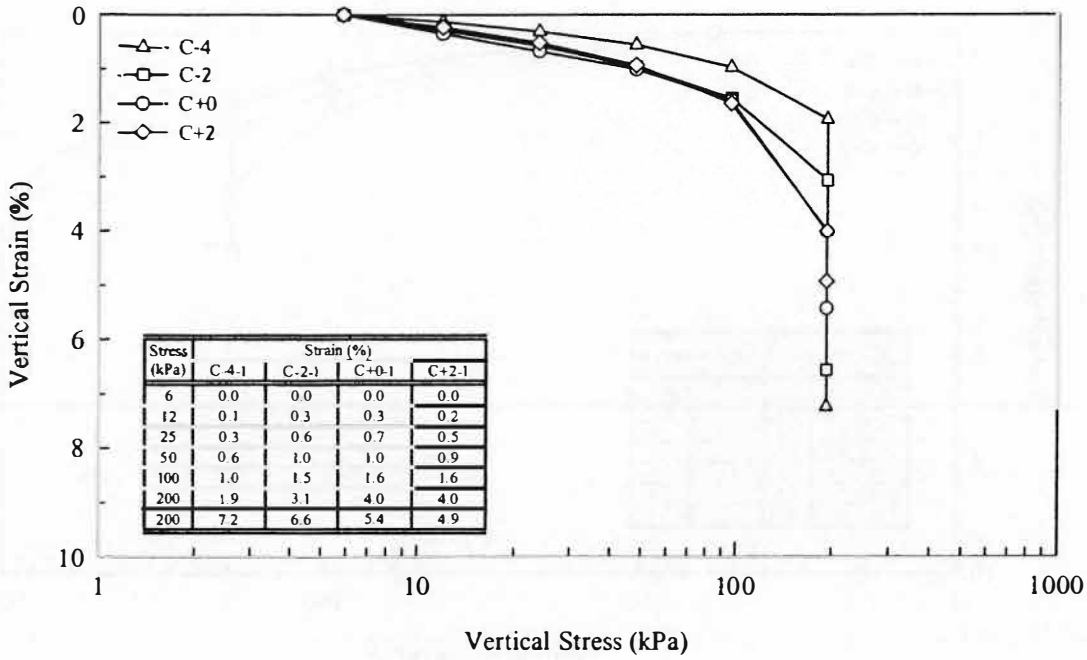

Stress (kPa)	Strain (%) C-4-1	C-2-1	C+0-1	C+2-1
6	0.0	0.0	0.0	0.0
12	0.1	0.3	0.3	0.2
25	0.3	0.6	0.7	0.5
50	0.6	1.0	1.0	0.9
100	1.0	1.5	1.6	1.6
200	1.9	3.1	4.0	4.0
200	7.2	6.6	5.4	4.9

Figure A-15: Results of single-oedometer test for Doolin Clay

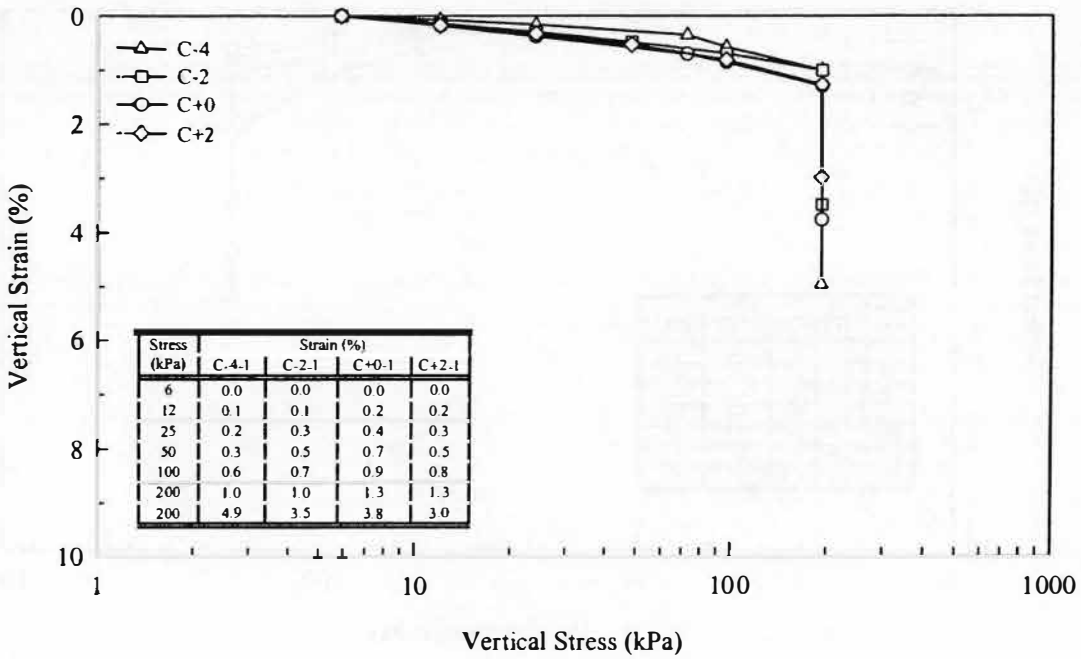

Stress (kPa)	Strain (%) C-4-1	C-2-1	C+0-1	C+2-1
6	0.0	0.0	0.0	0.0
12	0.1	0.1	0.2	0.2
25	0.2	0.3	0.4	0.3
50	0.3	0.5	0.7	0.5
100	0.6	0.7	0.9	0.8
200	1.0	1.0	1.3	1.3
200	4.9	3.5	3.8	3.0

Figure A-16: Results of single-oedometer test for Wellington Shale

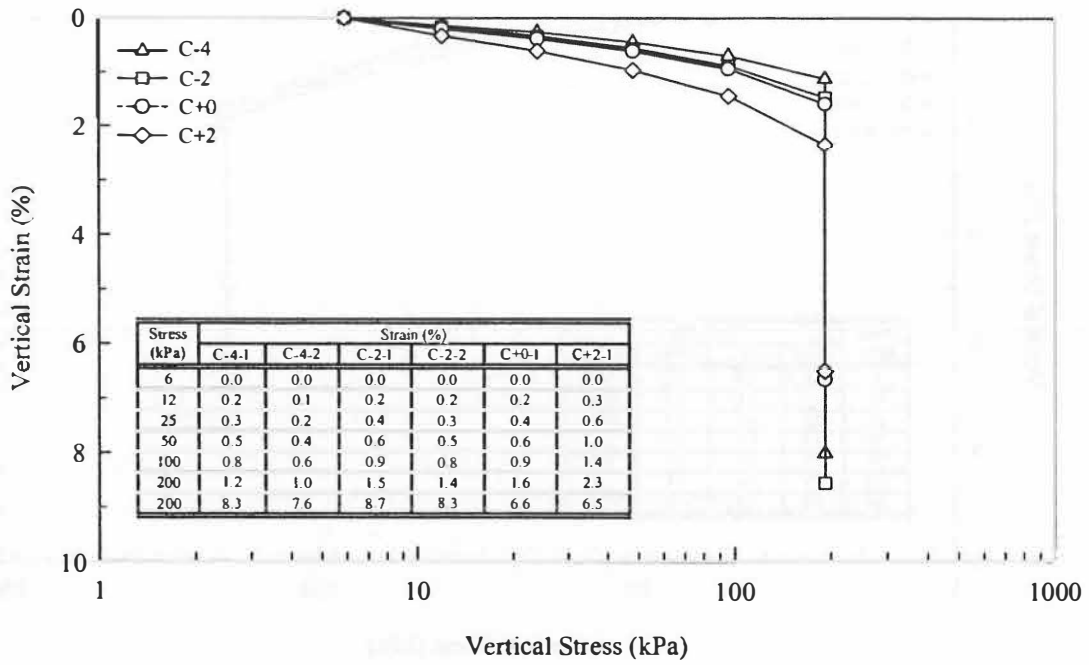

Stress (kPa)	Strain (%)					
	C-4-1	C-4-2	C-2-1	C-2-2	C+0-1	C+2-1
6	0.0	0.0	0.0	0.0	0.0	0.0
12	0.2	0.1	0.2	0.2	0.2	0.3
25	0.3	0.2	0.4	0.3	0.4	0.6
50	0.5	0.4	0.6	0.5	0.6	1.0
100	0.8	0.6	0.9	0.8	0.9	1.4
200	1.2	1.0	1.5	1.4	1.6	2.3
200	8.3	7.6	8.7	8.3	6.6	6.5

Figure A-17: Results of single-oedometer test for Boggy Shale

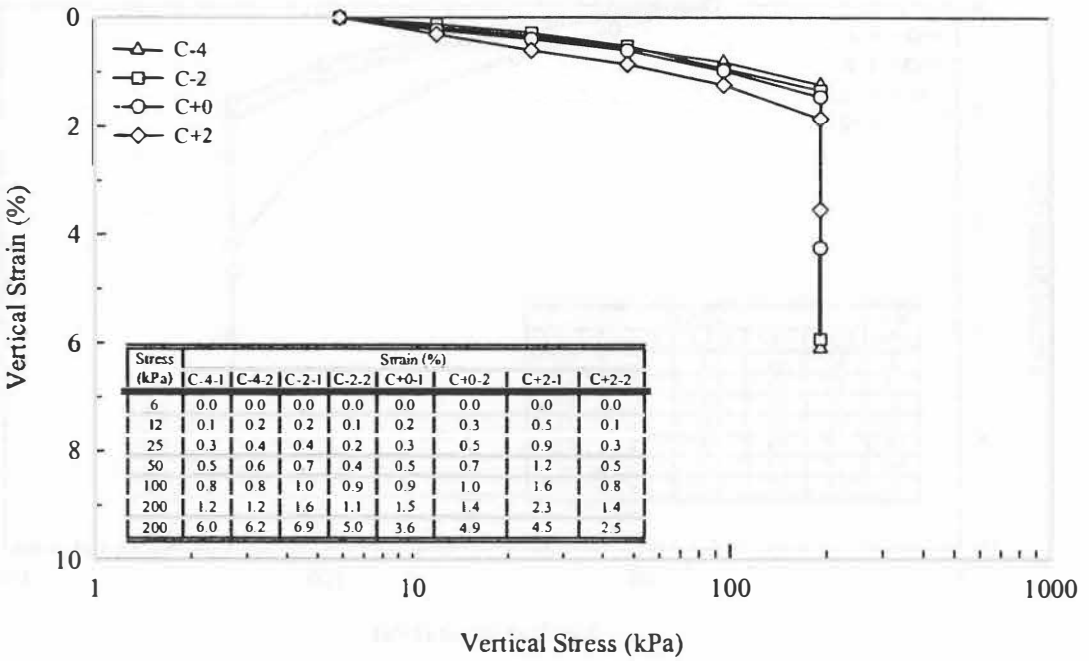

Stress (kPa)	Strain (%)							
	C-4-1	C-4-2	C-2-1	C-2-2	C+0-1	C+0-2	C+2-1	C+2-2
6	0.0	0.0	0.0	0.0	0.0	0.0	0.0	0.0
12	0.1	0.2	0.2	0.1	0.2	0.3	0.5	0.1
25	0.3	0.4	0.4	0.2	0.3	0.5	0.9	0.3
50	0.5	0.6	0.7	0.4	0.5	0.7	1.2	0.5
100	0.8	0.8	1.0	0.9	0.9	1.0	1.6	0.8
200	1.2	1.2	1.6	1.1	1.5	1.4	2.3	1.4
200	6.0	6.2	6.9	5.0	3.6	4.9	4.5	2.5

Figure A-18: Results of single-oedometer test for Bethany Clay

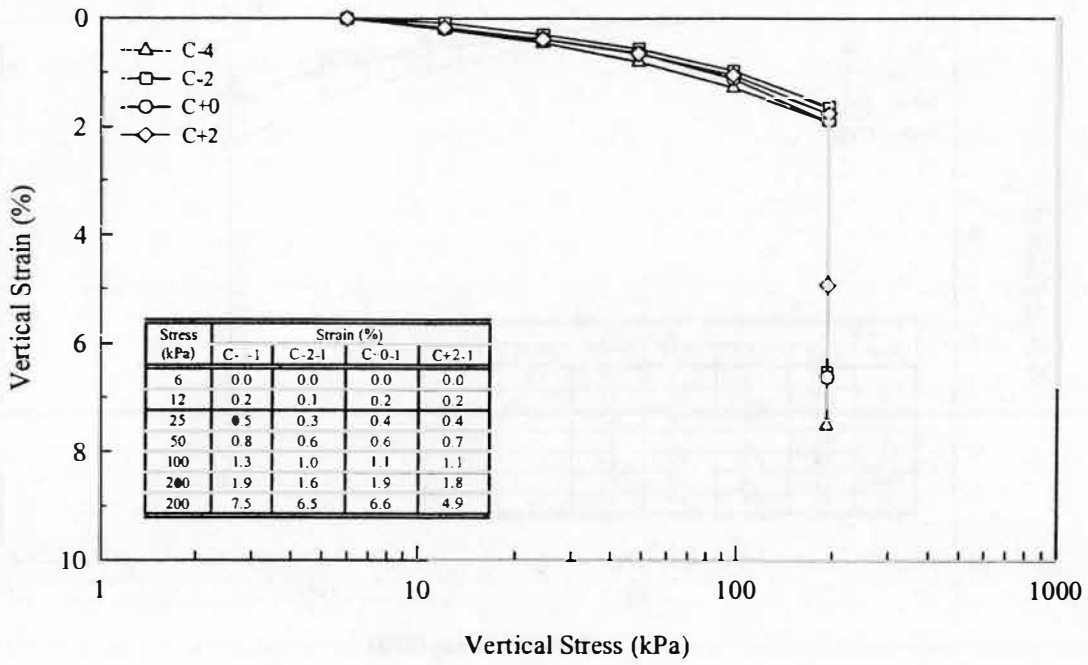

Stress (kPa)	Strain (%) C- -1	C-2-1	C-0-1	C+2-1
6	0.0	0.0	0.0	0.0
12	0.2	0.1	0.2	0.2
25	0.5	0.3	0.4	0.4
50	0.8	0.6	0.6	0.7
100	1.3	1.0	1.1	1.1
200	1.9	1.6	1.9	1.8
200	7.5	6.5	6.6	4.9

Figure A-19: Results of single-oedometer test for Heiden Clay

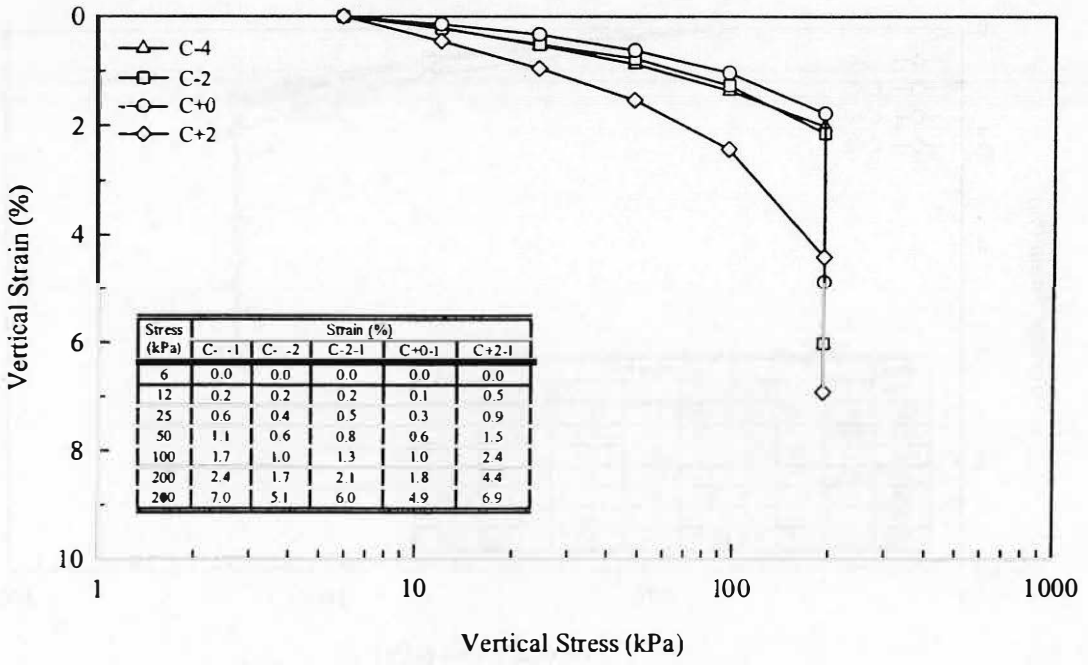

Stress (kPa)	Strain (%) C- -1	C- -2	C-2-1	C+0-1	C+2-1
6	0.0	0.0	0.0	0.0	0.0
12	0.2	0.2	0.2	0.1	0.5
25	0.6	0.4	0.5	0.3	0.9
50	1.1	0.6	0.8	0.6	1.5
100	1.7	1.0	1.3	1.0	2.4
200	2.4	1.7	2.1	1.8	4.4
200	7.0	5.1	6.0	4.9	6.9

Figure A-20: Results of single-oedometer test for Lomill Clay

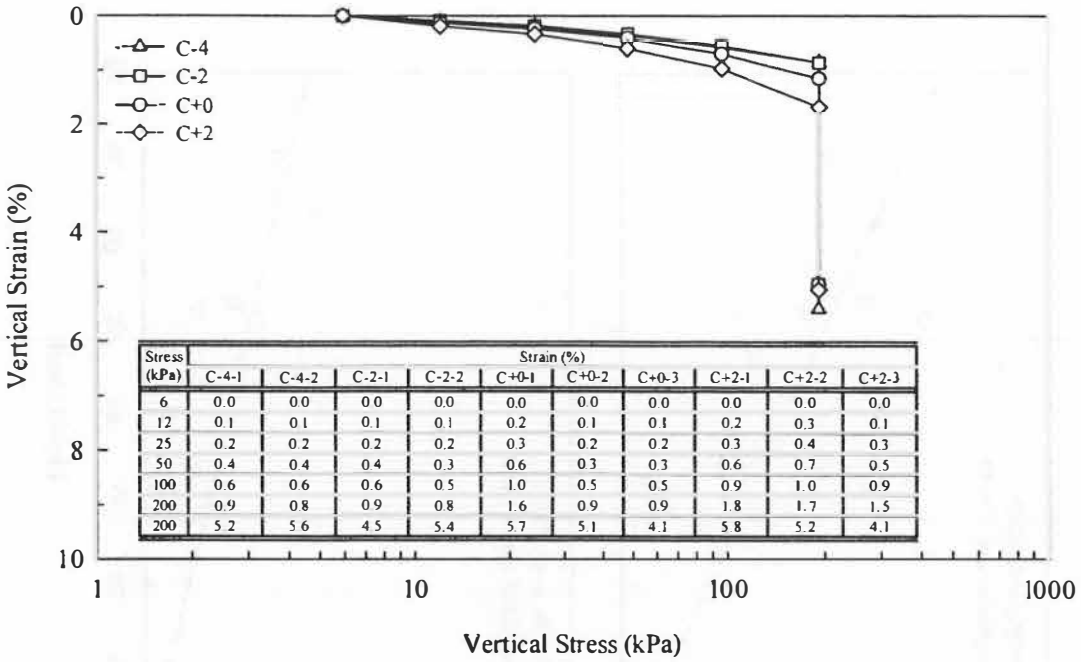

Stress (kPa)	Strain (%)									
	C-4-1	C-4-2	C-2-1	C-2-2	C+0-1	C+0-2	C+0-3	C+2-1	C+2-2	C+2-3
6	0.0	0.0	0.0	0.0	0.0	0.0	0.0	0.0	0.0	0.0
12	0.1	0.1	0.1	0.1	0.2	0.1	0.1	0.2	0.3	0.1
25	0.2	0.2	0.2	0.2	0.3	0.2	0.2	0.3	0.4	0.3
50	0.4	0.4	0.4	0.3	0.6	0.3	0.3	0.6	0.7	0.5
100	0.6	0.6	0.6	0.5	1.0	0.5	0.5	0.9	1.0	0.9
200	0.9	0.8	0.9	0.8	1.6	0.9	0.9	1.8	1.7	1.5
200	5.2	5.6	4.5	5.4	5.7	5.1	4.1	5.8	5.2	4.1

Figure A-21: Results of single-oedometer test for Bosville Clay

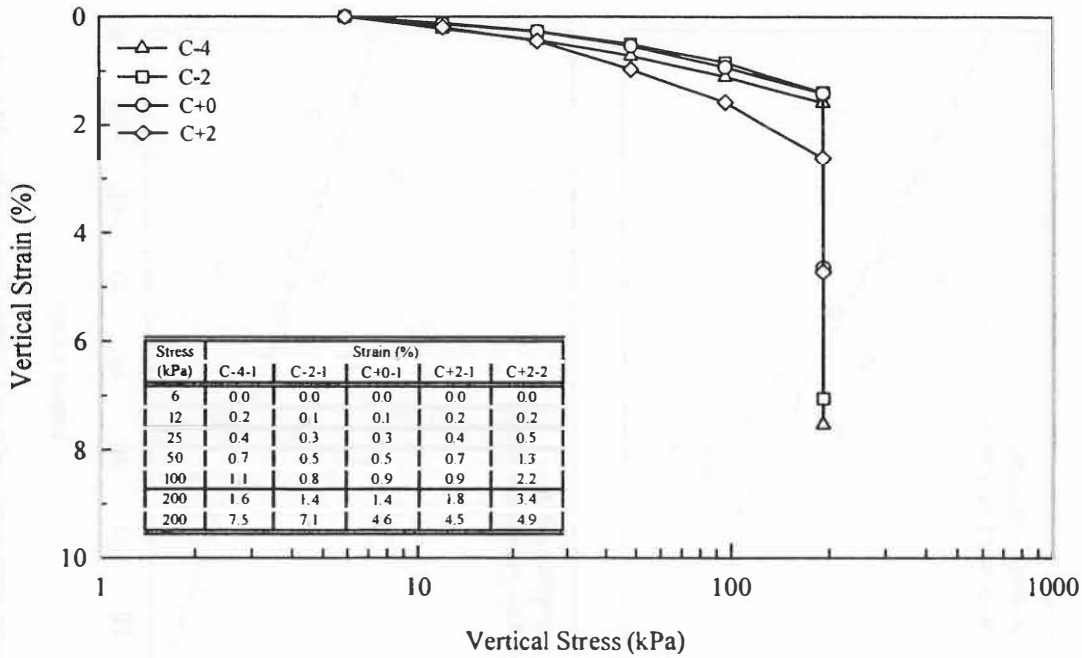

Stress (kPa)	Strain (%)				
	C-4-1	C-2-1	C+0-1	C+2-1	C+2-2
6	0.0	0.0	0.0	0.0	0.0
12	0.2	0.1	0.1	0.2	0.2
25	0.4	0.3	0.3	0.4	0.5
50	0.7	0.5	0.5	0.7	1.3
100	1.1	0.8	0.9	0.9	2.2
200	1.6	1.4	1.4	1.8	3.4
200	7.5	7.1	4.6	4.5	4.9

Figure A-22: Results of single-oedometer test for Dennis Clay

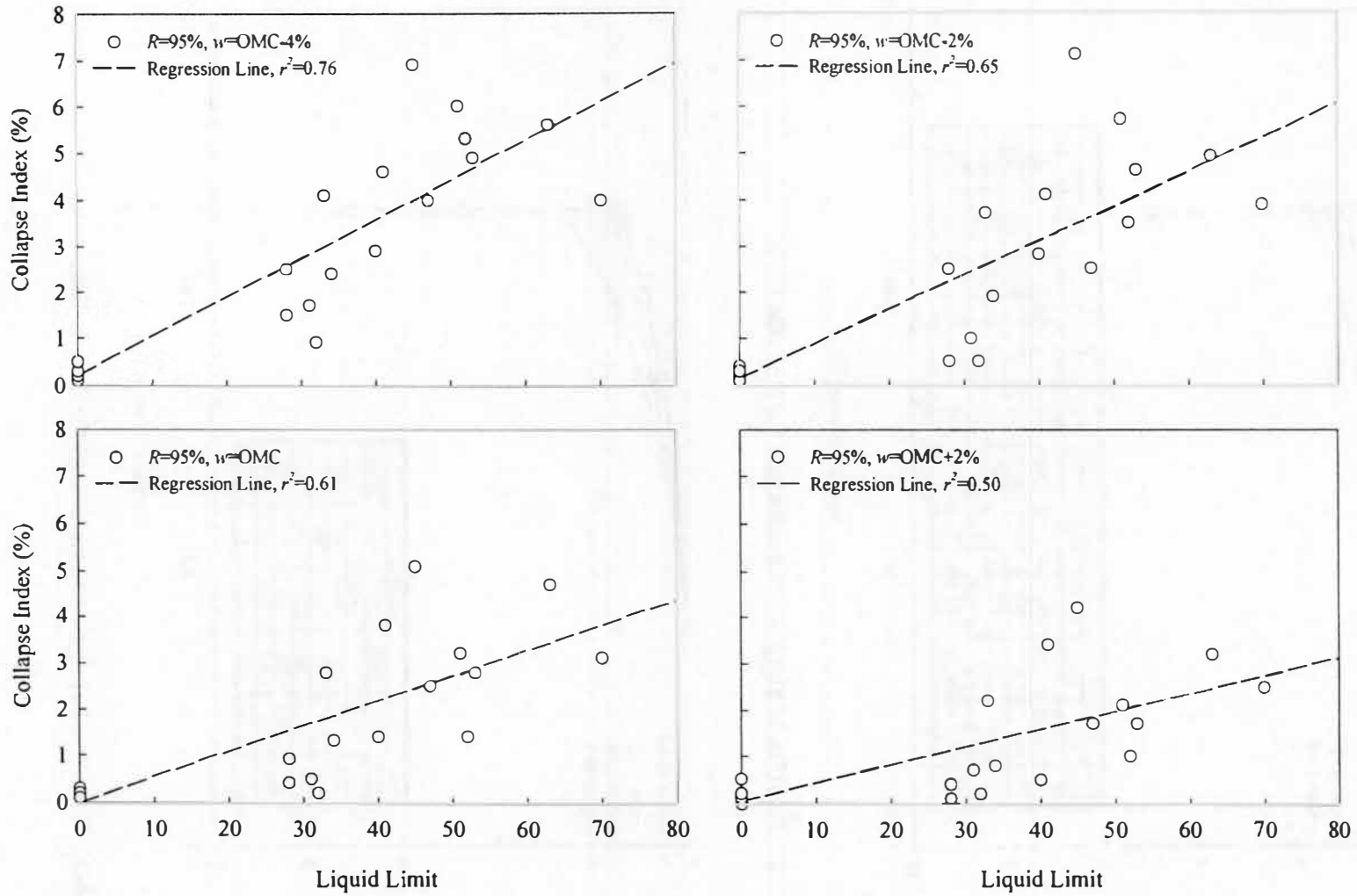

Figure A-23: Average value of collapse index versus liquid limit

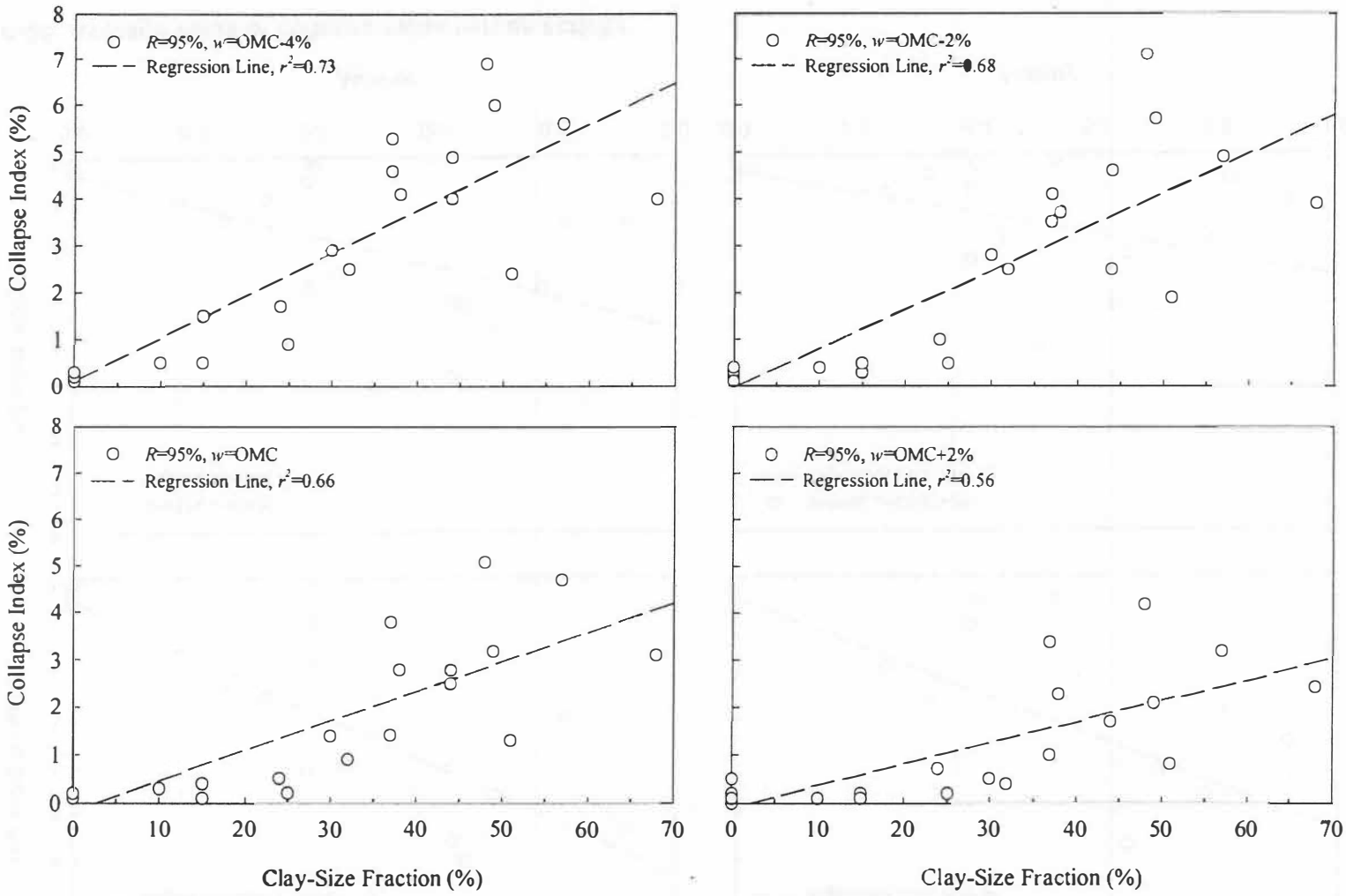

Figure A-24: Average value of collapse index versus clay-size fraction

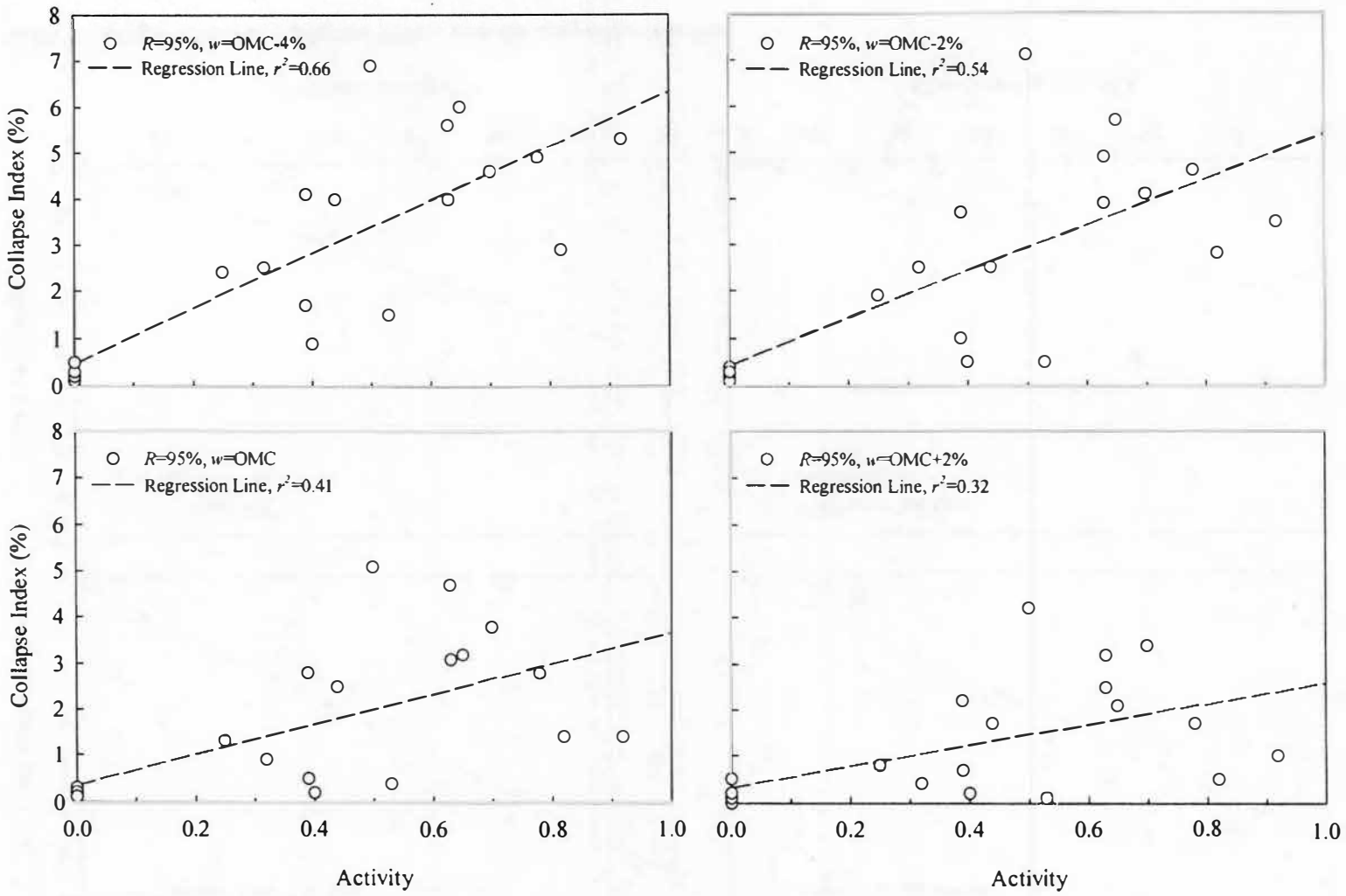

Figure A-25: Average value of collapse index versus activity

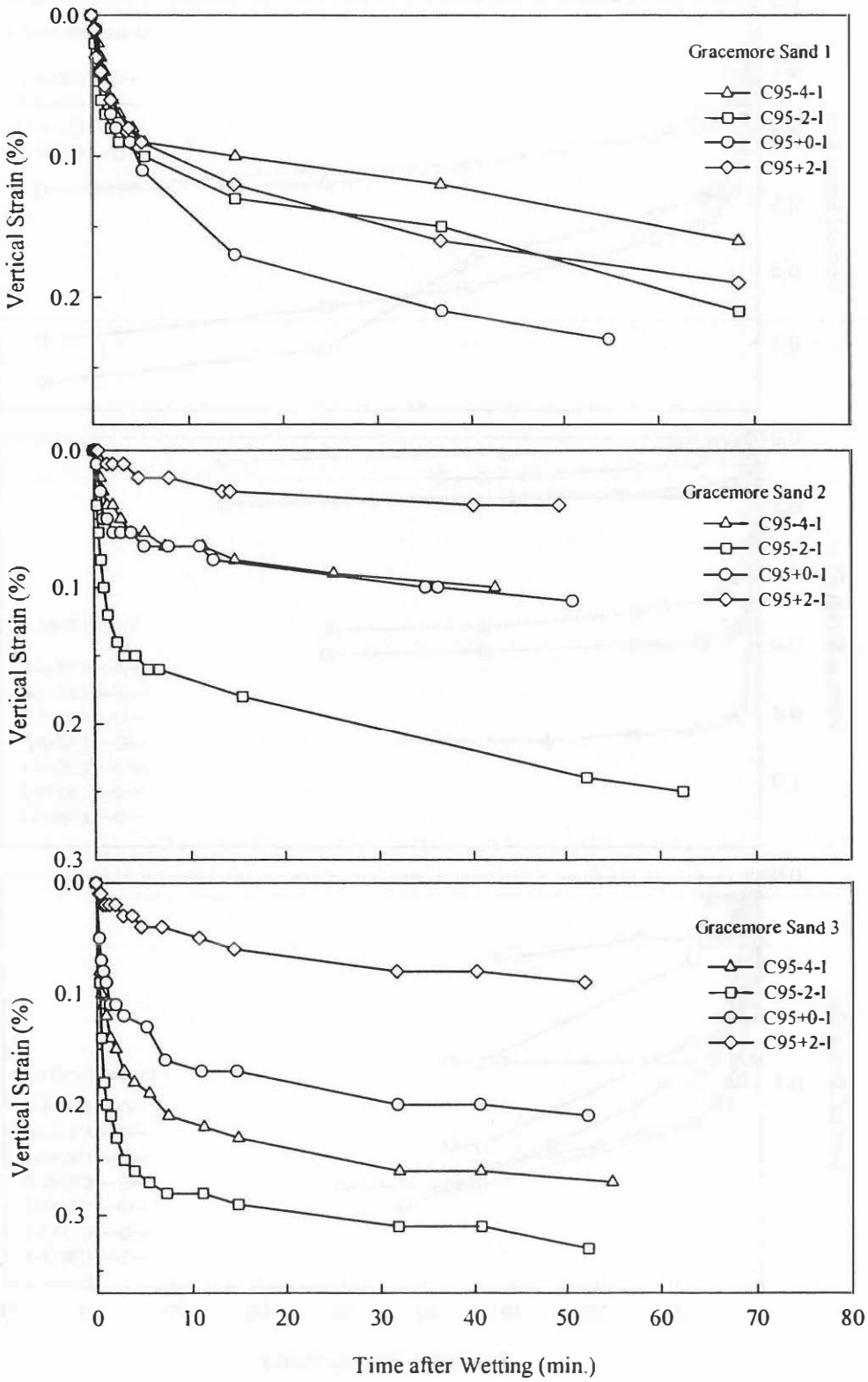

Figure A-26: Vertical strain versus time for Gracemore Sands 1, 2, and 3 during single-oedometer collapse at a vertical stress of 200 kPa

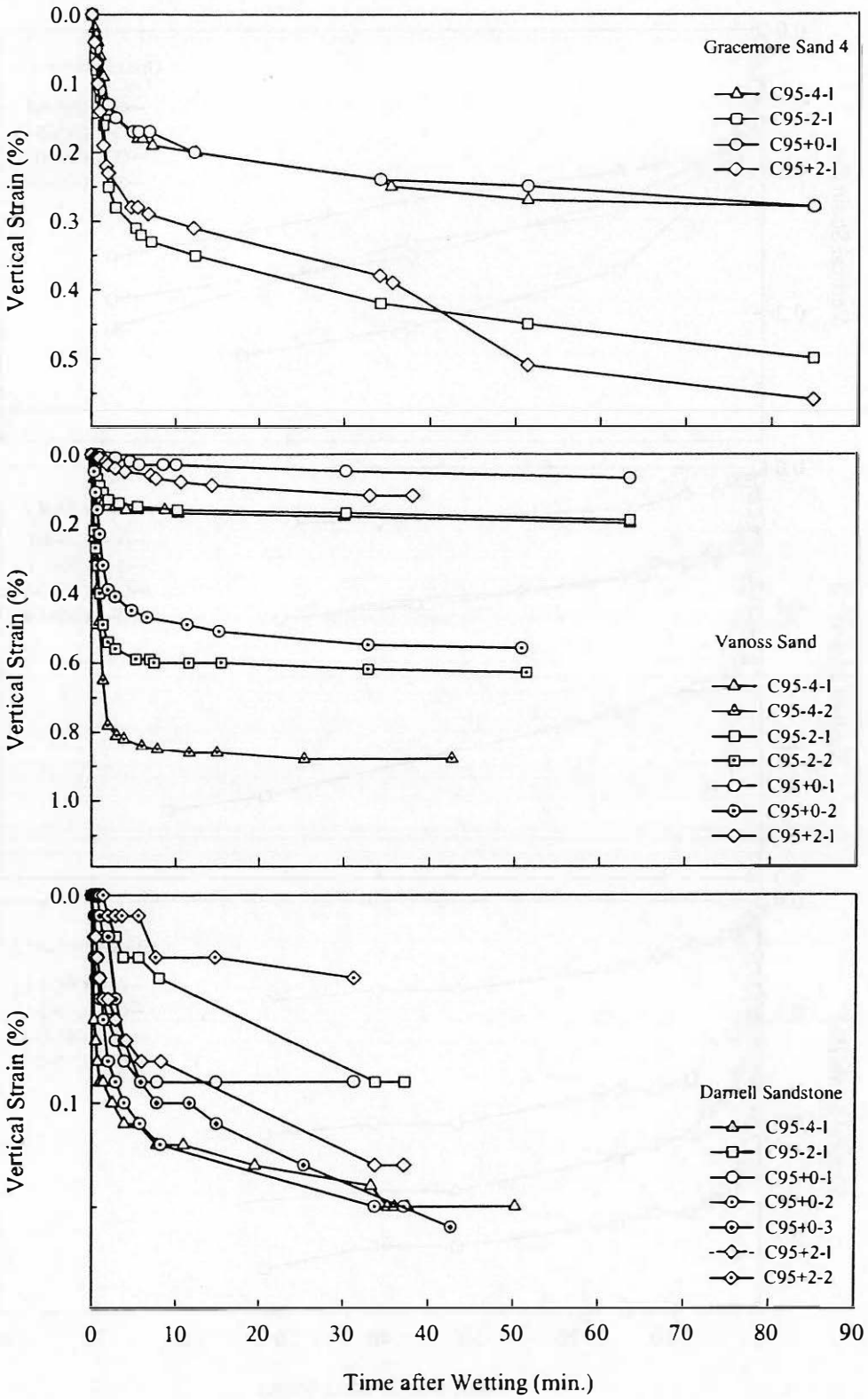

Figure A-27: Vertical strain versus time for Gracemore Sand 4, Vanoss Sand, and Darnell Sandstone during single-oedometer collapse at a vertical stress of 200 kPa

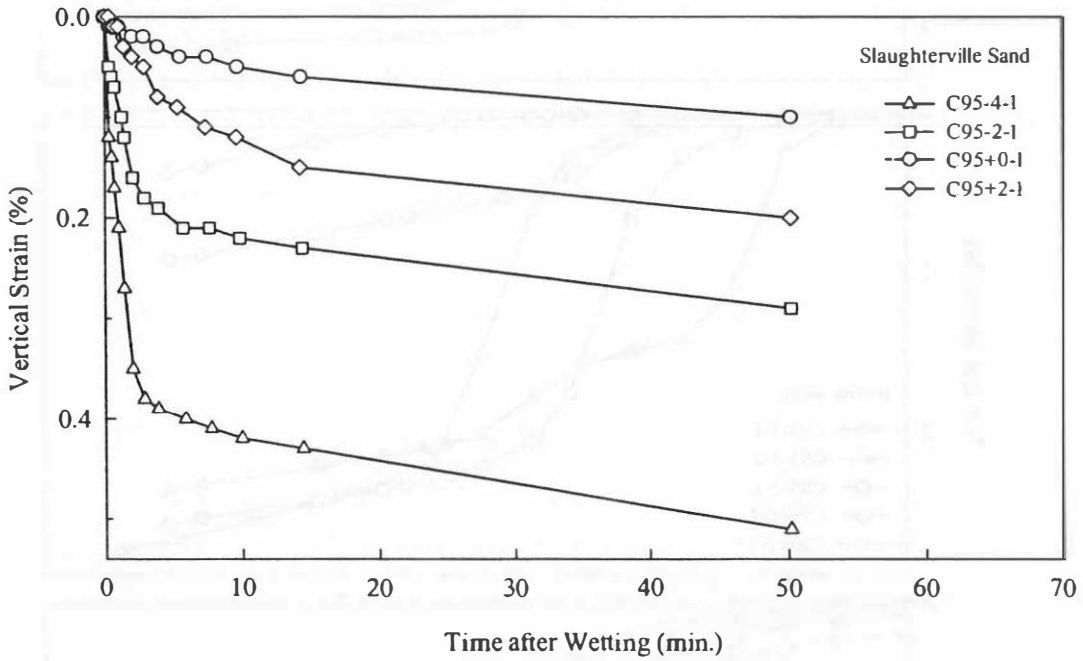

Figure A-28: Vertical strain versus time for Slaughterville Sand during single-oedometer collapse at a vertical stress of 200 kPa

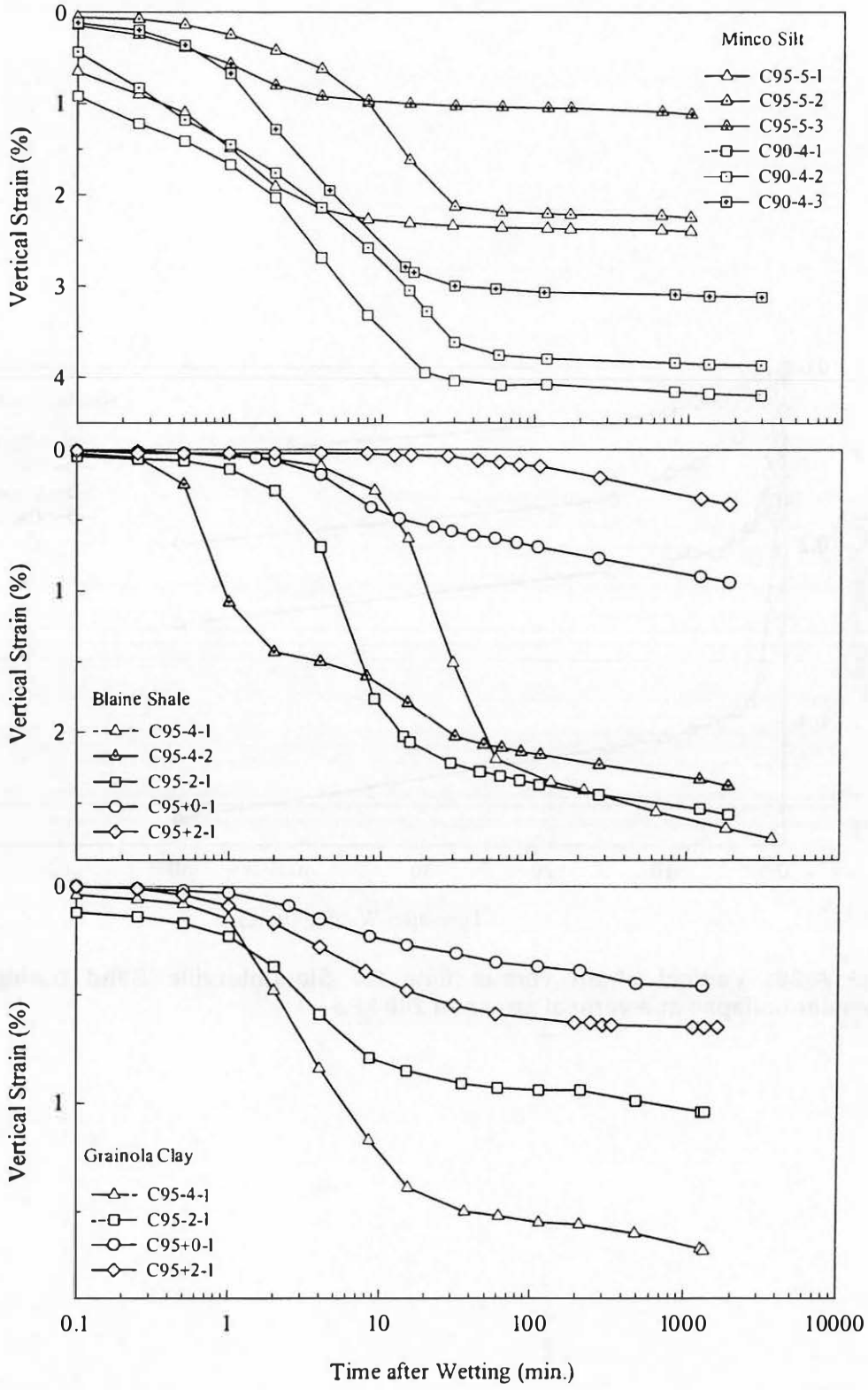

Figure A-29: Vertical strain versus time for Minco Silt, Blaine Shale, and Grainola Silt during single-oedometer collapse at a vertical stress of 200 kPa

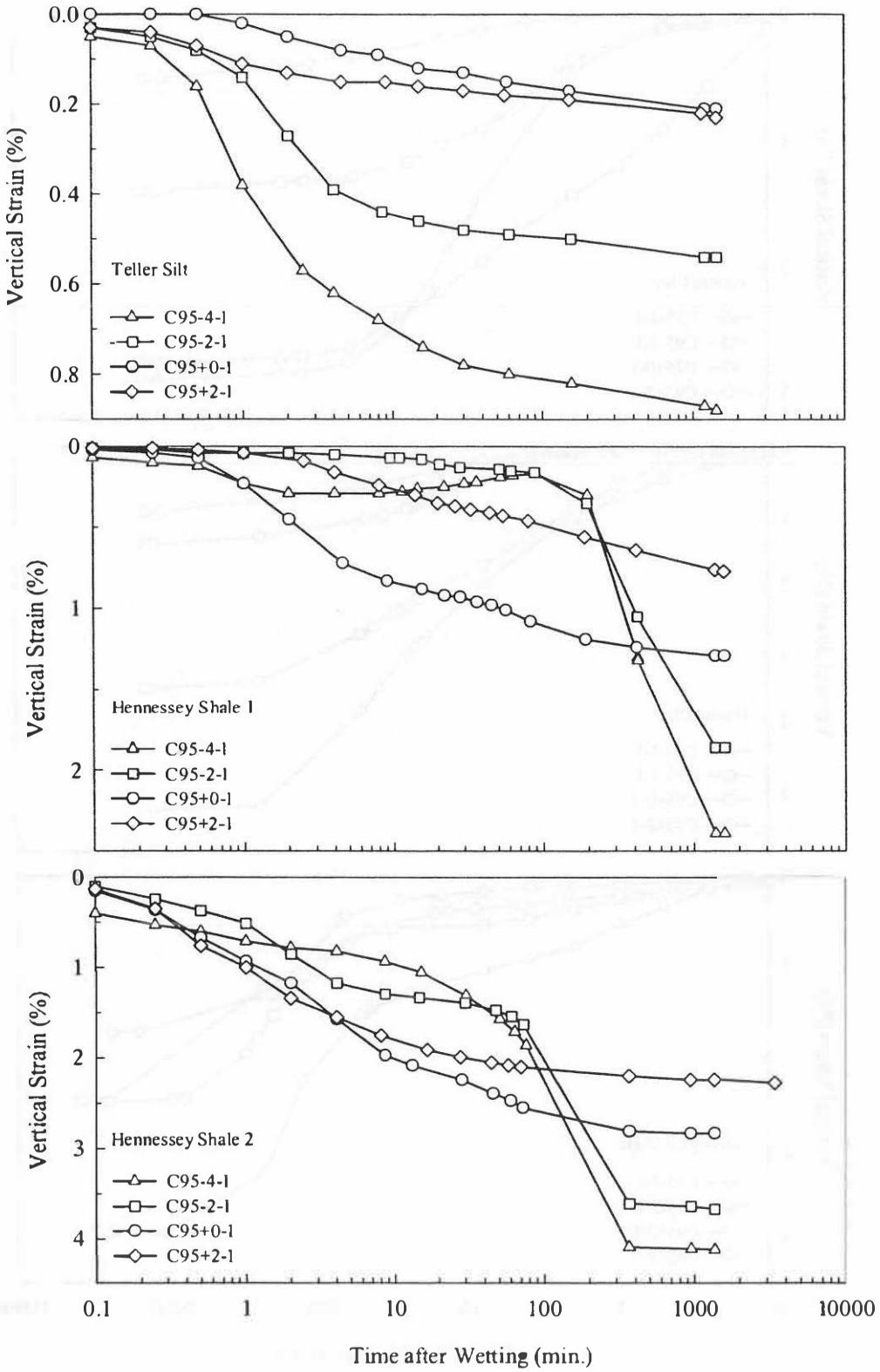

Figure A-30: Vertical strain versus time for Teller Silt, Hennessey Shales 1 and 2 during single-oedometer collapse at a vertical stress of 200 kPa

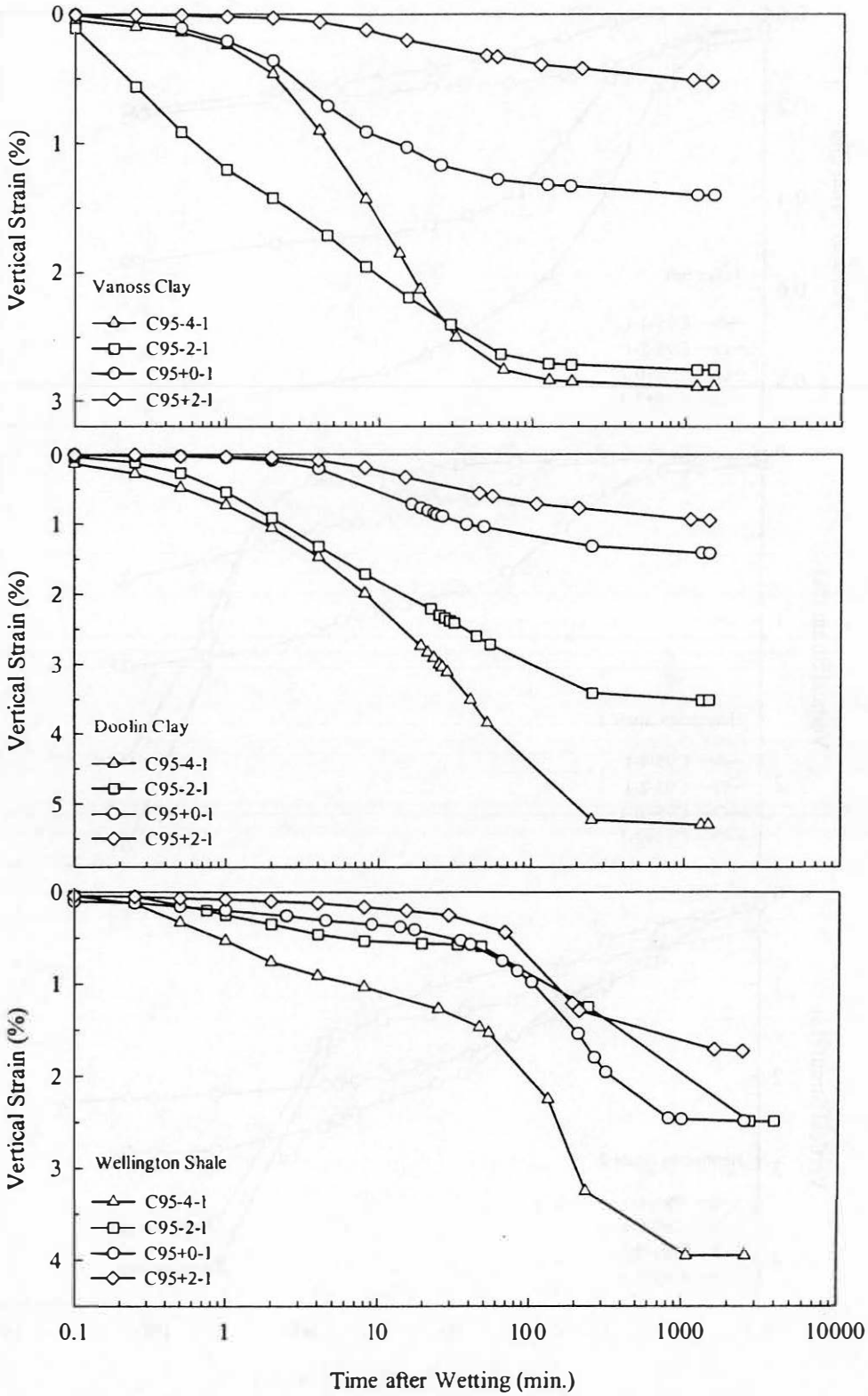

Figure A-31: Vertical strain versus time for Vanoss Clay, Doolin Clay, and Wellington Shale during single-oedometer collapse at a vertical stress of 200 kPa

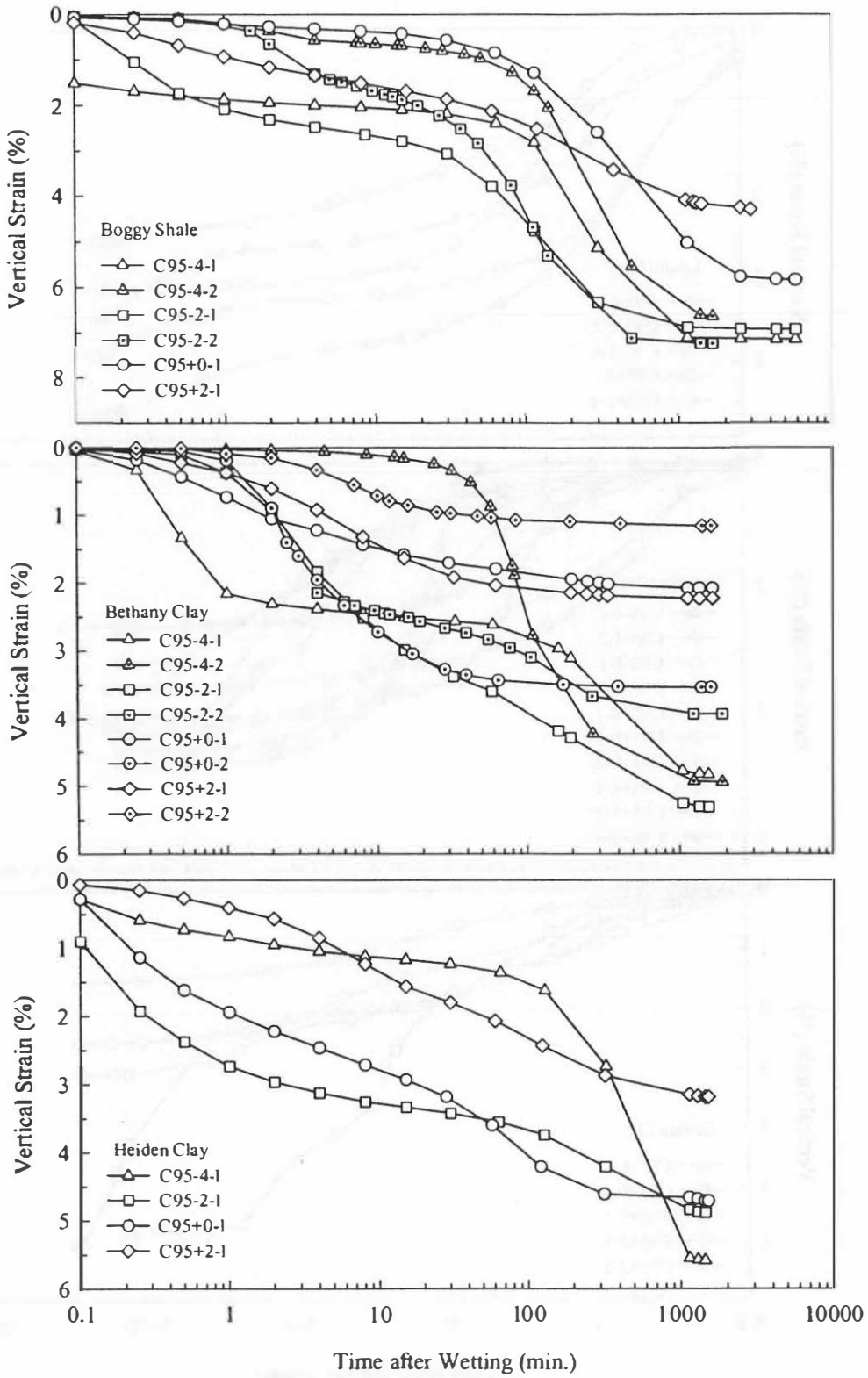

Figure A-32: Vertical strain versus time for Boggy Shale, Bethany Clay, and Heiden Clay during single-oedometer collapse at a vertical stress of 200 kPa

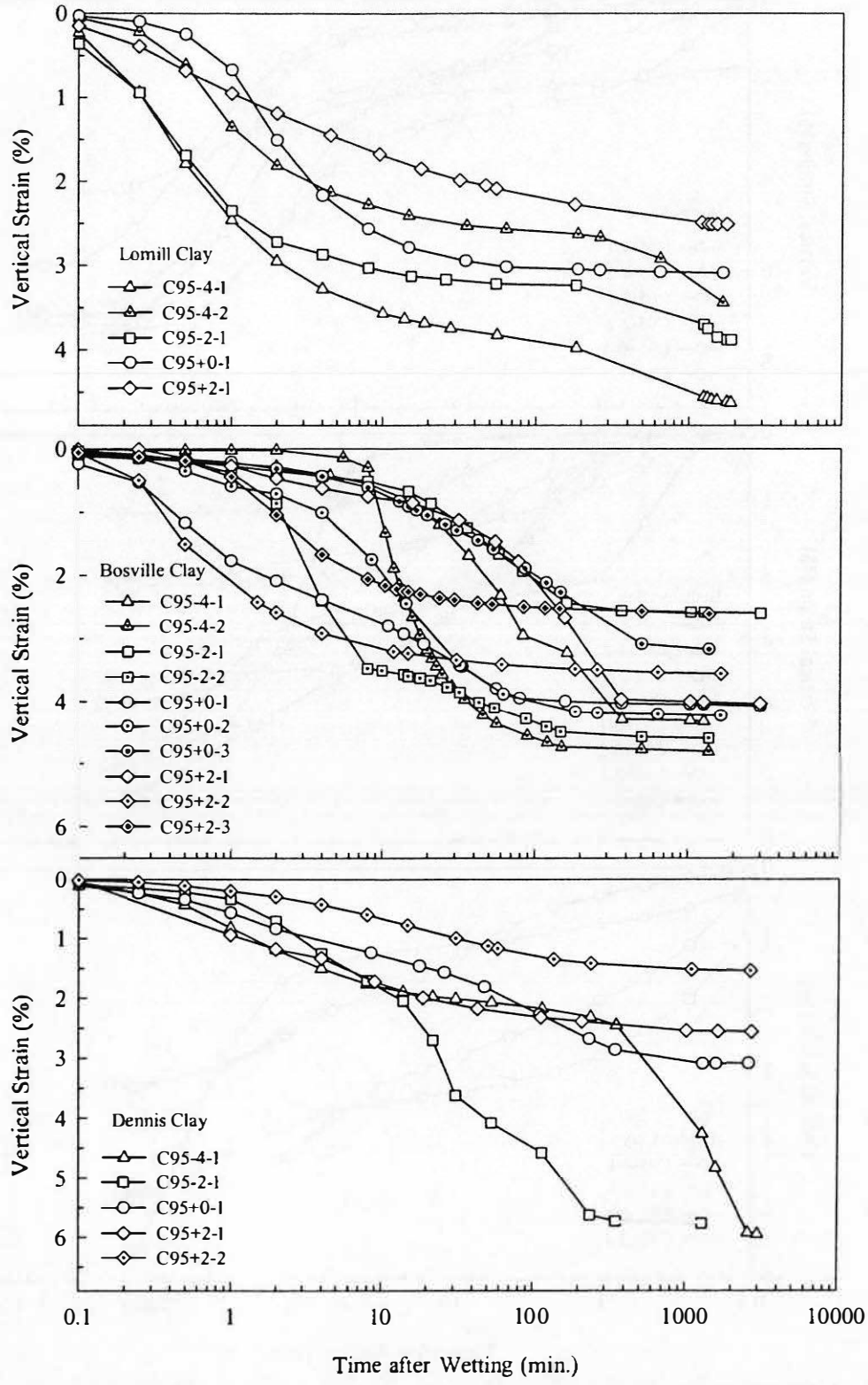

Figure A-33: Vertical strain versus time for Lomill Clay, Bosville Clay, and Dennis Clay during single-oedometer collapse at a vertical stress of 200 kPa

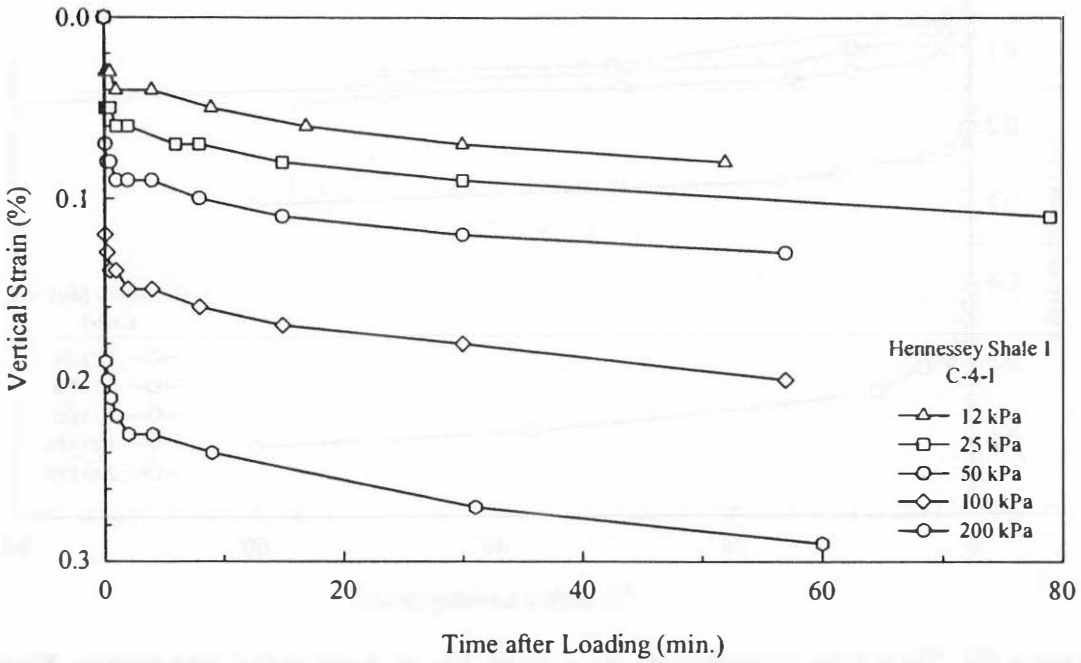

Figure A-34: Time rate of compression curves for as-compacted Hennessey Shale 1 (C-4-1)

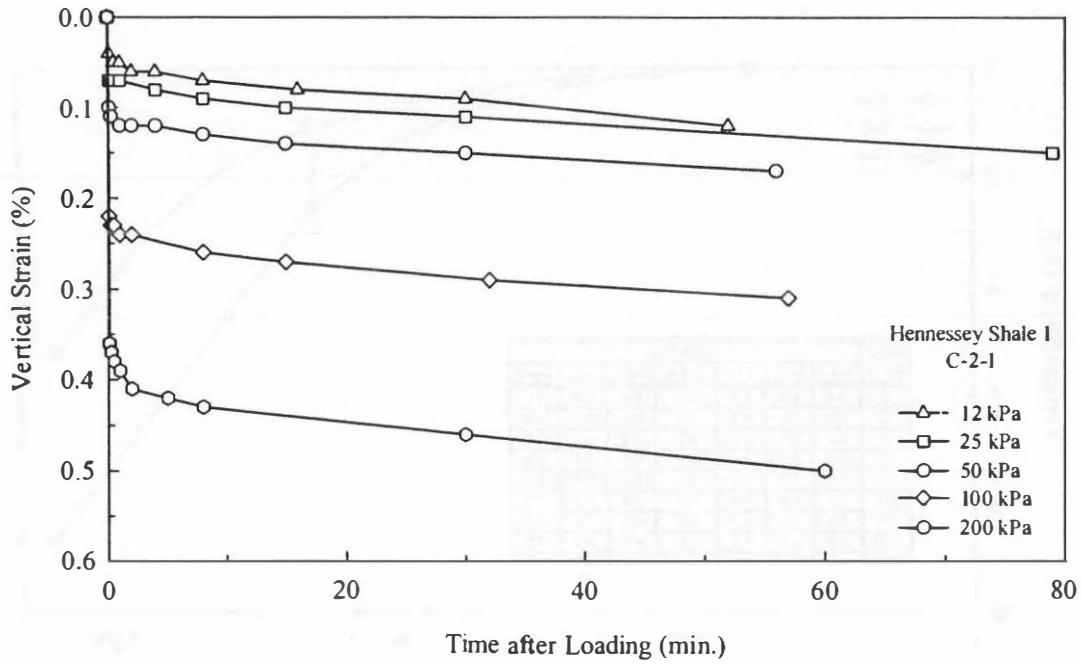

Figure A-35: Time rate of compression curves for as-compacted Hennessey Shale 1 (C-2-1)

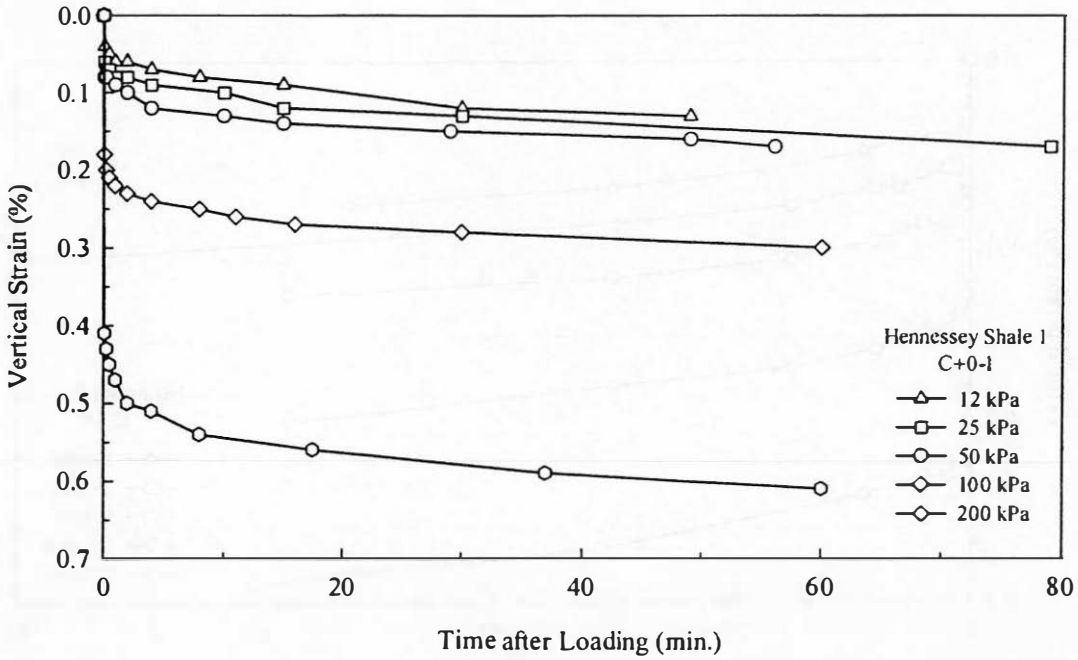

Figure A-36: Time rate of compression curves for as-compacted Hennessey Shale 1 (C+0-1)

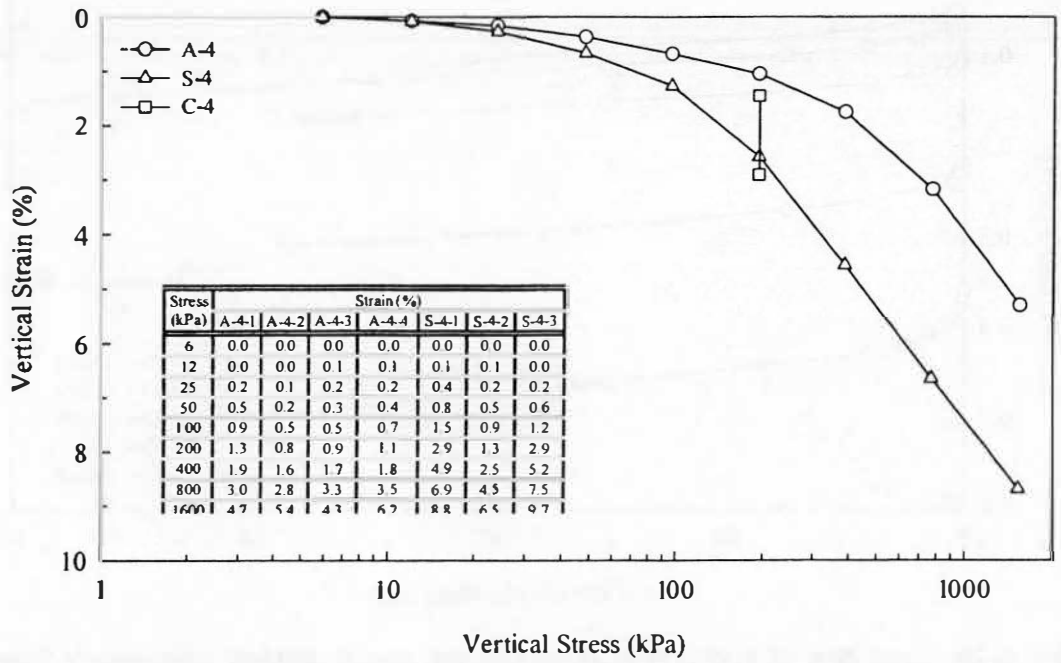

Stress (kPa)	Strain (%)						
	A-4-1	A-4-2	A-4-3	A-4-4	S-4-1	S-4-2	S-4-3
6	0.0	0.0	0.0	0.0	0.0	0.0	0.0
12	0.0	0.0	0.1	0.1	0.1	0.1	0.0
25	0.2	0.1	0.2	0.2	0.4	0.2	0.2
50	0.5	0.2	0.3	0.4	0.8	0.5	0.6
100	0.9	0.5	0.5	0.7	1.5	0.9	1.2
200	1.3	0.8	0.9	1.1	2.9	1.3	2.9
400	1.9	1.6	1.7	1.8	4.9	2.5	5.2
800	3.0	2.8	3.3	3.5	6.9	4.5	7.5
1600	4.7	5.4	4.3	6.2	8.8	6.5	9.7

Figure A-37: Results of double-oedometer test for Minco Silt

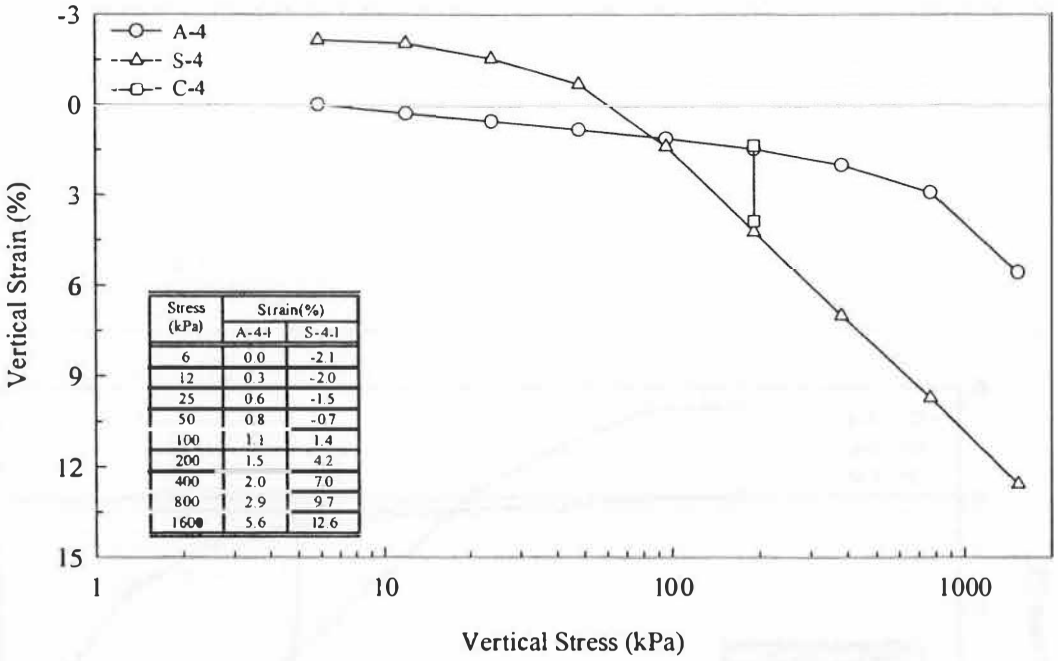

Stress (kPa)	Strain(%)	
	A-4-1	S-4-1
6	0.0	-2.1
12	0.3	-2.0
25	0.6	-1.5
50	0.8	-0.7
100	1.1	1.4
200	1.5	4.2
400	2.0	7.0
800	2.9	9.7
1600	5.6	12.6

Figure A-38: Results of double-oedometer test for Blaine Shale

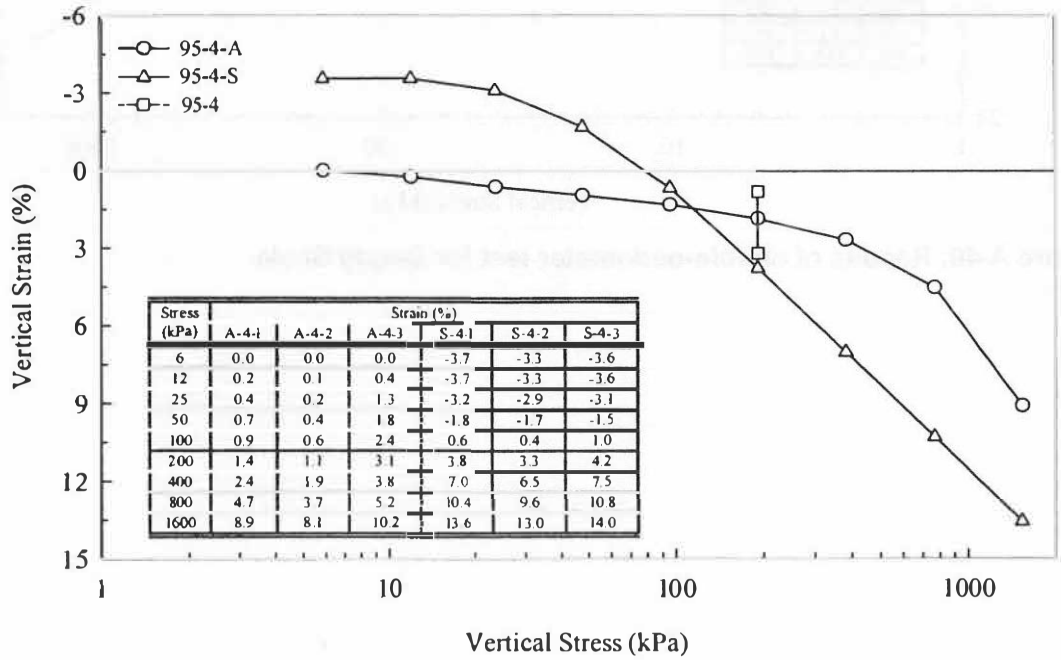

Stress (kPa)	Strain (%)					
	A-4-1	A-4-2	A-4-3	S-4-1	S-4-2	S-4-3
6	0.0	0.0	0.0	-3.7	-3.3	-3.6
12	0.2	0.1	0.4	-3.7	-3.3	-3.6
25	0.4	0.2	1.3	-3.2	-2.9	-3.1
50	0.7	0.4	1.8	-1.8	-1.7	-1.5
100	0.9	0.6	2.4	0.6	0.4	1.0
200	1.4	1.1	3.1	3.8	3.3	4.2
400	2.4	1.9	3.8	7.0	6.5	7.5
800	4.7	3.7	5.2	10.4	9.6	10.8
1600	8.9	8.1	10.2	13.6	13.0	14.0

Figure A-39: Results of double-oedometer test for Hennessey Shale 1

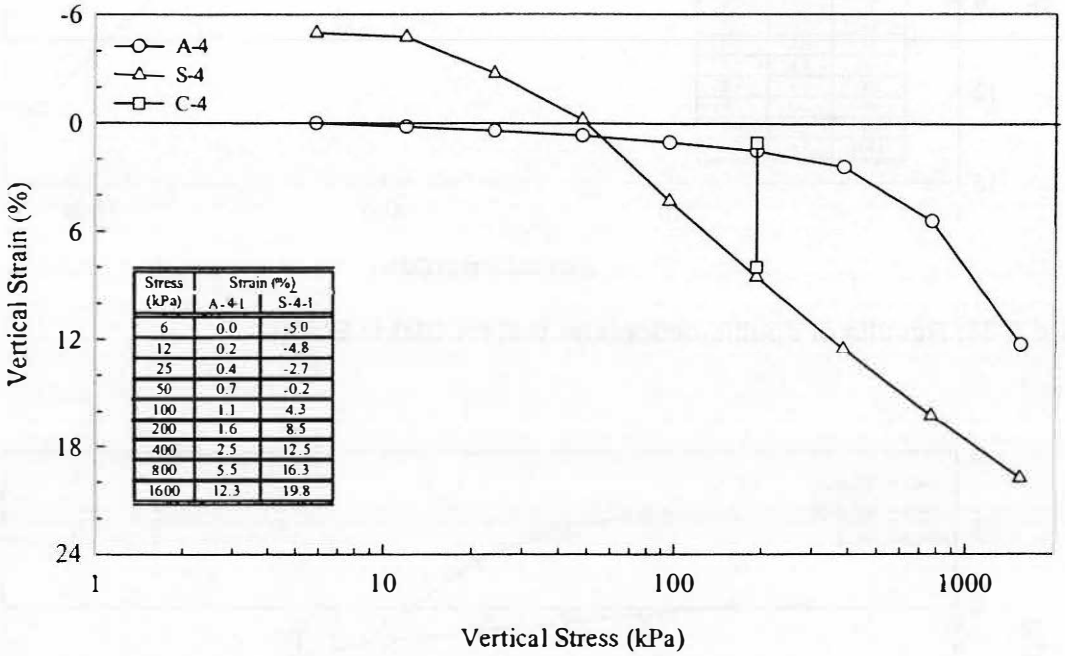

Stress (kPa)	Strain (%) A-4-1	S-4-1
6	0.0	-5.0
12	0.2	-4.8
25	0.4	-2.7
50	0.7	-0.2
100	1.1	4.3
200	1.6	8.5
400	2.5	12.5
800	5.5	16.3
1600	12.3	19.8

Figure A-40: Results of double-oedometer test for Boggy Shale

Appendix B : Centrifuge Test Data

Table B-1: Oedometer test data correspond to centrifuge Model No. 1

Vertical stress (kPa)	Vertical Strain (%)							
	As-compacted		Soaked			Single-oedometer		
6	0.00	0.00	0.04	0.00	0.00	0.00	0.00	0.00
12	0.06	0.24	0.18	0.04	0.05	0.09	0.11	0.15
25	0.19	0.40	0.35	0.23	0.23	0.20	0.21	0.32
50	0.36	0.59	0.57	0.44	0.50	0.36	0.44	0.50
100	0.62	0.87	0.93	0.75	0.93	0.61	0.71	0.76
200	1.03	1.34	1.71	1.36	1.69	1.00	1.16	1.21
400	1.78	2.22	2.91	2.64	3.09	1.75	1.97	1.99
800/400 [a]	2.92	3.69	4.27	---	4.55	2.46	2.67	2.96
1600	4.46	5.56	5.94	5.80	6.20	---	---	---

[a]800 kPa for double-oedometer data, 400 kPa for single-oedometer data; inundation at 400 kPa for single-oedometer tests.

Table B-2: Oedometer test data correspond to centrifuge Model No. 2

Vertical stress (kPa)	Vertical Strain (%)							
	As-compacted			Soaked		Single-oedometer		
6	0.00	0.00	0.00	0.07	0.06	0.00	0.00	0.00
12	0.07	0.32	0.19	0.13	0.15	0.10	0.07	0.12
25	0.19	0.52	0.44	0.28	0.36	0.22	0.18	0.33
50	0.42	0.77	0.70	0.62	0.76	0.39	0.34	0.56
100	0.70	1.08	1.03	1.33	1.79	0.65	0.59	0.84
200	1.23	1.54	1.54	3.00	3.40	1.13	1.07	1.31
400	2.49	2.59	2.48	4.92	5.44	2.41	2.45	2.33
800/400 [a]	4.70	4.72	4.55	6.81	7.40	6.61	6.31	5.44
1600	7.49	7.43	7.36	8.80	9.44	---	---	---

[a]800 kPa for double-oedometer data, 400 kPa for single-oedometer data; inundation at 400 kPa for single-oedometer tests.

Table B-3: Oedometer test data correspond to centrifuge Model No. 3

Vertical stress (kPa)	Vertical Strain (%)								
	As-compacted			Soaked			Single-oedometer		
6	0.00	0.00	0.00	-0.05	-0.05	-0.01	0.00	0.00	0.00
12	0.20	0.12	0.07	0.02	-0.02	0.03	0.13	0.09	0.05
25	0.42	0.25	0.16	0.15	0.16	0.13	0.29	0.21	0.12
50	0.66	0.38	0.29	0.39	0.36	0.40	0.51	0.37	0.23
100	0.92	0.56	0.47	0.93	0.69	0.81	1.24	0.55	0.40
200	1.23	0.80	0.73	1.98	1.82	1.77	1.61	0.86	0.71
400	1.70	1.18	1.17	3.71	3.42	3.28	2.28	1.43	1.33
800/400 [a]	2.57	2.08	2.21	5.45	5.08	5.01	4.64	3.66	2.36
1600	4.17	3.79	4.16	7.29	6.81	6.81	---	---	---

[a]800 kPa for double-oedometer data, 400 kPa for single-oedometer data; inundation at 400 kPa for single-oedometer tests.

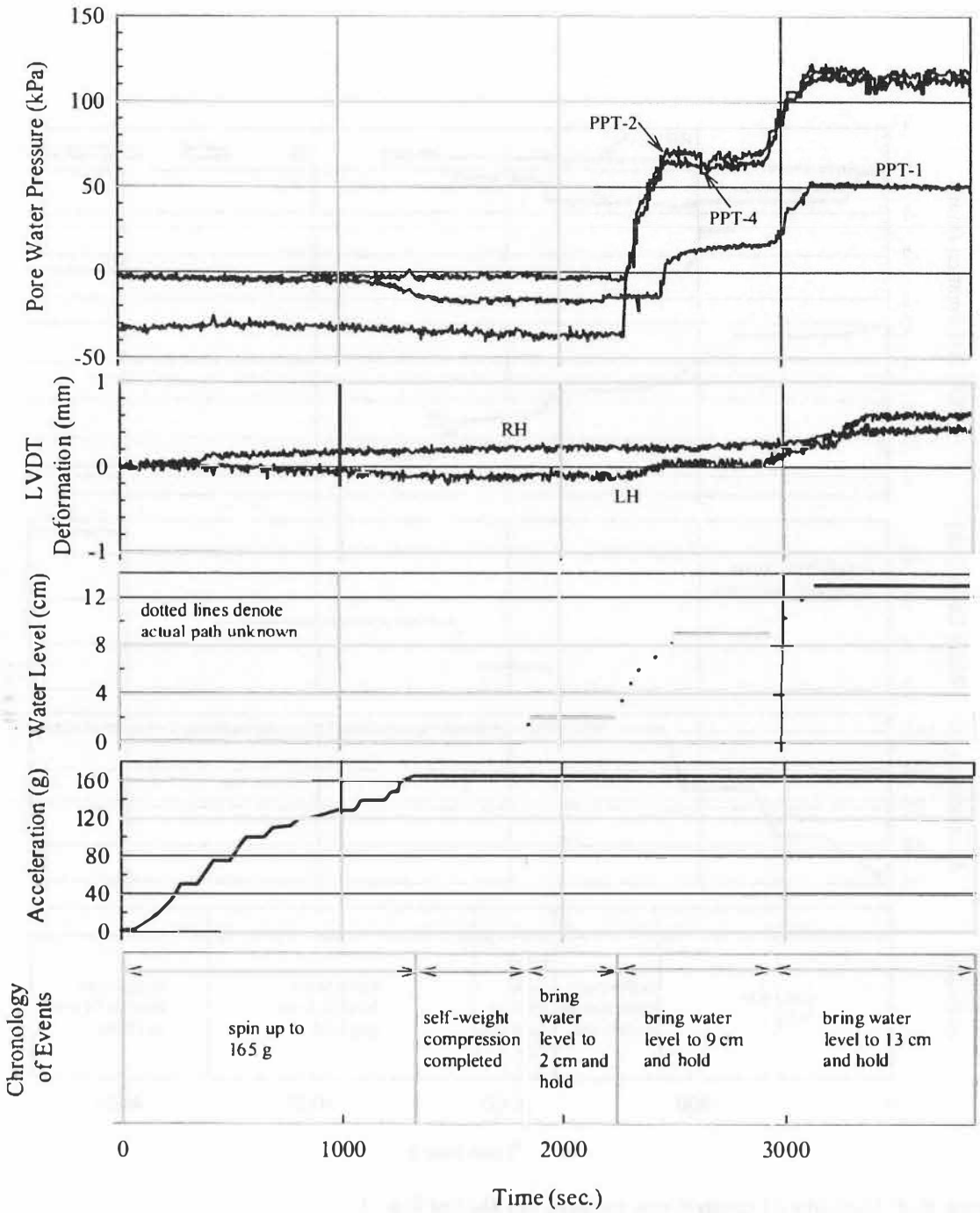

Figure B-1: Results of centrifuge testing on Model No. 1

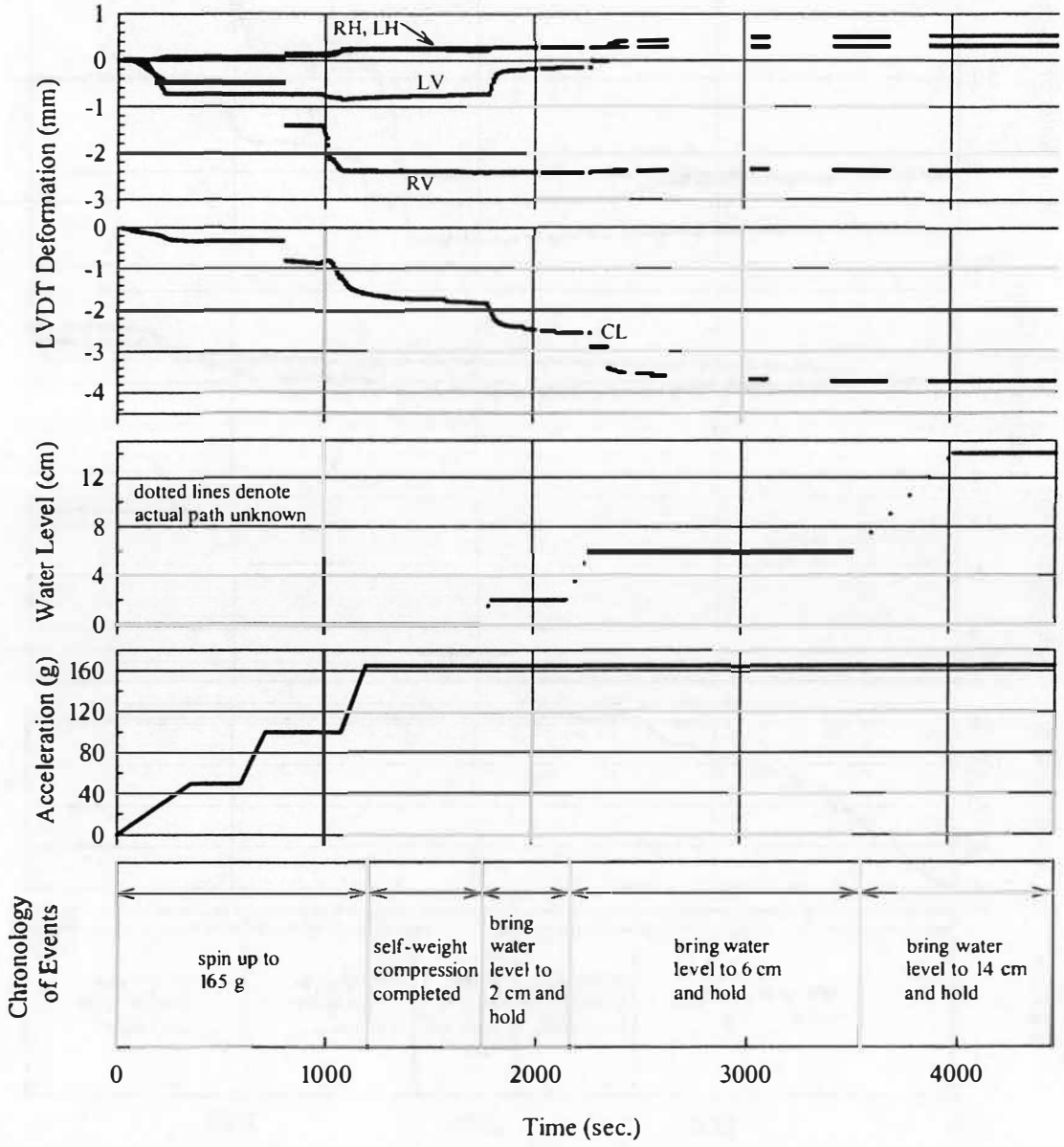

Figure B-2: Results of centrifuge testing on Model No. 2

Appendix C : Field Study Test Data

Table C-1: Oedometer data for Sample No. 1 from Boring No. 1

Vertical stress (kPa)	Vertical Strain (%)				
	As-compacted		Soaked		Single-oedometer
6	0.00	0.00	-2.52	-2.59	0.00
12	0.19	0.12	-2.44	-2.54	0.17
25	0.32	0.32	-2.07	-2.26	0.36
50	0.49	0.58	-0.85	-1.27	0.58
100	0.77	0.97	2.23	2.35	0.94
200	1.35	1.66	5.88	6.02	1.63
400	4.19	3.80	9.48	9.72	4.56
800/400 [a]	8.33	8.05	12.89	13.30	9.19
1600	12.29	12.05	16.47	16.90	---

[a]800 kPa for double-oedometer data, 400 kPa for single-oedometer data; inundation at 400 kPa for single-oedometer tests.

Table C-2: Oedometer data for Sample No. 2 from Boring No. 1

Vertical stress (kPa)	Vertical Strain (%)				
	As-compacted		Soaked		Single-oedometer
6	0.00	0.00	-3.11	-2.93	0.00
12	0.33	0.31	-3.04	-2.88	0.27
25	0.57	0.48	-2.76	-2.53	0.44
50	0.80	0.69	-1.78	-1.65	0.68
100	1.12	1.04	1.55	1.13	1.05
200	1.79	1.70	5.33	5.07	1.71
400	4.92	4.77	9.11	8.75	4.91
800/400 [a]	8.45	7.90	12.81	12.25	10.46
1600	12.52	11.76	16.43	15.65	---

[a]800 kPa for double-oedometer data, 400 kPa for single-oedometer data; inundation at 400 kPa for single-oedometer tests.

Table C-3: Oedometer data for Sample No. 3 from Boring No. 2

Vertical stress (kPa)	Vertical Strain (%)		
	As-compacted	Soaked	Single-oedometer
6	0.00	-8.01	0.00
12	0.13	-7.91	0.13
25	0.36	-7.25	0.36
50	0.68	-5.04	0.67
100	1.10	-1.70	1.15
200	1.55	1.90	1.57
400	2.39	5.72	2.41
800/400 [a]	4.86	9.96	5.80
1600	11.48	14.29	---

[a]800 kPa for double-oedometer data, 400 kPa for single-oedometer data; inundation at 400 kPa for single-oedometer tests.

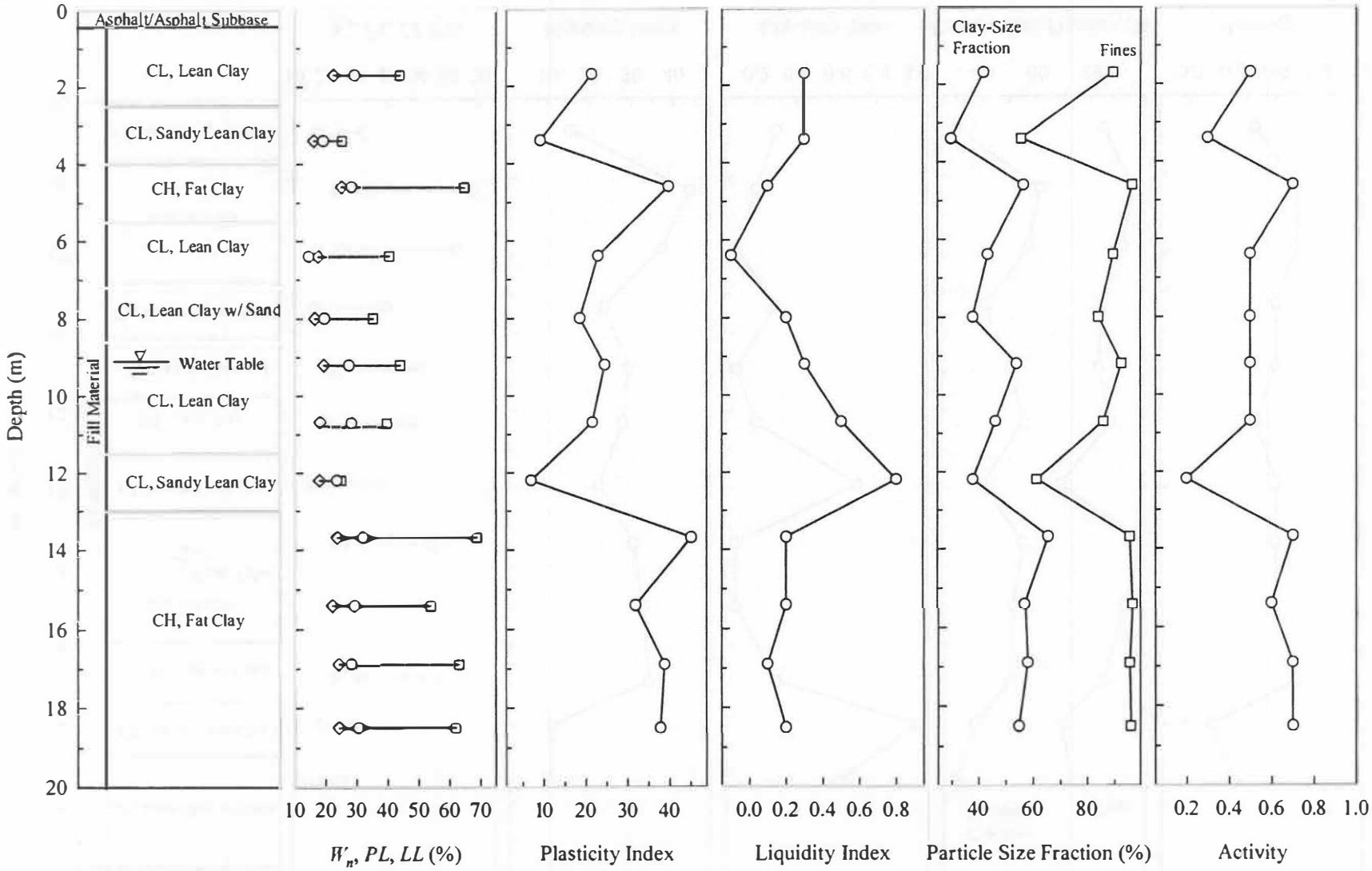

Figure C-1: Soil profile for Boring No. 1 at Embankment No. 2

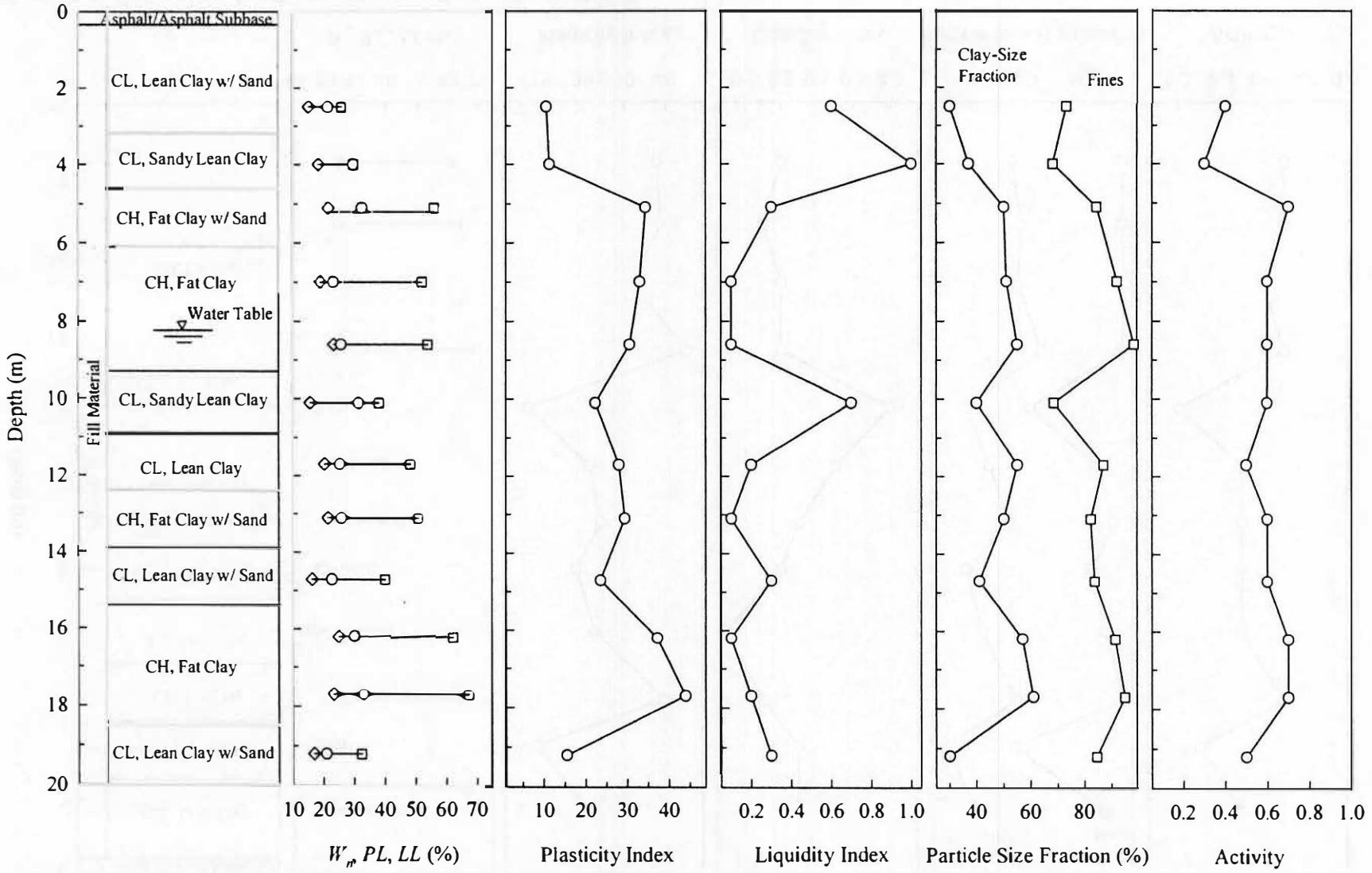

Figure C-2: Soil profile for Boring No. 2 at Embankment No. 2

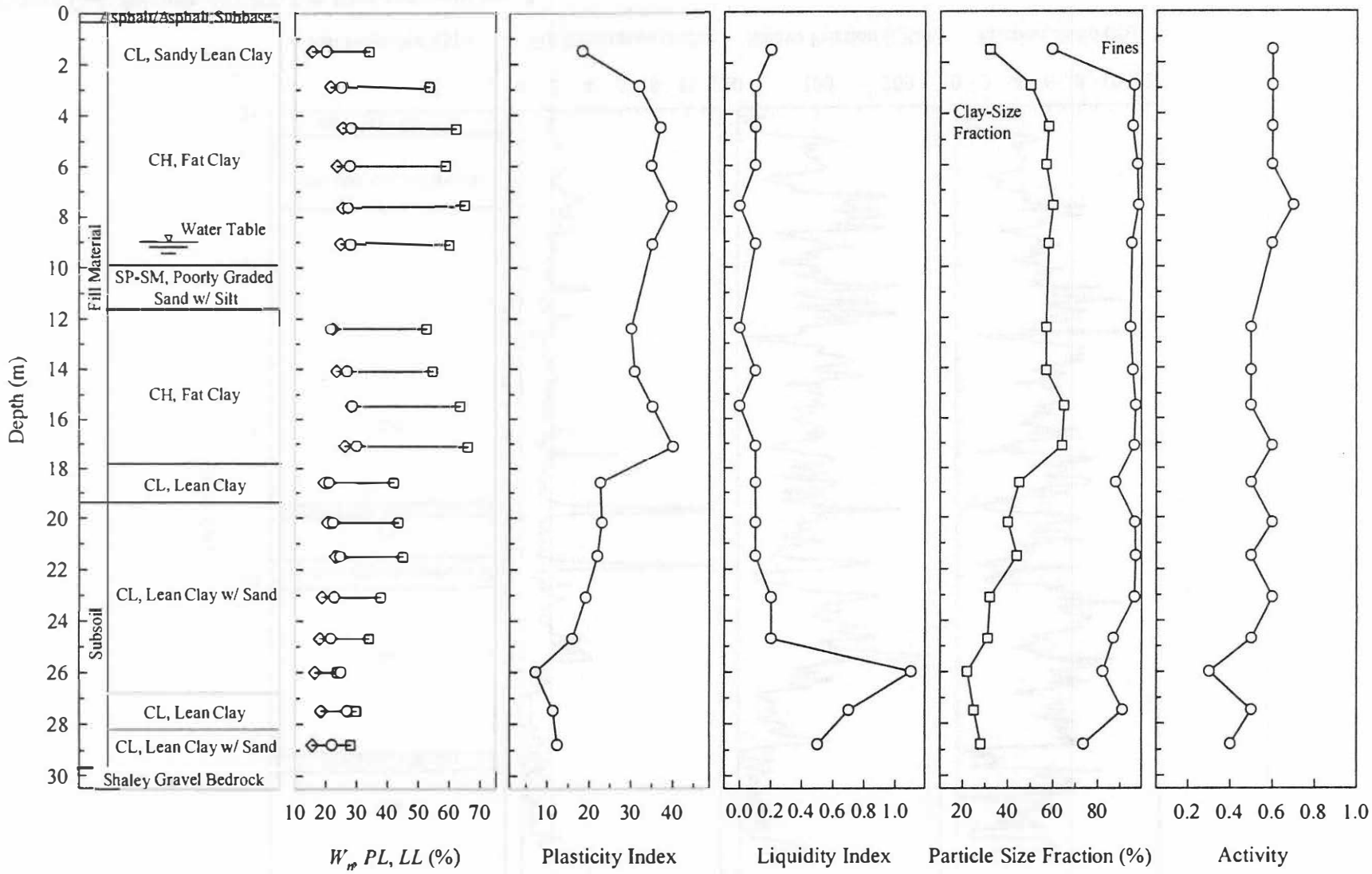

Figure C-3: Soil profile for Boring No. 3 at Embankment No. 2

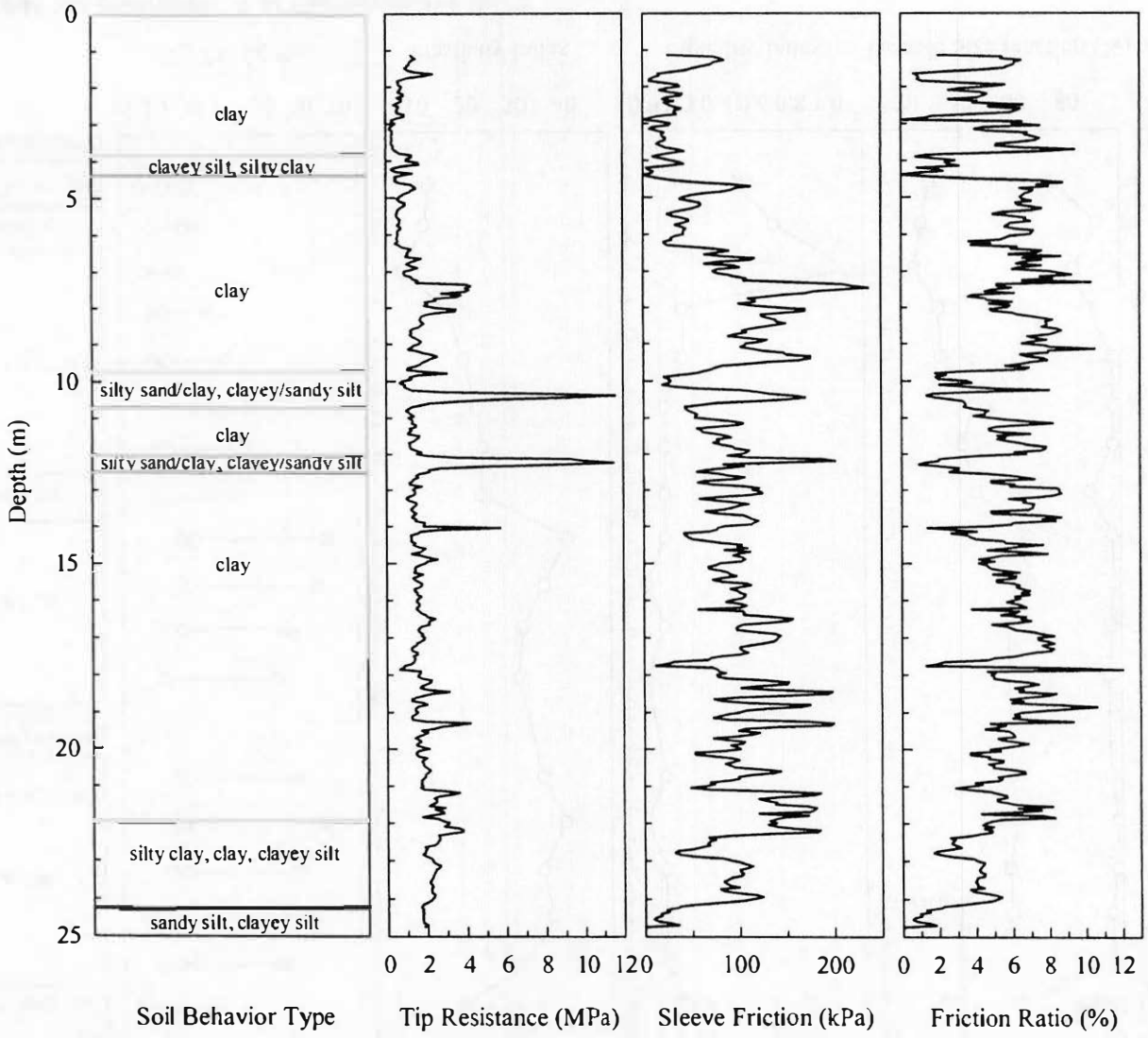

Figure C-4: Results of CPT-2 at Embankment No. 2

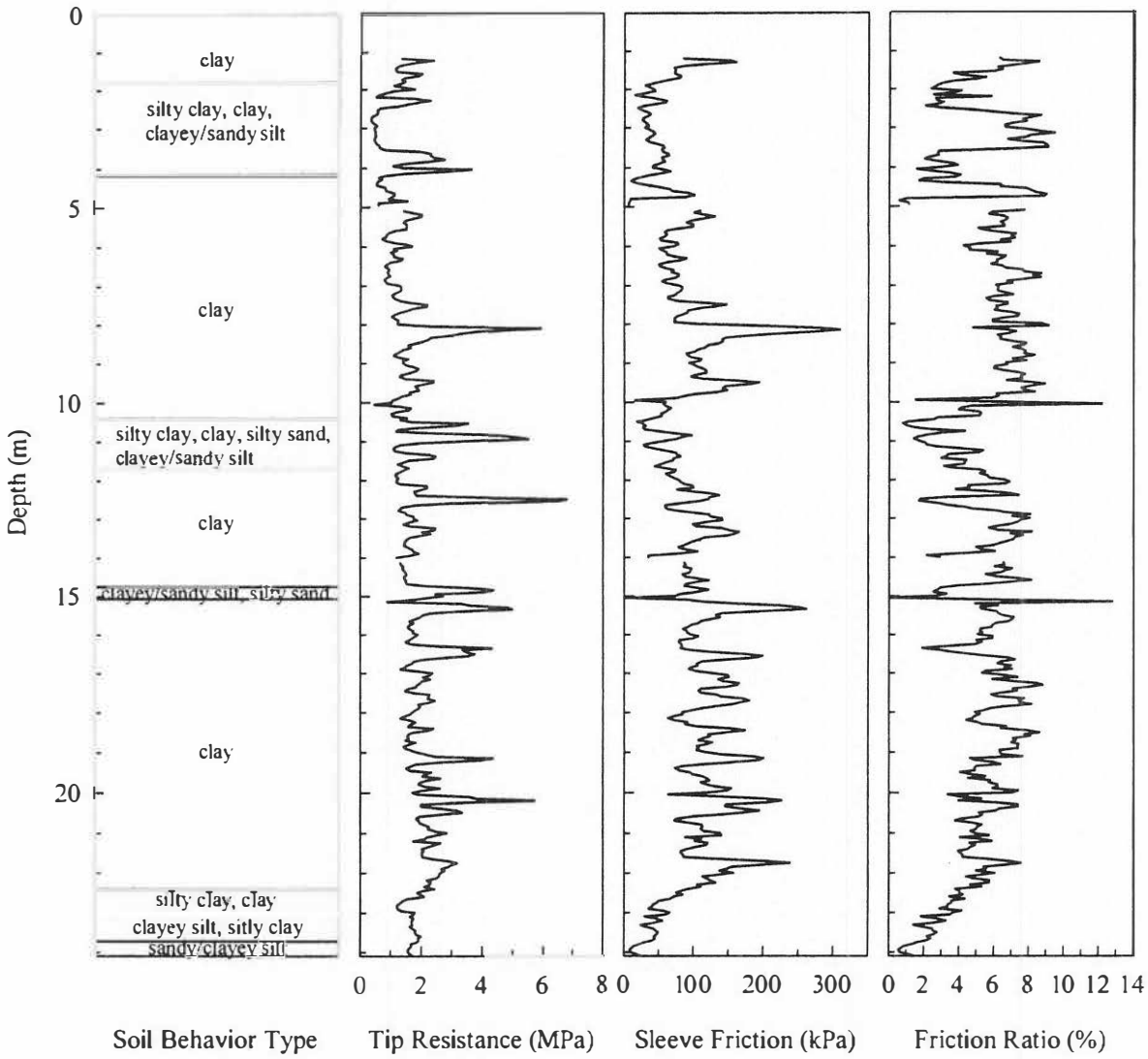

Figure C-5: Results of CPT-3 at Embankment No. 2